

**Effect of Roasting Processes on Some Properties of  
Sesame and Sesame Paste: Rheological, Color,  
Textural and Moisture Adsorption**

**Ph. D. Thesis  
in  
Food Engineering  
University of Gaziantep**

**Supervisor  
Assoc. Prof. Dr. Sevim KAYA**

**by  
Talip KAHYAOĞLU  
November 2005**

*Dedicated to*

*Canan*

*and*

*Tuğçe, Ömer Faruk, Emine Nida*

....

## ABSTRACT

### EFFECT OF ROASTING PROCESSES ON SOME PROPERTIES OF SESAME AND SESAME PASTE: RHEOLOGICAL, COLOR, TEXTURAL AND MOISTURE ADSORPTION

KAHYAOĞLU Talip

Ph.D. in Food Engineering

Supervisor: Assoc. Prof. Dr. Sevim KAYA

November 2005, 134 pages

Sesame seeds were roasted using conventional method at 120, 150, and 180°C for 120 min. The changes occurred in the moisture content, color values and textural properties (hardness and fracturability) of sesame seeds were simulated using exponential, kinetic and polynomial models for conventional roasting. Response surface methodology was applied to develop predictive models and optimize the hot air, electrical oven and vacuum oven roasting processes. As considering desirability function of each color and texture parameters, the optimum roasting temperature and time ranges for production of sesame paste were determined as 155-170°C and 40-60 min at hot air roaster, respectively. The effects of dehulling and roasting process on the moisture adsorption isotherms and thermodynamic properties of sesame seed were investigated. Though the trend of sorption isotherms of the samples were similar, equilibrium moisture content was decreased with dehulling and roasting process at a certain water activity. The Guggenheim-Anderson-de Boer (GAB) and Halsey models were found to adequately describe the sorption characteristics. The values of differential enthalpy and differential entropy decreased with application of dehulling and roasting process. The effects of gum type and temperature on the thixotropic behavior of sesame paste were determined. The different mathematical models were used for description of structural breakdown of paste. The first-order shear stress decay with non-zero equilibrium was determined as the most successful model.

**Key words:** Sesame, Sesame paste, Roasting, Moisture adsorption, Rheology

## ÖZET

### KAVURMA İŞLEMİNİN SUSAMIN VE TAHİNİN BAZI ÖZELLİKLERİNE ETKİSİ: REOLOJİK, RENK, DOKUSAL VE NEM SOĞURMA

KAHYAOĞLU Talip  
Doktora tezi, Gıda Mühendisliği  
Tez Danışmanı: Doç. Dr. Sevim KAYA  
Kasım 2005, 134 sayfa

Susamlar geleneksel kavurma yöntemi kullanılarak 120, 150 ve 180°C sıcaklıklarda 120 dakika süre ile kavruldu. Geleneksel kavurma sürecinde susamın nem, renk ve dokusal (sertlik ve kırılgenlik) özelliklerinde meydana gelen değışimler, üssel, kinetik ve polinomal eşitliklerle modellendi. Tepkisel yüzey yöntemi, sıcak hava, elektrik fırını ve vakum fırını ile gerçekleştirilen kavurma işlemlerinin, optimizasyonlarında ve tahmini modellerin geliştirilmesinde kullanıldı. Her bir renk ve dokusal parametrelerin istenirlik fonksiyonu dikkate alınarak, sıcak hava kavurma yöntemi ile tahin üretimi için optimum kavurma sıcaklık ve zaman sınırları sırasıyla 155-170°C ve 40-60 dakika olarak belirlendi. Kavurma ve kabuk soyma işlemlerinin susamın nem soğurma eşsıcaklık eğrisine ve termodinamik parametrelerine olan etkileri incelendi. Susamın belirli su aktivitelerindeki denge nem miktarının, kavurma ve kabuk soyma işlemlerinin etkisi ile düştüğü gözlemlendi. Guggenheim-Anderson-de Boer (GAB) ve Halsey modellerinin soğurma davranışlarını yeterince tanımladıkları bulundu. Diferansiyel entalpi ve entropi değerlerinin kavurma ve kabuk soyma işlemi ile düştüğü tespit edildi. Gam çeşitlerinin ve sıcaklığın tahinin tiksotropik davranışı üzerine olan etkileri incelendi. Farklı matematiksel modeller, tahindeki yapısal yıkımın tanımlanması için kullanıldı. Denge değerine sahip birinci mertebe gerilim azalma modeli, en başarılı model olarak belirlendi.

**Anahtar Kelimeler:** Susam, Tahin, Kavurma, Nem soğurma, Reoloji

## ACKNOWLEDGEMENTS

I wish to express my gratitude to my supervisor Dr. Sevim Kaya for her encouragement and invaluable suggestions throughout this study. I am grateful for her support, guidance and motivation.

I would like to thank specially to my committee members, Dr. Medeni Maskan and Dr. Sadettin Kapucu for their enlightening suggestions throughout study.

Thanks to Mr. Süleyman Buzcu, owner of Özen Food, for providing opportunity to me study in his sesame paste factory also for sharing his invaluable practical knowledge about sesame and it's processing with me.

I also would like to thank Dr. Ahmet Kaya for his interest and helps.

I would like to thank to our students, Ferdi Sümbül, Hamdi Aydın, and Fatih Balcı, for their efforts and helps.

I wish to extend my thanks to Dr. Hüseyin Bozkurt, Dr. Mustafa Bayram, Aylin Altan, Sibel Yağcı and my roommate, Ozan Nazım Çiftçi for their assistance, useful discussions, listening and many encouraged words.

I wish to thank each member of my pretty family for their endless support.

## CONTENTS

ABSTRACT.....	ii
ÖZET.....	iii
ACKNOWLEDGEMENTS.....	iv
CONTENTS.....	v
LIST OF FIGURES.....	viii
LIST OF TABLES.....	xii
NOMENCLATURE.....	xiv
CHAPTER 1 GENERAL INTRODUCTION.....	1
CHAPTER 2 ABOUT SESAME AND ITS PRODUCTS.....	4
2.1 Botany of Sesame.....	4
2.2 Composition and Nutritional Chemistry of Sesame.....	7
2.3 Use of Sesame in Food Industry.....	12
2.4 Sesame Market Worldwide.....	15
CHAPTER 3 MODELING AND OPTIMIZATION OF VARIOUS ROASTING PROCESS OF SESAME SEEDS.....	19
3.1 Sesame Roasting.....	19
3.2 Mathematical Models and Kinetic Analysis of Changes during Roasting.....	21
3.3 Response Surface Methods (RSM) and Process Optimization.....	23
3.4. Materials and Methods.....	26
3.4.1 Conventional roasting (CR).....	26
3.4.2 Hot air roasting (HAR).....	26
3.4.3 Electric oven roasting (EOR).....	28
3.4.4 Vacuum oven roasting (VOR).....	28
3.4.5 Chemical analysis.....	29
3.4.6 Color measurements.....	30
3.4.7 Texture measurements.....	30

3.4.8 Statistical analysis and modeling.....	31
3.5 Results and Discussion.....	31
3.5.1 Conventional roasting (CR).....	32
3.5.2 Hot air roasting (HAR).....	46
3.5.3 Electric oven roasting (EOR).....	53
3.5.4 Vacuum Oven Roasting (VOR).....	60
3.6 Conclusions.....	66
CHAPTER 4 INFLUENCE OF DEHULLING AND ROASTING PROCESS ON THE THERMODYNAMICS OF MOISTURE ADSORPTION IN SESAME SEED.....	69
4.1 Introduction.....	69
4.2 Isotherm Models.....	70
4.3 Net Isotheric Heat of Adsorption.....	71
4.4 Differential Entropy.....	72
4.5 Spreading Pressure.....	72
4.6 Net integral enthalpy and entropy.....	73
4.7 Materials and Methods.....	74
4.7.1 Preparation of the sesame seed samples.....	74
4.7.2 Moisture sorption measurements.....	74
4.8 Results and Discussion.....	75
4.8.1 Adsorption isotherms.....	75
4.8.2 Isotherm equations.....	77
4.8.3 Net isotheric heat of adsorption.....	79
4.8.4 Differential entropy.....	80
4.8.5 Spreading pressure.....	80
4.8.6 Net integral enthalpy and entropy.....	82
4.9 Conclusions.....	84
CHAPTER 5 STEADY AND OSCILLATORY FLOW PROPERTIES OF SESAME PASTE WITH DIFFERENT GUMS.....	86
5.1. Introduction.....	86
5.2 Food Rheology.....	87
5.3 Basic rheology and its terms.....	88
5.3.1 Thixotropy.....	91
5.3.1.1 Mathematical theories for thixotropy .....	93
5.3.2 Dynamic Rheological Methods.....	94
5.4 Use of gums in improving food texture.....	96

5.5 Materials and Methods.....	98
5.5.1 Preparation of gum and paste mixture.....	98
5.5.2 Rheological measurements.....	99
5.5.3 Hysteresis loop.....	99
5.5.4 Shear stress decay with recovery test.....	99
5.5.5 Frequency sweep tests.....	100
5.5.6 Temperature sweep tests.....	100
5.6 Results and Discussions.....	100
5.6.1 Steady-shear flow measurements.....	100
5.6.1.1 Flow curve tests.....	100
5.6.1.2 Shear stress decay test.....	105
5.6.2 Dynamic small oscillatory tests.....	110
5.6.2.1 Frequency sweep tests.....	110
5.6.2.2 Temperature sweep tests.....	112
5.7 Conclusions.....	115
CHAPTER 6 CONCLUSIONS.....	116
6.1 Further Recommendations.....	116
REFERENCES.....	118
APPENDICES.....	125
CURRICULUM VITAE.....	133



## LIST OF FIGURES

Figure 2.1	Sesame plant.....	5
Figure 2.2	Sesame seed capsules.....	6
Figure 3.1	Experimental hot air roaster: A, motor to rotate the product basket; B, product basket; C, heat gun; D temperature measurements points.....	27
Figure 3.3	Moisture content changes of sesame seed conventionally roasted at different temperatures. Symbols show the actual data points. Mesh lines represent the fitted line by Eq. (3.19) (A), and Eq. (3.20) (B).....	35
Figure 3.4	Changes in the color parameters of sesame seeds during roasting at different temperatures studied (120, 150 and 180°C) for 120 minutes.....	36
Figure 3.5	Changes in the L-values of sesame seed conventionally roasted at different temperatures studied. Symbols show the actual data points. Mesh lines represent the fitted line by Eq. (3.21).....	41
Figure 3.6	Changes in the a-values of sesame seed conventionally roasted at different temperatures studied. Symbols show the actual data points. Mesh lines represent the fitted line by Eq. (3.21).....	42
Figure 3.7	Changes in the b-values of sesame seed that conventionally roasted at different temperatures studied. Symbols show the actual data points. Mesh lines represent the fitted line by Eq. (3.21).....	42
Figure 3.8	Effect of roasting temperature and time on the hardness of sesame seeds.....	43
Figure 3.9	Effect of roasting temperature and time on the fracturability of sesame seeds.....	44
Figure 3.10	Response surface for color whiteness (L-value) of sesame seeds roasted in a hot air roaster.....	48
Figure 3.11	Response surface for redness (a-value) of sesame seeds roasted in a hot air roaster.....	49
Figure 3.12	Response surface for yellowness (b-value) of sesame seeds roasted in a hot air roaster.....	49
Figure 3.13	Response surface for browning index (BI) of sesame seeds roasted in a hot air roaster.....	50

Figure 3.14	Response surface for textural parameters of sesame seeds roasted in a hot air roaster	51
Figure 3.15	Desirability function response surface for the sesame seeds roasted in a hot air roaster.....	53
Figure 3.16	Response surface plots for L-value of sesame seeds that roasted in an electrical oven.....	55
Figure 3.17	Response surface plots for a-value of sesame seeds that roasted in an electrical oven.....	56
Figure 3.18	Response surface plots for b-value of sesame seeds that roasted in an electrical oven.....	56
Figure 3.19	Response surface for browning index (BI) of sesame seeds roasted in an electrical oven.....	57
Figure 3.20	Response surface plots for hardness of sesame seeds that roasted in an electrical oven.....	58
Figure 3.21	Response surface plots for fracturability of sesame seeds that roasted in an electrical oven.....	59
Figure 3.22	Response surface plots for moisture content of sesame seeds that roasted in an electrical oven.....	59
Figure 3.23	Desirability function response surface plot for the sesame seeds that roasted in an electrical oven.....	60
Figure 3.24	Response surface plots for L-value of sesame seeds that roasted in a vacuum oven.....	62
Figure 3.25	Response surface plots for a-value of sesame seeds that roasted in a vacuum oven.....	62
Figure 3.26	Response surface plots for b-value of sesame seeds that roasted in a vacuum oven.....	63
Figure 3.27	Response surface plots for BI-value of sesame seeds that roasted in vacuum oven.....	63
Figure 3.28	Response surface plots for hardness of sesame seeds that roasted in a vacuum oven.....	64
Figure 3.29	Response surface plots for fracturability of sesame seeds that roasted in a vacuum oven.....	65
Figure 3.30	Response surface plots for moisture content of sesame seeds that roasted in a vacuum oven	65
Figure 3.31	Desirability function response surface plot for the sesame seeds that roasted in vacuum oven.....	66
Figure 4.1	Sorption isotherms of whole sesame seed (WS), dehulled sesame seed (DS), and dehulled-roasted sesame seed (DRS) at different temperatures studied.....	76
Figure 4.2	Application of GAB and Halsey models to adsorption data of dehulled sesame seed at all temperature range studied.....	78

Figure 4.3	Net isosteric heat values of sesame seed samples (WS: whole sesame seed, DS: dehulled sesame seed, and DRS: dehulled-roasted sesame seed) as a function of equilibrium moisture content.....	79
Figure 4.4	Differential entropy of sesame seed sesame seed samples (WS: whole sesame seed, RS: dehulled sesame seed, and DRS: dehulled-roasted sesame seed) as a function of equilibrium moisture content.....	81
Figure 4.5	Spreading pressure adsorption isotherms for whole sesame seed (WS), dehulled sesame seed (DS), and dehulled-roasted sesame seed (DRS) at different temperatures studied.....	81
Figure 4.6	Net integral enthalpy values of sesame seed samples (WS: whole sesame seed, DS: dehulled sesame seed, and DRS: dehulled-roasted sesame seed) as a function of equilibrium moisture content.....	83
Figure 4.7	Net integral entropy values of sesame seed samples (WS: whole sesame seed, DS: dehulled sesame seed, and DRS: dehulled-roasted sesame seed) as a function of equilibrium moisture content.....	84
Figure 5.1	Basic shear diagram of shear rate versus shear stress for classification of time independent flow behavior of fluid foods: Newtonian (N), Pseudoplastic (P), Bingham (B), and Dilatant (D).....	89
Figure 5.2	Time-dependent flow behaviors of fluids.....	92
Figure 5.3	Flow curves of pure sesame paste (control) and paste containing guar gum 1% (wt) (GG1) or 5% (wt) (GG5) at 5° and 25°C.....	101
Figure 5.4	Apparent viscosity versus shear rate for pure sesame paste (control) and paste containing guar gum 1% (wt) (GG1) or 5% (wt) (GG5) at 5° and 25°C.....	101
Figure 5.5	Flow curves of pure sesame paste (control) and sesame paste/xanthan gum mixture.....	104
Figure 5.6	Effect of locust bean gum concentration on the thixotropic behavior of the sesame paste.....	106
Figure 5.7	Effect of temperature on the thixotropic behavior of the sesame paste/guar gum mixture.....	107
Figure 5.8	Storage modulus ( $G'$ : solid line) and loss modulus ( $G''$ : dotted line) of the pure sesame paste.....	111
Figure 5.9	Storage modulus ( $G'$ : solid line) and loss modulus ( $G''$ : dotted line) of the sesame paste/locust bean gum mixture (1% wt).....	112
Figure 5.10	Phase angle values of sesame paste/gum mixtures (GG5, XG5, KG5 and LBG5 contains 5% wt of guar gum, xanthan gum, kappa-carrageen gum, and locust bean gum respectively).....	112

Figure 5.11	Temperature dependency of phase angle of pure sesame paste (control), sesame paste/locust bean gum mixtures (LBG1 and LBG5 contains 1 and 5% wt of locust bean gum respectively).....	113
Figure 5.12	Temperature dependency of phase angle of pure sesame paste (control), sesame paste/gum mixtures (GG1, KG1 and LBG1 contains 1%wt of guar gum, kappa-carrageen gum and locust bean gum respectively).....	114
Figure 5.13	Temperature dependency of phase angle of pure sesame paste (control), sesame paste/gum mixtures (XG5, KG5 and LBG5 contains 5%wt of xanthan gum, kappa-carrageen gum and locust bean gum respectively).....	114
Figure A.1	Hot air roasting system.....	126

## LIST OF TABLES

Table 2.1	Composition of whole and dried sesame seeds (USDA, 2004).....	7
Table 2.2	Fatty acid composition of sesame oil (g / 100g).....	9
Table 2.3	Amino acid composition of sesame (mg/g protein)* .....	11
Table 2.4	Sesame food uses.....	12
Table 2.5	Sesame seed world production (FAO, 2004).....	17
Table 2.6	Trade of sesame around the world (FAO, 2004).....	18
Table 3.1	Coded and actual variables for the experimental design for the optimization of the roasting process of sesame seed accomplished in the hot air roaster.....	28
Table 3.2	Coded and actual variables for the experimental design for the optimization of the roasting process of sesame seed that accomplished in electrical oven.....	29
Table 3.3	Coded and actual variables for the experimental design for the optimization of the roasting process of sesame seed that accomplished in vacuum oven.....	29
Table 3.4	Physical and compositional properties of sesame seeds under study.....	32
Table 3.5	Two-parameter exponential and Page models parameters and fitting criteria for moisture loss of sesame seeds during roasting...	34
Table 3.6	Parameters and fitting criteria of zero-, first-order, quadratic and cubic models for the color values of sesame seed during conventional roasting operation.....	39
Table 3.7	Parameters and fitting criteria of zero- and first-order kinetics for modeling of L-value in the lightening period of roasting of sesame seed.....	40
Table 3.8	Constants and fitting criteria obtained from generalized model (Eq. (3.21)) for color parameters of sesame seed during conventional roasting operation.....	40
Table 3.9	Parameters and fitting criteria of zero-, first-order, quadratic and cubic models for the textural change of sesame seed during conventional roasting operation.....	45
Table 3.10	Regression equation coefficients for response parameters of sesame seed roasted in the hot air in terms of coded terms <sup>a</sup> .....	47
Table 3.11	Regression equation coefficients for response parameters of sesame seed that roasted in an electrical oven in terms of coded terms <sup>a</sup> .....	54

Table 3.12	Regression equation coefficients for response parameters of sesame seed that roasted in the vacuum oven in terms of coded terms <sup>a</sup> .....	61
Table 4.1	Estimated parameters and criteria of GAB model for the sesame seed samples.....	77
Table 4.2	Estimated parameters and criteria of Halsey model for the sesame seed samples.....	78
Table 5.1	Material functions used to describe viscoelastic behavior.....	95
Table 5.2	Source, function and main applications of some types of gums (Williams and Philips, 2003).....	97
Table 5.3	Coefficients of power law-model for forward measurements of sesame paste/ gum mixtures at studied temperatures (5 and 25°C)	103
Table 5.4	Thixotropic and relative thixotropic area values of sesame paste/gum mixtures at 5 and 25°C.....	105
Table 5.5	Viscosity ratio and structural breakdown rate constant for second order kinetic model for the sesame pastes with varying gums.....	107
Table 5.6	Weltman model parameters for the sesame pastes with varying gums .....	108
Table 5.7	Coefficients of first-order stress decay with zero-equilibrium stress value, for a shearing time of 1200 s for the sesame pastes with varying gums.....	109
Table 5.8	Parameters of the first-order stress decay model with non-zero equilibrium for the sesame pastes with varying gums.....	110
Table 5.9	Thixotropic and relative thixotropic areas of the sesame paste/gum mixtures after shearing 1200 s for 200 s <sup>-1</sup> .....	110
Table A.1	Experimental data for response parameters of sesame seeds roasted in the hot air roaster.....	127
Table A.2	ANOVA and model fitting for response parameters of roasted sesame seeds in the hot air roaster.....	128
Table A.3	Experimental data for response parameters of sesame seeds that roasted in the electrical oven.....	129
Table A.4	ANOVA and model fitting for response parameters of roasted sesame seeds in the electrical oven.....	130
Table A.5	Experimental data for response parameters of sesame seeds that roasted in the vacuum oven.....	131
Table A.6	ANOVA and model fitting for response parameters of roasted sesame seeds in the vacuum oven.....	132

## NOMENCLATURE

$a_w^*$	geometric mean water activity
$\lambda$	latent heat of vaporization of pure water (kJ/kg)
a, b, r, C, k	sorption isotherm constants
$A_m$	surface area of a water molecule in $m^2$ ( $1.06 \times 10^{-19} m^2$ )
$a_w$	water activity
BI	browning index
E	mean relative deviation
i	number of terms
K	Boltzman's constant ( $1.380 \times 10^{-23} J/K$ )
k	reaction rate constant, $k^{-n}$
$k_{ref}$	frequency factor
L-, a-, and b-values	color dimensions
m	moisture content of samples, % dry basis
$m_e$	equilibrium moisture content
$M_i$	moisture content (experimental value), % dry basis
$m_o$	monolayer moisture content, % dry basis
$M_{pi}$	moisture content (predicted value), % dry basis
MR	moisture ratio
n	Page model parameter, number of experimental data
$Q_{in}$	net integral enthalpy (kJ/kg)
$Q_{st}$	isosteric heat of adsorption (kJ/kg)

$q_{st}$	net isosteric heat of adsorption (kJ/kg)
$R$	universal gas constant (8.314 J/mol K)
$r^2$	coefficient of determination
$S_d$	differential entropy (J/g K)
SEE	standard error of estimate
$S_{in}$	net integral entropy (J/g K)
$T$	temperature (K)
$t$	time (min)
$\Phi$	spreading pressure (J/m)



## CHAPTER 1

### GENERAL INTRODUCTION

Sesame (*Sesamum indicum* L., Pedaliaceae) is a unique food (Namiki, 1995). It has been used extensively for thousands of years as a seed of worldwide significance for edible oil, paste, cake, confectionary purposes, and flour. It is considered to be one of the first recorded plants for its seed and thought to have originated in Africa or India.

There are various rumors about origin of sesame and its usage. Early Assyrians believed that their gods drank sesame wine as a prelude to creating the world. A drawing on an Egyptian tomb of 4,000 years ago depicts a baker adding sesame seeds to dough. Around the same time, the Chinese were burning sesame oil to make soot for ink. Ancient Greek soldiers carried sesame seeds as energy boosting emergency rations and the Romans made a kind of hummus from sesame and cumin. Sesame also has been considered a symbol of good luck and signifies immortality to Brahmins. The English term sesame traces back to the Arabic *simsim*, Coptic *semsem*, and early Egyptian *semsent*.

The extensive usage of sesame may be due to its highly stable oil content, nutritious protein, and savory nutty roasted flavor. It is also considered as a food beneficial to health in oriental countries. Many scientific studies have been conducted to investigate the health-promoting effects of sesame (Shyu and Hwang, 2002).

Sesame seeds are consumed in various forms. Whole sesame seeds are generally used for oil production and some types of bakery foods. Dehulled seeds also have been consumed in baked goods such as breads, hamburger buns, cakes, cookies, confections and snack foods. In many countries (Middle-East, Mediterranean and

Oriental) dehulled roasted sesame seeds are used for producing sesame paste (called tahin, tehina, tehineh, tahina or matahina) (El-Adawy and Mansour, 2000; Lokumcu and Ak, 2005).

Global production of sesame seed is estimated by FAO at 3.25 million tones in 2004 having risen from 1.4 million tones in the early 1960's. The increased consumer concern for healthy eating, and the beneficial image of sesame in this sector, is held to be responsible for this development in the market.

Since global competition, regulation, and consumer demands are ever increasing in the food industry, manufacturers to meet consumer expectations should produce high quality foods. To achieve this aim, understanding the phenomena that occur during processing, the design of unit operation and the control of them are necessary and all of them are the main inherent objectives of food engineering. Throughout the world, sesame is mostly utilized as a whole seed in condiments or as additives on breads, biscuits and other cereal products. The seed has fairly hard coat and is not easily digested and is therefore undesirable for general consumption. For sesame to be more digestible, it should be used as ground sesame or a paste (tahin). For more popular use of the sesame, research in food science and technology should be initiated to improve its flavor and texture (Namiki, 1995). Therefore in this dissertation, two main subjects are considered to improve the quality of sesame's products; roasting of sesame and rheology of sesame paste.

Roasting is the main unit operation for sesame's products particularly sesame paste and sesame oil production. Therefore uniform and controlled roasting is required to produce sesame's products at good quality. Sesame paste producers have considered the determination of optimum conditions for roasting as one of their main problems. Thus one of the main objectives of this study was to characterize and model the physical changes in sesame by different roasting methods. The ultimate aim was to ascertain, for each roasting method, which parameters and models could be used to establish optimum roasting time and temperature to produce optimally roasted sesame. Chapter 3 is related with the development of mathematical models and optimization procedures for various roasting methods of sesame seeds.

Chapter 4 covers the study about the effects of roasting and dehulling process on the moisture adsorption isotherms and thermodynamic properties of sesame seed. The application of thermodynamic principles to sorption isotherm data has been used to obtain more information about the properties of water, food microstructure, and physical phenomena on the food surfaces, and sorption kinetic parameters. For these reasons the effective design of roasting, drying and storage systems for both three forms of sesame seeds (whole, dehulled and dehulled-roasted) needs knowledge of their energy requirements and the state and model of the moisture sorption with them (Aviara and Ajibola, 2002).

Sesame paste is one of the concentrated colloidal suspension basically contains protein and oil. The better and wider understanding of the rheology of sesame paste is important for its processing and new product formulation. Sesame paste is used as an ingredient for helva (sweetened sesame paste with saponin extract) and many local sauces. Besides, there has been great interest in the production of sesame seed containing commercial creamy product. In order to achieve that goal, gums are used widely as thickening and gelling agents. Because of the difference in gum structure and extrinsic condition with fluid food system the rheological particularly thixotropic behavior is quite different and complex, and varies from one gum to other. The important parameter is related with thixotropy is spreadability because a food product should gain its viscosity to prevent drainage after spreading and this affects directly the consumer acceptance. Therefore a good understanding behavior of thixotropic and shear-thinning behavior of sesame paste/gum mixture is useful for food manufacture. In Chapter 5, the detailed study on the rheological behavior of sesame paste with various gums, are described.

## CHAPTER 2

### ABOUT SESAME AND ITS PRODUCTS

In the following sections, the current knowledge about sesame's botany and chemistry, its uses in food industry and its market conditions, are given.

#### 2.1 Botany of Sesame

Sesame belongs to the *Sesamum* genus, one of the 16 genres of the family Pedaliaceae. *Sesamum* has 36 species, most of which are wild, distributed mainly in African savanna, India, the East Indies, Mexico and Australia (Namiki, 1995; Morris, 2002). A cultivated species, *Sesamum indicum* L., is the major commercial source of sesame. The use of sesame is as old as the use of wheat or rice, based on Egyptian records, which date back 6000 years. Based on the archeological findings, two possible routes for the spread of sesame from central Africa, believed that the actual origin was in Sudan, are considered. One route was eastward over the ocean to India, to central Asia, then to China and Japan, to Southeast Asia islands and to Australia. The other route was northward to Egypt, and through the Mediterranean countries, then to Arabia, central Asia, China, and finally Europe.

Sesame is an erect annual plant that can reach 100-120 cm in height when the plant early under the high moisture conditions. Sesame is a broadleaf summer crop that has bell-shaped flowers and opposite leaves (Figure 2.1). The tubular, two-lipped flower is about 4-5 cm long with a pink or white corolla. One to three attractive flowers, which later develop into the seed pods (capsules), are borne in each axil. Flowers appear about 30-45 days after planting with 2 flowers per stem per day for about 35-40 days. Some varieties have 6 flowers per stem per day for 25-40 days.

The upright capsules split open at top. The suture splits, and the seeds are forcibly ejected. The Arabic incantation (magic word) “open sesame” is said to have originated from the movement of the opening of the sesame capsules. There are approximately 50 to 80 seeds per capsule (Figure 2.2). The seeds vary considerably in color size, and the texture of the seed coat. The color differs from white through various shades of brown, gold, gray, via lot and black. The seed coat may be either rough or smooth. Black sesame commonly has a thick seed coat. The seeds are tiny and weigh 2-3.5 g/1000 seeds (Namiki, 1995).



Figure 2.1 Sesame plant

Sesame flourished originally from tropic African savanna plains, but now it is cultivated worldwide, in tropical and sub tropical region between the north and south parallels of about 45°. It is scarcely cultivated in the USA or Europe, not only because of climate but also because of the low returns per unit area. Sesame is adapted to fertile, well-drained soils and is not salt tolerant. Cultivation requires a frost-free growing period. Growth and fruiting are favorable as the average temperature is around 25°C. Sesame varieties grown commercially require 90 to 110 days from planting to reach physiological maturity. A good rule of thumb is not to plant until at least a month after the last killing frost in the spring. The plant is one of the most drought tolerant crops in the world and can grow in areas where there is sufficient rainfall to grow dry land sorghum and cotton.

It is important that crop should be dry before harvesting. Dry down of sesame plants prior to harvest can seem slow relative to a crop like soybeans. When planted in early June, sesame will normally drop its leaves and begin drying down in early October, but it can take a while for the last of the green to disappear from the stem and upper seed capsules. To deal with the indeterminate nature of the crop, some farmers have windrowed it. Harvest should be done before frost if at all possible, because frost can damage the appearance of the seed (important for whole seed confectionery use) and sometimes the quality of the seed.

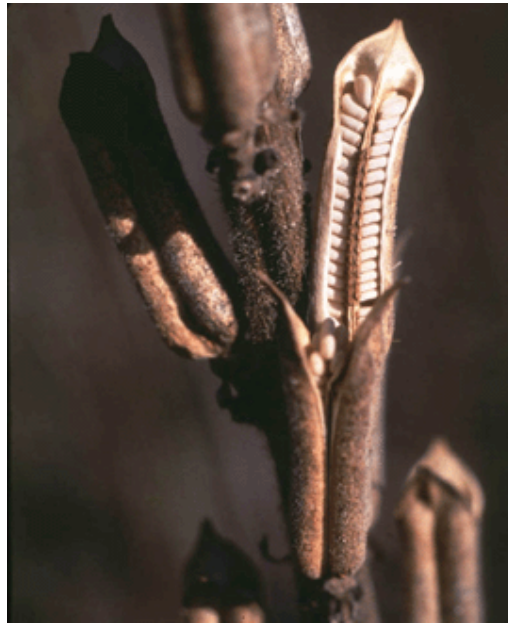


Figure 2.2 Sesame seed capsules

Since sesame is a small flat seed, it is difficult to move much air through it in a storage bin. Therefore, it is recommended that the seed should be harvested as dry as possible, and stored at moisture of 6% or less. If the seed is too moist, it can quickly heat up and become rancid. Freshly harvested seed above 6% should not be left sitting on a truck for long to avoid spoilage. Idle trucks with sesame on board should generally not be trapped on a sunny day, since the trap can increase heat build up. Sesame grain is sold on a weight basis rather than a bushel basis.

Seed yields range from 2350 to 1700 kg/ha depending on the varieties used cultivation techniques. According to FAO records, the average yield is 488 kg/ha in 2004. This is considerably lower than for other oilseeds, such as soybean (2200

kg/ha) and sunflower seed (1200 kg/ha). Improved varieties, better cultivation techniques, and the development of machine harvesting are necessary to increase the yield and production of sesame.

## 2.2 Composition and Nutritional Chemistry of Sesame

The composition of sesame seeds varies considerably, depending on the varieties, in size, color and coat thickness. They differ in major and minor components. Sesame seeds mainly composed of oil, protein and carbohydrate. The average composition of whole and dried sesame seeds is given in Table 2.1 (USDA, 2004).

Sesame is a high-energy food containing approximately 50% oil, and the cells of the cotyledon and the residual endosperm are filled with oil droplets. The oil content of sesame seeds varies widely from 24 to 64% according to their species and cultivation conditions (Namiki, 1995). Ozcan (1993) reported that the oil content of Turkish variety sesame seeds changes between 52 to 61 %. Namiki (1995) also found that the oil contents varied inversely with the percentage of the hull, the average oil content for the white-seeded strains was 55%; and for the black-seeded strains, 47.8%, as the hulls of the black seeded strains were thicker than white ones.

Table 2.1 Composition of whole and dried sesame seeds (USDA, 2004)

<b>Nutrient</b>	<b>Value per 100 g<sup>*</sup></b>
Moisture	4.69 g
Energy	573 kcal
Protein	17.73 g
Total lipid (fat)	49.67 g
Ash	4.45 g
Carbohydrate, by difference	23.45 g
Fiber, total dietary	11.8 g
Sugars, total	0.30 g
<b>Vitamins</b>	
Thiamin	0.791 mg
Riboflavin	0.247 mg

**Table 2.1/cont.**

Niacin	4.515 mg
Vitamin B-6	0.790 mg
Folate, total	97 mcg
Vitamin E (alpha-tocopherol)	0.25 mg
<b>Minerals</b>	
Calcium, Ca	975 mg
Iron, Fe	14.55 mg
Magnesium, Mg	351 mg
Phosphorus, P	629 mg
Potassium, K	468 mg
Sodium, Na	11 mg
Zinc, Zn	7.75 mg
Copper, Cu	4.082 mg
Manganese, Mn	2.460 mg
Selenium, Se	5.7 mcg

Sesame oil contains mainly oleic and linoleic acids, with small amounts of palmitic and stearic acids but with only trace amounts of linolenic acid. The fatty acid composition of sesame oil is given in Table 2.2. It has been known for many years that sesame oil is highly resistant to oxidative deteriorations as compared to other edible oils (Budowski, 1962). The remarkable stability of sesame oil is due to the presence of unique unsaponifiable constituents namely lignans and tocopherols.

Lignans, low molecular weight compounds produced by oxidative coupling of *p*-hydroxyphenylpropane, are in minor amount but very important functional components of sesame. The main sesame lignans are sesamin and sesamol. Sesamin has been found in other plants also, but sesamol seems to be characteristics of sesame. Although they possess no antioxidant activity (Kamal-Eldin and Appelqvist, 1994), during roasting sesamol is transformed to sesamol dimmers, while it is transformed to sesamol and sesaminol during chemical refining and bleaching (Nagata et al. 1997). These components are believed



to play important role in oxidative stability of sesame oil. These compounds possess strong antioxidant activity and may have the potential of inhibiting the process of aging in man and in biological systems.

Table 2.2 Fatty acid composition of sesame oil (g / 100g)

<b>Fatty acids,</b>	<b>A</b>	<b>B</b>	<b>C</b>
<b>Total saturated</b>	15.2	10.62	13.3
12:0 - Lauric	0.29	-	-
14:0 - Myristic	0.14	-	0.2
16:0 - Palmitic	9.4	9.87	8.3
18:0 - Stearic	4.76	Trace amount	3.9
20:0 - Arachidic	0.58	0.75	0.9
<b>Total monounsaturated</b>	39.99	41.86	35.9
16:1 - Palmiloteic	0.30	-	0.3
18:1 - Oleic	39.1	41.86	35.6
20:1 - Gadoleic	0.21	-	-
22:1 - Erucic	0.38	-	-
<b>Total polyunsaturated</b>	40.46	48.3	51.2
18:2 - Linoleic	40.0	47.63	51.0
18:3 - Linolenic	0.46	0.67	0.2

A: Namiki (1995); B: Ozcan and Akgül, (1994); C: Yoshida and Takagi (1997)

The other main component of sesame is protein. This protein is nutritionally valuable because it is rich in methionine and other essential amino acids (Table 2.3). It is one of the main sources of cheap protein yielding 20–25% total dry mass depending on the variety (Elezar et al. 2003). Sesame protein is slightly lower in lysine but richer in other amino acids when compared with soybean and FAO standards. However, it contains more sulphur containing amino acids (methionine and cystine) than soybean. Thus sesame is mixed with soybean in oriental countries, and also mixed with cooked chickpeas “hommes”, very popular dishes, in the Middle East, to complete amino acid profile of those products.

Most developing countries of the world today face the problem of inadequate protein intake by a large section of their population (Egbekun and Ehieze, 1997). The utilization of plant protein from legumes and oilseeds would provide an economical and readily available source of protein because the average protein intake is less than desirable. In fact, some attempts have been made to use it as a source of protein for human consumption. Defatted sesame seed has been used as part replacement to study the effect of sesame seed flour on millet biscuit characteristics (Alobo, 2001) and to analyze the nutritional value of table bread fortified with defatted soybean and sesame meals amongst other uses. El-Adawy (1997) reported that addition of sesame products to wheat flour improved the nutritional value of product by the computation of essential amino acid index, protein efficiency ratio and chemical score of breads.

Carbohydrate content of sesame is about 18-20%. The presence of low amounts of glucose and fructose has been reported (El Adawy and Mansour, 2002). However no starch is present. Sesame seed is rich in mineral constituents, as shown in Table 2.1. It is especially rich in calcium (120 mg/100g) and iron (9.6 mg/100 g) as well as phosphorus, potassium, magnesium, zinc, and selenium. Calcium and iron, which are often deficient in modern diets, are found in high concentration in sesame.

Sesame has long been regarded as healthy food, which provides energy and prevents aging therefore much attention should be focused to examine the minor constituents of sesame that have health-promoting effect on human beings.

Table 2.3 Amino acid composition of sesame (mg/g protein)\*

Amino acids	Sesame	Soybean	Recommended daily intake**	
			Child	Adult
Tryptophan	18	14	4	3.5
Threonine	39	41	35	7
Isoleucine	42	51	30	10
Leucine	75	82	45	14
Lysine	31	68	60	12
Methionine	36	16		
Cystine	25	17		
Phenylalanine	51	58		
Tyrosine	39	37		
Valine	54	52	33	10
Arginine	140	81		
Histidine	29	30		
Alanine	51	46		
Aspartic acid	91	120		
Glutamic acid	200	190		
Glycine	55	46		
Proline	42	57		
Serine	47	50		
Met + Cys	61	33	27	13
Phe + Tyr	90	95	27	14

\*Namiki (1995); \*\*FAO reference

### 2.3 Use of Sesame in Food Industry

Sesame is used in food industry mainly in three basic forms. These are its seeds, paste and edible oil (Table 2.4).

Table 2.4 Sesame food uses

Form	Products	Description uses
Seeds	Confectionery	Fried seeds may be bound together with sugar syrup to give sweetmeats.
Seeds	Biscuits	The whole seeds can be baked into biscuits.
Seeds (dehulled)	Bakery	Popular in Northern Europe either incorporated into breads or as decorative toppings. May be used as dehulled or whole seed.
Seeds (roasted or unroasted)	Oil	Particularly used in oriental cuisine. The flavor is quite strong and rarely compatible with traditional Western style cooking but also used as a salad oil.
Oil	Margarine	Once an important use, now other cheaper vegetable oils are available.
Dehulled seeds	Sesame paste	Used as an ingredient in Eastern Mediterranean and Middle Eastern foods.
Paste	Dips & spreads	Various ingredients, such as chickpeas or eggplants, are added to paste to make dips and spreads such as hummus.
Paste	Helva	A sweet made from sesame paste and sugar with other added flavorings
Cake	Animal feed	Protein rich useful supplement.
Cake from dehulled seeds	Ingredient	Used in some Indian cooking. Also as a snack.

Sesame is widely used as an ingredient in baked goods and confectionary products (Namiki, 1995). Dehulled sesame seeds undergo a special hulling process that produces a clear white seed. These seeds are then double washed, dried, and used on hamburger buns. This special process allows the seed to stick to the bun while maintaining a white color after baking. About one-third of the imported crop from Mexico is purchased by McDonalds for their sesame seed buns (The Nut Factory, 1999). The seeds are also used on bread and then eaten in many countries. Sesame

seed has a nutty taste when the seed is roasted. Bread, breadsticks, cookies, chocolate, and ice cream are ideal products for roasted natural sesame seed. In Mediterranean countries, seeds are used in cakes, while in Togo; Africa seeds are a main soup ingredient. Sesame flour is an edible, creamy and light brown powder from sesame seeds.

Tahin is sesame paste and named in different region as tehineh, tahini, benne, simsim, gingelly and tehina. It is used as a local food in the Middle East, China and Mediterranean countries. Sesame paste is manufactured using only the selected sesame seeds and seeds dehulled, roasted and ground into wholesome paste. Sesame paste is used as a main raw material in helva and consumed as mixture with pekmez, honey and some local foods in Turkey (Özcan and Akgül, 1994). The popularity of sesame paste among the people of Middle East is evidenced by its use in several popular foods in the region. It is usually mixed with cooked chickpeas and the product is called “Humus tehineh” or mixed with eggplants to obtain “Baba ganouj” which are very popular dishes in Middle Eastern areas, and also mixed with legumes and fresh green vegetables in a salad form. Sesame paste is also added to some types of bread and used as a sauce for fish and meat and is a major constituent of helva (~50%) and other sweets, pastries and snack foods (Sawaya, 1985). Sesame paste is known to be rich in protein and one of the best energy sources for human life. Sesame paste is of a high nutritive value; for it is rich in lipids (57-65 wt %); proteins (23-27 wt %); carbohydrate (6.4-9 wt %), niacin (4.5 mg/100 mg), thiamin (1.08 mg/100 g) and some minerals such as calcium (100 mg/100g), phosphorus (807-840 mg/100 mg), and iron (9 mg/100g) (Abu-Jdayil and Al-Malah, 2002). It is easily digestible because its high alkaline mineral content neutralizes the acid end products of the protein. Because of its non-acid nature, sesame paste is an ideal protein source for people with weak digestive systems, invalids and young children, and can be used as a source of quick energy for active people and athletes. Interest in sesame paste was sparked by an interesting discovery. During both World War II and the Korean War, Turkish aviators became well known for their physical and mental endurance. Upon investigation, it was discovered that sesame paste was an important part of their daily diet. Since then, growing interest in ethnic foods has introduced many peoples to sesame paste.

The production methods used vary from country to country and also factory to factory; however basic principles for the preparation of sesame paste are the same, the method the old conventional one or the newly automated ones.

Sesame paste production steps are as follows (Ozcan, 1993):

- **Cleaning of seeds:** Organic and inorganic contaminants, foreign particles are separated by sieving (dry cleaning) or using brine solution (wet cleaning)
- **Tempering:** Cleaned seeds are waited in water for 5-15 hours for easy separation of hulls. The tempering time depends on water temperature.
- **Dehulling:** Seeds are dehulled either by passing them through propellers or by steam injection.
- **Separation of hulls:** Dehulled sesame seeds are separated from their hulls by using brine solution.
- **Water separation:** Water on the surface of the seeds are removed by centrifuge or filtered via cloth.
- **Roasting:** Seeds are roasted in conventional roaster, steam boiler or automatic roasting machines (at 100-150°C for 2.5-3 hour). The roasting process gives special flavor to sesame paste. In literature, different roasting temperature and time combinations were reported (Sawaya, 1985).
- **Milling:** Roasted seeds are ground either by stones mills or by high speed automatic mills to a viscous paste.
- **Packaging:** Sesame paste is packed in glass or plastic jars.

Most of the sesame seeds are used for production of oil in Oriental countries. Due to its high oil content, sesame oil could be readily produced by simple, primitive techniques of expressing oil from roasted sesame seeds. Although the conventional process for preparation of sesame oil involves cleaning, roasting, grinding, cooking and pressing, but not refining (Fukuda and Namiki, 1988), currently two different types of sesame oil are produced. One of them is from roasted seeds and the other, cooked with steam. The former is classified according to the roasting temperatures and time (e.g. 140°C-150°C, 160°C-180°C, and about 200°C; from several minutes to 10-30 min.) (Namiki, 1995). The color, flavor intensity and also antioxidant activity of oil depends on the roasting degree.

The latter called as unroasted, raw or salad sesame oil is processed by degumming, alkali washing, water washing, decolorization, and deodorization. The processed oil has a mild odor and a pleasant taste and, as such, is a natural salad oil requiring little or no winterization. It is used as cooking oil, in shortening and margarine, as a soap fat, in pharmaceuticals and as a synergist for insecticides. Roasted and unroasted sesame seed oils are widely used in the Eastern Asian countries, especially in Japan and China. Especially, roasted sesame oil is indispensable in Chinese, Korean, and Japanese cooking because of its flavor. It is used after blending with other cooking oils.

The resultant sesame oils have been known as being resistant to oxidative deterioration (Nagata et al. 1987). Refined sesame oil is fine because of its antioxidant properties allow for greater shelf-life plus improving its flavor and taste. Roasted sesame oil resists rancidity due to the antioxidants formed during seed roasting and particular roasted sesame flavor improves taste of fired products.

Several pharmaceutical uses have been identified from sesame oil and sesame in literature. Sesame oil is a pharmaceutical aid used as a solvent for intramuscular injections and has nutritive, demulcent, and emollient properties (Tyler et al. 1976) and has been used as a laxative. The oil was used during the fourth century by the Chinese as a remedy for toothaches and gum disease (Morris, 2002). Other uses include the treatment of blurred vision, dizziness, and headaches. The Indians have used sesame oil as an antibacterial mouthwash, to relieve anxiety and insomnia. A recent clinical trial proved that sesame oil was significantly more effective for treating nasal mucosa dryness to a dry winter climate than isotonic sodium chloride solution (Morris, 2002). The sesame paste oil is called as “şirik” in Turkish, and it is used also for many pharmaceutical purposes in Turkey. Due to these outstanding characteristics, sesame oil is often considered the “queen” of vegetable oils.

#### **2.4 Sesame Market Worldwide**

Global production of sesame seed is estimated by FAO at 3.25 million in 2004 having risen from 1.4 million tones in the early 1960's (Table 2.5). The largest producers are China and India, each with an annual harvest around 650,000 tones followed by Myanmar (550,000 tones) and Sudan (325,000 tones) (Table 2.5). These figures are only rough estimates of the situation as sesame is a smallholder crop and

much of the harvest is consumed locally, without record of the internal trade and domestic processing.

Global exports of sesame seed are estimated to have reached 799,000 tones in 2003, having risen from 427,000 tones in 1988. The 2003 exports were valued at 541 million dollar. India is now the single largest exporter of sesame seed, with exports of some 189,000 tones, with Sudan in second exporting over 172,000 tones per year. In 1988 China was the principal exporter in the world.

The rise in international trade in sesame seed noted above is also shown in the increased imports. All the major importers show strong increase in consumption over the past 10 years. Japan dominates the purchasing side of the trade for sesame seed, with an annual requirement up to 150,000 tones. Sesame oil, particularly from roasted seed, is an important component of Japanese cooking and traditionally this is the principal use of the seed. However, much of the recent increase seems to have come from expanding demand for sesame in other forms, either whole or processed. The trade estimates that 30% of imports are used in forms other than oil, either as a powder, a paste, a roasted condiment or whole.

The increased consumer concern for healthy eating, and the beneficial image of sesame in this sector, is held to be responsible for this development in the market. Although, Turkey was the one of the main suppliers of sesame seed in fifties (Can, 1964), unfortunately it became the fourth largest importers in 2003. Probably due to the unplanned planting and low efficiency, sesame production gradually decreased during past fifty years. The sesame and sesame products are indispensable for Turkish diet. Thus more detailed plan and working are necessary to enhance sesame production. According to GAP master plan, sesame production is planned as 5% in total products.



Table 2.5 Sesame seed world production (FAO, 2004)

Country	Production (tones)	Country	Production (tones)
Angola	1,700	Kenya	10,000
Bangladesh	50,000	Korea, Republic of	11,977
Benin	15,500	Laos	6,150
Brazil	15,500	Lebanon	250
Burkina Faso	29,000	Mali	7,500
Cambodia	10,500	Mexico	22,593
Cameroon	3,300	Morocco	1,220
Central African Republic	42,800	Mozambique	6,000
Chad	35,000	Myanmar (Burma)	550,000
China	650,620	Nicaragua	5,491
Colombia	2,040	Niger	22,000
Congo, Dem Republic of	4,200	Nigeria	76,000
Congo, Republic of	300	Pakistan	68,000
Côte d'Ivoire	3,000	Paraguay	34,000
Ecuador	25	Saudi Arabia	2,212
Egypt	37,000	Senegal	15,912
El Salvador	1,691	Sierra Leone	1,900
Eritrea	4,965	Sri Lanka	4,000
Ethiopia	61,462	Sudan	325,000
Gambia	2,100	Syrian Arab Republic	4,000
Greece	90	Tajikistan	300
Guatemala	35,049	Tanzania, United Rep of	41,000
Guinea	400	Thailand	40,000
Haiti	3,800	Togo	1,300
Honduras	2,272	Turkey	22,000
India	680,000	Uganda	110,000
Iran, Islamic Rep of	28,000	United States of America	0
Israel	50	Uzbekistan	18,000
Italy	1,700	Venezuela, Bolivar Rep of	20,806
Japan	0	Viet Nam	21,000
Jordan	80	West Bank	0

Table 2.6 Trade of sesame around the world (FAO, 2004)

<b>Exporters</b>	<b>Quantity (tones)</b>	<b>Importers</b>	<b>Quantity (tones)</b>
India	189,000	Japan	149,000
Sudan	172,000	China	98,000
China	104,000	Korea	81,000
Ethiopia	71,000	Turkey	66,000
Burma	41,000	Netherlands	41,000
Netherlands	34,000	Egypt	38,000
Turkey	4,000	USA	37,000

It is expected that, due to the constant increase in fast and convenience foods on one side and the health concerns on the other, the consumption of sesame seed will grow. As long as there are still several advantages of sesame seed and its oil, which have not been fully researched, the growth will be limited. Nevertheless, it is expected that through increased research in the health and medical capacities of sesame seeds, the knowledge and better use of these advantages will increase.

## **CHAPTER 3**

### **MODELING AND OPTIMIZATION OF VARIOUS ROASTING PROCESSES OF SESAME SEEDS**

#### **3.1 Sesame Roasting**

Roasting is the most significant step in coffee, nut and bean processing, that causes important physical, chemical, structural and sensorial changes (Özdemir and Devres, 2000; Pittia et al. 2001; Saklar et al. 2001). It is also the basic unit operation for production of sesame's products. The sesame roasting is carried out for promoting more flavor, desired color and texture changes that ultimately increases the overall palatability. There are many forms of using roasted sesame. Sesame paste (butter) called as tahina, tehneh, tahin are produced by milling of mechanically dehulled roasted sesame. Sesame oil prepared from roasted sesame seeds also has a distinctive flavor and extended shelf-life (Kikugawa et al. 1983). Bread, breadsticks, cookies, crackers, chocolate, and ice cream are the other ideal products for roasted sesame seed.

Roasting of sesame can be accomplished in a number of ways for sesame paste production. Sawaya et al. (1985) reported that sesame seeds were roasted at 90-100°C for a few minutes in electrically heated tunnel for sesame paste production. El-Adawy and Mansour (2000) studied the effect of steam roasting, vacuum roasting, hot plate and hot air roasting methods on the nutritional properties of sesame paste, and they advised hot air roasting at 130°C for 1 h. On the other hand, Özcan and Akgül (1994) reported that sesame should be roasted at 100-150°C for 2.5-3 h for the production of sesame paste. In Turkey, substantial quantities of sesame are processed in rotary drum roasters for use in sesame paste and confectionary products. Since the roasting affects the product quality, the control of roasting process is significant.

The control of roasting in sesame paste production is carried out by experienced operators as many food processing operations. On the other hand, sesame paste producers considered that determination of optimum conditions for roasting of sesame was one of the main problems. Hence, the optimum roasting conditions should be established in order to make good quality of sesame paste.

Color is one of the parameter that used for process control during roasting, because the brown pigments increase as the browning and caramelization reactions progress (Moss and Otten, 1989). Browning of foods may result from both enzymatic and non-enzymatic reactions. Hussain et al. (1986) reported that both non-enzymatic browning and phospholipids degradation were responsible for color formation in sesame oil. The chemistry of browning reactions is complex but the kinetics is an important tool of control model. To optimize and control the process, the determination of kinetic parameters (reaction order, reaction rate constant, activation energy) or modeling of changes are necessary. The non-enzymatic browning reaction in foods is generally first-order or zero-order, and the effect of temperature on non-enzymatic browning reaction is usually shown using Arrhenius-type relationship. The polynomial equations were also used for modeling of color changes; Moss and Otten (1989) used second-degree polynomial in describing L- and a-values of the color in peanut roasting; Ozdemir and Devres (2000a) also used third-degree polynomial for modeling of color changes (L- and a-values) during roasting of hazelnut.

In addition to the color, texture is another important control parameter for sesame roasting. During the roasting, seeds become more crumble and brittle, which are typical characteristics of the roasted products. The reaching of a certain degree of texture is very important for the production of sesame paste. Experienced operators also control the roasting process by eating sesame for production of sesame paste. This type of measurement is called as subjective test. Textural measurements that performed on instruments originally, developed for material science, are considered as objective tests. With the better objective tests, assessment of the textural aspects of foods might be made more quickly, cheaply and sensitively and, since the mechanical parameters can be referred to specific aspects of the shape, chemistry, water content, etc. of the food item, quality control would become more of an

objective science and so rendered much easier (Vincent, 2004). The most commonly used objective texture tests can be categorized into three groups: flexure, shear and compression tests. The latter are probably the most commonly employed because of their similarities with the mastication process. In these tests, the specimen is compressed either between two parallel plates or by a plunger compressing the sample held in a cylinder. Samples can be tested individually or as bulk when contained in a cell (Nixon and Peleg, 1995). Saklar et al. (1999) reported that changes in the texture of hazelnuts due to the roasting are attributed to crispness and crunchiness. Pittia et al. (2001) also concluded that moisture content and roasting process influence the textural properties of coffee beans and high temperature roasting caused fragile and brittle texture.

This part of the study aimed to characterize and modeling the moisture, color and texture changes of sesame during application of different roasting methods. The ultimate aim is to ascertain, for each roasting method, which parameters and models could be used to be able to establish optimum roasting time and temperature to produce optimally roasted sesame. Our objective was firstly to determine the moisture, color and texture changes during conventional roasting of sesame seeds and then to improve the mathematical models for describing the observed changes. Response surface methodology was also used to improve the predictive model for describing the color, texture and moisture changes of sesame seeds during hot air, vacuum and electrical oven roasting and to determine the optimization procedure for the roasting operations.

### **3.2 Mathematical Models and Kinetic Analysis of Changes during Roasting**

The essential purpose of mathematical models is to describe sufficiently a set of obtained data. This model can be used for many purposes such as prediction, process control, optimization and simulation. Empirical models are widely used in modeling of food processing due to the complexity of reactions and non-homogeneous structure of food products. Also from pragmatic perspective, for practical purposes simple mathematical expressions can be easily used to control the process.

Exponential models have been used most widely to describe moisture loss (drying) of food products. One of the empirical drying correlation models is Page equation (Eq. (3.1)) (Moss and Otten, 1989);

$$MR = \exp(-kt^n) \quad (3.1)$$

In these models, MR is the dimensionless moisture ratio and equals to  $(m - m_e)/(m_o - m_e)$ , where  $m$  is the moisture content of the product any each time,  $m_o$  is the initial moisture content of the product and  $m_e$  is the equilibrium moisture content. The values of  $m_e$ , are relatively small compared to  $m$  or  $m_o$  it could be assumed as zero. Thus, moisture ratio can be reduced to  $MR = m/m_o$ .

Another important analytical approach to model process and reaction in food systems is kinetic approach. This approach is based on general reaction rate equation (Eq. (3.2)).

$$\frac{dP}{dt} = \pm kP^n \quad (3.2)$$

The order of chemical reaction for quality degradation in a food system is generally zero (Eq. (3.3)) or first (Eq. (3.4)):

$$P = P_o - kt \quad \text{when } n=0 \quad (3.3)$$

$$P = P_o . e^{-kt} \quad \text{when } n=1 \quad (3.4)$$

This does not mean that the reactions taking place are very simple reactions rather, it shows complex systems can be made to fit simple mathematical models (Labuza, 1980). General reaction rate equation (Eq. (3.2)) can be correlated with environmental factors (temperature, pressure, etc.) and composition (concentration, pH etc.). Some valuable general functional relationship has been found for temperature, concentration, water activity and moisture content, oxygen, and mixed-models effects (Saguy and Karel, 1980). The most common and general valid assumption is that temperature dependence of reaction rate constant will follow Arrhenius type relationship (Eq. (3.5)).

$$k = k_{ref} \exp\left(\frac{-E_a}{RT}\right) \quad (3.5)$$

Functions other than the Arrhenius type relation such as linear, exponential and hyperbolic have been also used to correlate reaction rate with temperature (Saguy and Karel, 1980). One-step nonlinear regression method is recommended by several authors for calculation of activation energy and temperature dependency of parameter (Rapasusas and Discroll, 1995). For zero-order process, if Eq. (3.5) is substituted into Eq. (3.3), it becomes:

$$P = P_o - k_{ref} \exp\left(-\frac{E_A}{RT}\right)t \quad (3.6)$$

### 3.3 Response Surface Methods (RSM) and Process Optimization

When many factors and interactions affect the desired yield, response surface methodology (RSM) is an effective tool for optimising a process. RSM is a collection of mathematical and statistical techniques that are useful for modeling and analysis of problems in which a response of interest is influenced by several variables and one's objective is to optimise this response (Montgomery, 2001).

RSM has been successfully applied to many food process modeling and optimisation problems. Saklar et al. (2001) used the response surface methodology for the determination of hazelnut roasting conditions, and they reported that this technique is suitable for determining the optimum roasting conditions. Similarly, Özdemir and Devres (2000b) obtained successful predictive models for describing the changes in L-, a-, and b-values of whole-kernel, ground-state and cut-kernel hazelnuts during roasting, using RSM. Hebbar and Ramesh (2005) determined optimum drying conditions for cashew kernels with testa using RSM.

In this study, response surface method was used to model the response variables (L-, a-, b-, and BI-values, hardness, fracturability, moisture content) with respect to independent parameters (roasting temperature and roasting time) for hot air, electrical oven and vacuum oven roasting methods. Since true functional relation between the responses and the independent variables was unknown, the first-order or

second-order polynomial expressions for a selected experimental region approximated the actual response surfaces.

The first-order model for the case of two independent variables (roasting temperature ( $x_1$ ) and roasting time ( $x_2$ )) is

$$y = b_0 + b_1x_1 + b_2x_2 + \varepsilon \quad (3.7)$$

$$E(y) = y - \varepsilon \quad (3.8)$$

where  $E(y)$  is the equation of a plane, if there is an interaction between these variables, interaction term is added:

$$y = b_0 + b_1x_1 + b_2x_2 + b_{12}x_1x_2 + \varepsilon \quad (3.9)$$

where interaction term promotes small curvature into the response function. If high curvature is present, the response surface possibly described by a second-order model. Thus the second-order model surface will be a parabolic, a hyperboloid, or some other conic shape. The second-order model for the variables  $x_1$  and  $x_2$ , is

$$y = b_0 + b_1x_1 + b_2x_2 + b_3x_1x_2 + b_4x_1^2 + b_5x_2^2 + \varepsilon \quad (3.10)$$

where  $b_0, b_1, b_2, b_3, b_4$  and  $b_5$  are regression equation coefficients,  $y$  is the response,  $E(y)$  is the expected value of response and  $\varepsilon$  is the random error.

Almost in all RSM problems, one or both of these models are used. For the simplification of mathematical labor of statistical analysis, it is convenient to convert actual variables to coded variables (Montgomery, 2001). The coding was performed as follows

$$z_{i1} = \frac{x_{i1} - (\max x_{i1} + \min x_{i1})/2}{(\max x_{i1} - \min x_{i1})/2} \quad (3.11)$$

where  $z$  is the coded term.

The model parameters can be estimated most effectively if proper experimental designs are used to collect the data. Designs for fitting response surfaces are called



response surface designs. A 2-factor ( $x_1$  and  $x_2$ ), 5-level (-1.414, -1, 0, +1, +1.414) central composite designs were used for all roasting experiments.

The polynomial equations were fitted to the data to obtain the regression equations. Then, statistical significance of the terms in the regression equation was investigated (İbanoğlu, 2003). The goodness of fit of the predicted models was tested by lack of fit value. The procedure is to partition of the sum of squares for error ( $SS_E$ , residual error) into two parts, one due to experimental (pure) error and one due to the lack of fit.

$$SS_E = SS_{PE} + SS_{LOF} \quad (3.12)$$

where  $SS_{PE}$  is the sum of squares due to pure error and  $SS_{LOF}$  is the sum of squares due to lack of fit (Montgomery, 2001). The F-statistics for lack of fit is used for testing a hypothesis that the model is appropriate for the response,

$$F = \frac{MS_{LOF}}{MS_{PE}} \quad (3.13)$$

where  $MS_{LOF}$  and  $MS_{PE}$  are the mean square error of the lack of fit and pure error respectively. Ideally, the F-ratio for the lack of fit should be not significant for good fitting.

Optimization is the ultimate aim of the response surface methodology. Many response surface problems involve the analysis of several responses. Simultaneous consideration of multiple responses involves first building an appropriate response surface model for each response and then trying to find a set of operating conditions that in some sense optimizes all responses or at least keeps them in desired ranges. For this purposes, the use of desirability functions is one of the useful approach to optimization of multiple response. In this technique, the general approach is to first convert each response  $y_i$  into an individual desirability function  $d_i$  that varies over the range,  $0 \leq d_i \leq 1$  where if response  $y_i$  is at its target value, then  $d_i=1$ , and if it is outside an acceptable region,  $d_i = 0$ . Then the design variables were chosen to maximize the overall desirability as:

$$D = (d_1 * d_2 * \dots * d_m)^{\frac{1}{m}} \quad (3.14)$$

where m is the number of responses.

### **3.4. Materials and Methods**

Turkish cultivars brown sesame seeds (*Sesamum indicum* L; Gaziantep region, season 2003) were used in this study. Mechanically dehulled sesame seeds are generally used in the production of sesame paste. Therefore, sesame seeds were dehulled as follows: First the seeds were sieved to remove foreign materials, and then soaked in water ( $T = 18 \pm 2^\circ\text{C}$ ) for 12 h. The soaked seeds were strained off and passed through a mechanical peeler for removing the hulls from the seeds. The hulls and other remaining foreign materials were separated from seed by using salt solutions. The seeds were taken from the surface of solution batches and then washed with water several times to remove the salt. The cleaned sesame seeds were centrifuged to reduce the water content from the surface (wet dehulled sesame seeds). The wet dehulled sesame seeds were used for roasting processes in this study.

#### **3.4.1 Conventional roasting (CR)**

The conventional roasting process was carried out in a local factory. The wet dehulled sesame seeds (25 kg, initial moisture content was 33 %) were roasted using a temperature-controlled rotary roasting machine (Gürmaksan Co., Turkey) at roasting temperatures of 120, 150 and 180°C, which all are used commercially, sesame roasting for paste and confectionary productions. During roasting process samples were taken at different time intervals (20-120 min) and they were immediately equilibrated to room temperature ( $20 \pm 2^\circ\text{C}$ ) to prevent further heating. Roasted seeds were packed in polyethylene plastic bags and stored ( $5 \pm 2^\circ$ ) for further analysis. Two replicates were performed for each roasting process.

#### **3.4.2 Hot air roasting (HAR)**

An experimental hot air roasting system was designed and used for the roasting experiments (Figure 3.1). The system consisted of a heat gun (Varitemp®, Heat Gun, VT 752C, Master Appliance Corp., USA), a circular meshed product basket (diameter = 6.5 cm), and a motor to rotate the basket on horizontal axis (Figure A.1).

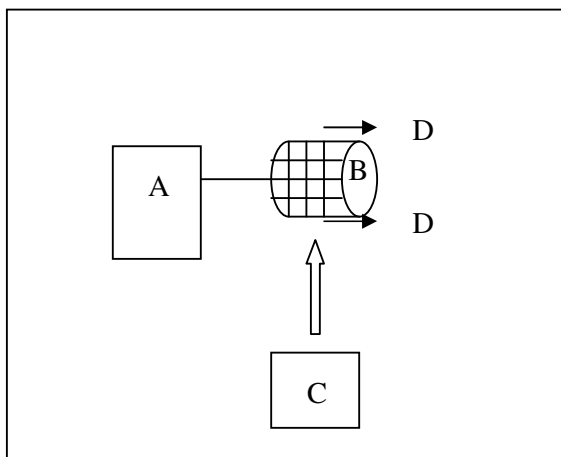


Figure 3.1 Experimental hot air roaster: A, motor to rotate the product basket; B, product basket; C, heat gun; D temperature measurements points

The air temperature was measured at inlet and exit of the product basket. The average of them was used. Air velocity was measured using an anemometer (Airflow Inst. LC600, UK precision of  $\pm 0.01$  m/s). Some pre-trials were conducted to determine the acceptable ranges. The air temperature and exposure time ranges were selected as  $120-180 \pm 2^\circ\text{C}$  and 30-60 min. Before roasting, temperature of air was set at the desired values and the mean value of the air velocity was measured as  $1.2 \pm 0.01$  m/s. The roaster was run for 10 minutes to achieve a steady state. Then, sesame seeds ( $3 \pm 0.2$  g) were roasted for a period of time (Table 3.1). The position of the product basket and the distance between the heating source (10 cm) and samples were fixed for all experimental runs for promoting uniform heating. After roasting, the sesame seeds were immediately equilibrated at room temperature ( $20 \pm 2^\circ\text{C}$ ) for preventing further heating.

Table 3.1 Coded and actual variables for the experimental design for the optimization of the roasting process of sesame seed accomplished in the hot air roaster

Run	Coded		Actual	
	Temperature (°C)	Time (min)	Temperature (°C)	Time (min)
1	0	-1.414	150	24
2	1.414	0	193	45
3	-1	-1	120	30
4	0	0	150	45
5	1	-1	180	30
6	-1	1	120	60
7	0	1.414	150	66
8	-1.414	0	108	45
9	0	0	150	45
10	1	1	180	60
11	0	0	150	45
12	0	0	150	45
13	0	0	150	45

### 3.4.3 Electric oven roasting (EOR)

The slightly dried sesame seeds (initial moisture content was around 11%) were selected (unhulled, small and big seeds were removed) and placed as a single layer in Pyrex Petri dishes (8 cm diameter) and then roasted in an electric oven (Heraeus, Hanau, Germany) between 120-150±3°C for 30-60 min. For experimental design, response surface methodology was used (Table 3.2). Two dishes were roasted once at each of the different roasting temperatures and times to obtain sufficient sample material for analysis and testing. Roasted samples were equilibrated to room temperature (20±2°C) for 24 h and physical analyses (color, texture and moisture content) were carried out after one the day of production.

### 3.4.4 Vacuum oven roasting (VOR)

The properties of sesame seeds and experimental conditions were the same as in the case of EOR, but in a different manner only roasting was carried out in a vacuum oven (Nüve, EV018) at air temperatures between 120°-150±3°C for 30-60 min at 60 Torr (Table 3.3).

Table 3.2 Coded and actual variables for the experimental design for the optimization of the roasting process of sesame seed that accomplished in electrical oven

Run	Coded		Actual	
	Temperature (°C)	Time (min)	Temperature (°C)	Time (min)
1	1	-1	150	30
2	-1	-1	120	30
3	0	0	135	45
4	1	1	150	60
5	0	0	135	45
6	0	0	135	45
7	-1	1	120	60
8	0	0	135	45
9	0	0	135	45
10	-1.414	0	114	45
11	0	0	135	45
12	0	1.414	135	67
13	1.414	0	157	45
14	0	-1.414	135	24

Table 3.3 Coded and actual variables for the experimental design for the optimization of the roasting process of sesame seed that accomplished in vacuum oven

Run	Coded		Actual	
	Temperature (°C)	Time (min)	Temperature (°C)	Time (min)
1	1	-1	150	30
2	-1	-1	120	30
3	0	0	135	45
4	1	1	150	60
5	0	0	135	45
6	0	0	135	45
7	-1	1	120	60
8	0	0	135	45
9	0	0	135	45
10	-1.414	0	114	45
11	0	0	135	45
12	0	1.414	135	67
13	1.414	0	157	45
14	0	-1.414	135	24

### 3.4.5 Chemical analysis

The composition of sesame seeds was measured according to the procedures listed in AOAC (AOAC, 1990). The Kjeldahl method (AOAC method 950.48, 1990) was used for the determination of protein content with factor 6.25. Oil content was determined using the Soxhlet method (AOAC method 960.39, 1990). Moisture

(AOAC method 925.09, 1990) , and ash (AOAC method 923.03, 1990) determinations were performed using gravimetric procedures. The remaining percentage of the composition was assumed to be the total carbohydrate content. The results of the compositional analysis were the mean of three measurements of two replicates.

### 3.4.6 Color measurements

Color measurements of sesame seeds were conducted after one day of roasting. The color measurements were done using HunterLab ColorFlex (A60-1010-615 Model Colorimeter, Hunter Lab, and Reston VA). The color values are expressed as L- (whiteness or darkness), a- (redness/greenness), and b- (yellowness/ blueness). The L-, a-, and b-values are three dimensions of the measured color which gives specific color value of the material. The browning index (BI) (Eq. (3.15)) is also used to estimate purity of brown color in the systems where enzymatic or nonenzymatic browning occurs (Maskan, 2001).

$$BI = \frac{[100(x - 0.31)]}{0.17} \quad (3.15)$$

where

$$x = \frac{(a + 1.75L)}{(5.645L + a - 3.012b)} \quad (3.16)$$

Three measurements were done for each sample. The instrument was calibrated against a standard reference tile (L = 91.10, a = -1.13, b = 1.26, YI = 1.52).

### 3.4.7 Texture measurements

The textural analyses of the sesame seeds was performed using a TA.XT2 Texture Analyzer (Texture Technologies Corp., Scarsdale, NY/Stable Microsystems, Godalming, UK). In Texture Profile Analysis (TPA) test, sesame seeds were placed individually on the plate, and double compression was applied using a cylindrical probe (diameter = 5.0 mm) at a test, pre-test and post-test speed were adjusted as 0.1 mm/s. The deformation was selected as 0.3 mm for samples. Sesame seeds have elliptical shape and the dimensions were measured over 150 kernels as length 3.30-3.50 mm, width 1.85-1.90, and thickness 0.90-0.95 mm. Sesame seeds were placed horizontally and force was applied on thickness. Ten measurements were performed

for each sample. Textural properties were derived from the force time curves (Bourne, 1982). Two textural parameters; fracturability (N) (first peak of first compression) and hardness (N) (maximum peak of first compression) were considered to evaluate textural properties of sesame seed samples.

#### **3.4.8 Statistical analysis and modeling**

The moisture contents, color values, and textural parameters of roasted sesame seeds were analyzed by the two-way analysis of variance method (ANOVA) to determine the effect of temperature and time on these responses. The exponential, zero-order, first-order, quadratic and cubic models were assessed to fit of experimental data. The coefficient of determination ( $r^2$ ) and standard error of estimate (SEE) were used as criteria for adequacy of fit. The data were fitted to models using commercial software (SigmaPlot 6.0, Jandel Scientific, San Francisco, USA) via the Marquardt-Levenberg algorithm. The ANOVA tests were performed using SPSS 9.0 (SPSS Inc., Chicago, IL, USA).

A commercial statistical package, Design-Expert trial version 6.01 (Statease Inc., Minneapolis, USA) was used for response surface analysis and optimisation. Since the individual desirability functions are not differentiable, numerical optimization methods cannot be used (Montgomery, 2001). The direct search methods are used by Design-Expert software to maximize the desirability function.

### **3.5 Results and Discussion**

The physical and chemical properties of the seeds are presented in Table 3.4. The similar composition for Gaziantep variety sesame seeds had been reported by Ozcan and Akgül (1994). However, the oil content of sesame seed was found higher than that reported by Namiki, (1995). The average oil content for the white-seeded strains was reported as 55.0%, for brown-seeded 54.2%, and for black-seeded strains 47.8% (Namiki, 1995).

Sesame contains approximately 20% protein (Namiki, 1995). Turkish brown-seeded had also similar protein content (20.30%). Carbohydrate content of our sesame sample was found as 13.47% that is lower than reported in literature (18-20%).

Table 3.4 Physical and compositional properties of sesame seeds under study

Physical and chemical properties	Number of measurements	Mean	SD <sup>a</sup>	SEM <sup>b</sup>
Mass (g)	25	0.0035	1.98x10 <sup>-4</sup>	3.96x10 <sup>-5</sup>
Length (mm)	25	3.46	0.16	0.033
Width (mm)	25	1.88	0.08	0.016
Thickness (mm)	25	0.93	0.05	0.010
Moisture (g /kg <sup>-1</sup> )	4	34.0	0.06	0.021
Protein (g /kg <sup>-1</sup> )	4	203.0	0.06	0.021
Oil (g /kg <sup>-1</sup> )	4	579.6	0.27	0.087
Carbohydrate (g/kg <sup>-1</sup> )	4	134.7	0.21	0.067
Ash (g/kg <sup>-1</sup> )	4	48.7	0.06	0.019

<sup>a</sup> Standard deviation; <sup>b</sup> Standard error of the mean

### 3.5.1 Conventional roasting (CR)

The changes in the moisture content of sesame seeds during roasting at 120, 150, and 180°C as a function of the roasting time are presented in Figure 3.2. Similar trends in the changes of moisture content were observed at three roasting temperature. The changes in the moisture of sesame seeds showed a steep decrease up to 40 min of roasting time. As it was expected, faster moisture loss occurred as roasting temperature increased.

Some empirical models were tested for the description of moisture changes during sesame seed roasting. Two-parameter exponential decay model and Page models were found as the best models with good fitting criteria (Table 3.5). Although, both two-parameter exponential and Page models had higher coefficient of determinations ( $r^2 \geq 0.990$ ) and small SEE, the Page model had better fitting criteria than those of the two-parameter exponential model. Similar findings were reported by Madamba et al. (1996a) for drying of garlic slices, Ozdemir and Devres (1999) for hazelnut roasting, and Doymaz (2004) for okra drying.



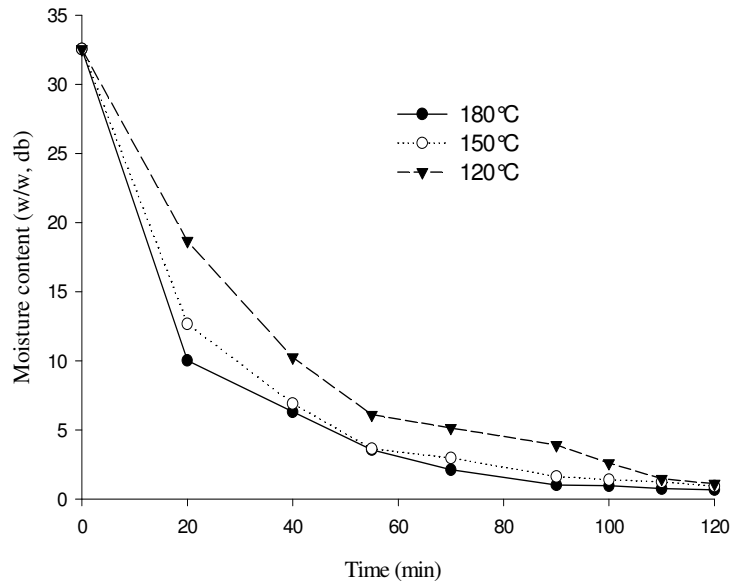


Figure 3.2 Relationship between roasting time and moisture loss of sesame seeds roasted in a conventional rotary roaster at different temperatures studied

The estimated parameter ( $n$ ) of the Page model exhibited temperature dependence (Table 3.5). As roasting temperature was increased,  $n$  value decreased. However, Senadeera et al. (2003) reported that  $n$  was independent of drying air temperature as Page model was used for simulation of drying curves of bean, potato and pea. Similarly, Simal et al. (2005) also concluded that the  $n$  was constant with air temperature for modeling of drying of kiwifruit. As shown in Table 3.5, the rate constants  $k$  and  $a$  also increased with increase of the roasting temperatures of sesame seeds. To find the relationship between roasting temperature and roasting time, the drying coefficients ( $a$  and  $k$ ) of two model were related to roasting temperature using linear regressions (Eqs. (3.17 and 3.18)), respectively

$$a = c + dT \quad (3.17)$$

$$k = e + fT \quad (3.18)$$

After linear regression, the coefficients of Eq. (3.17) and Eq. (3.18) were used as initial parameters for nonlinear regression analysis. The good estimation of initial parameters in nonlinear regression analysis is important for success of fitting.

Table 3.5 Two-parameter exponential and Page models parameters and fitting criteria for moisture loss of sesame seeds during roasting

Roasting Temperature (°C)	Two-parameter exponential model $MR = a \exp(-kt)$				Page model $MR = \exp(-kt^n)$			
	a	k (min <sup>-1</sup> )	r <sup>2</sup>	SEE	k (min <sup>-n</sup> )	n	r <sup>2</sup>	SEE
120	0.9961	0.0277	0.996	0.0208	0.0337	0.950	0.998	0.0210
150	0.9848	0.0404	0.992	0.0304	0.0968	0.759	0.999	0.0095
180	0.9834	0.0475	0.986	0.0402	0.1521	0.671	0.996	0.0151

The final form of the two-parameter exponential model (Eq. (3.19)) and Page model (Eq. (3.20)) that adequately described moisture ratio as a function of temperature and roasting time became as follows:

$$MR = (1.0572 - 0.0002T) \exp((0.1133 - 0.0004T)t) \quad (r^2 = 0.991) \quad (3.19)$$

$$MR = \exp((-0.173 - 0.0006T)t^{0.8239}) \quad (r^2 = 0.995) \quad (3.20)$$

The MR values, which were predicted using Eq. (3.19) and Eq. (3.20), are given in Figure (3.3). Although the empirical models do not provide mechanistic information and the estimated parameters have no physical meaning, it is possible to simulate accurately the drying curves from a practical point of view (Simal et al., 2005). Consequently, Eqs. (3.19) and (3.20) can be used to simulate the moisture content changes of sesame seeds during conventional roasting. The individual control model should be developed for each roasting or drying conditions.

Color is one of the most important appearance attributes of food materials, since it influences consumer acceptability (Maskan, 2001). Besides of consumer acceptability, color is also used for process control. Especially roasting operations are controlled by degree of color formation because the brown pigments increase as the browning and caramelization reactions progress (Saklar et al. 2001).

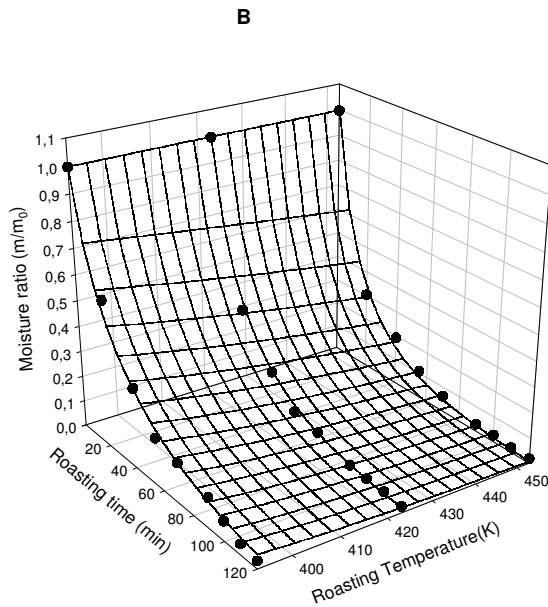
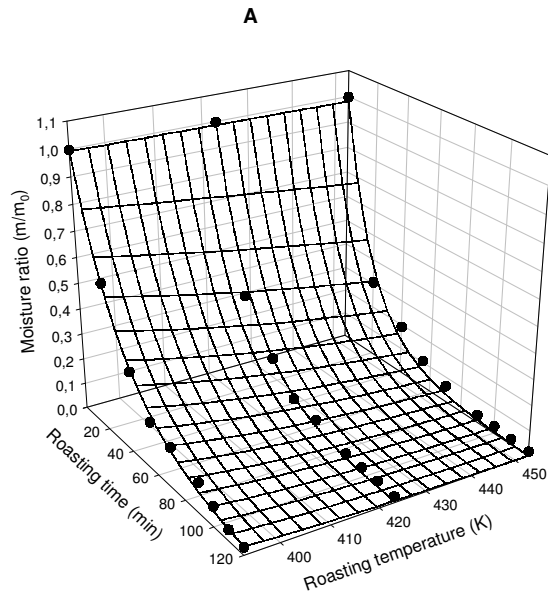


Figure 3.3 Moisture content changes of sesame seed conventionally roasted at different temperatures. Symbols show the actual data points. Mesh lines represent the fitted line by Eq. (3.19) (A), and Eq. (3.20) (B)

The changes in the Hunter L-, a-, b- and BI values of sesame seed roasted at different temperatures are shown in Figure 3.4. The performed two-way ANOVA indicated that temperature and time significantly ( $P < 0.05$ ) affected the color values of sesame seeds during roasting.

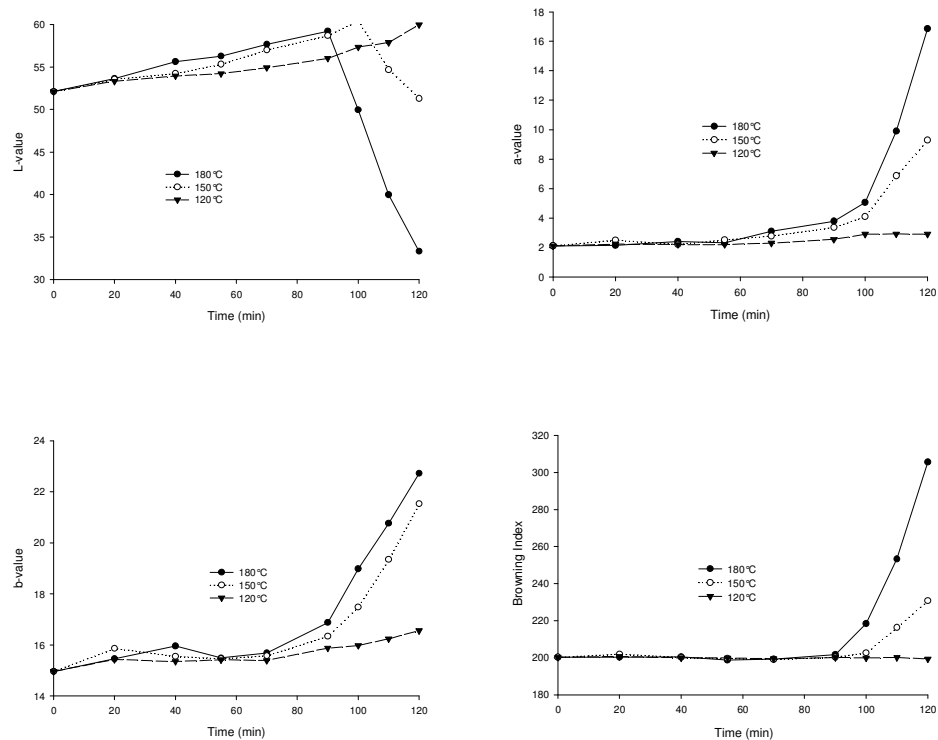


Figure 3.4 Changes in the color parameters of sesame seeds during roasting at different temperatures studied (120, 150 and 180°C) for 120 minutes

The L-value shows whiteness of product. At the initial period of roasting, a gradual increase in the L-value was observed. This period is called as initial lightening. Similar results were observed for peanuts by Moss and Otten (1989) and hazelnuts by Özdemir and Devres (2000). The reasons of lightening explained by Moss and Otten (1989) as the glazed appearance of the slightly roasted nuts after grinding but Özdemir and Devres (2000) concluded that this explanation was not valid for hazelnuts since they observed the lightening in whole-kernel also. The low-moisture content, denaturation of proteins, and the concentrated amount of oil particles embedded in protein matrix could be reasons of lightening during roasting of sesame. The oil particles may also impart whiteness to seeds by scattering light. After the initial lightening, there was a decline in the L-values (darkening) of seeds at higher roasting temperatures (150 and 180°C). However, no reduction was observed in the L-value during roasting at 120°C. As the roasting temperature was increased, the lightening period became shorter.

The a-value shows redness for roasted products and the variation in the a-value during sesame roasting was presented in Figure 3.4. An induction period was also observed for the a-value. Up to 70-90 minutes a-value remained nearly constant then increased sharply for sesame seed roasted at 150°C and 180°C. However, the a-values of seeds roasted at 120°C did not increase sharply. The increasing in the a-value was due to the formation of brown pigments through the non-enzymatic browning and phospholipids degradation. Increase in the a-value during processing was correlated with decrease in the L-value.

The b-value shows the degree of yellowness (Figure 3.4). The b-values increased with increasing roasting time and temperature. Similar trend as in the a-value was observed for the changes of b-value during roasting. Moss and Otten (1989) also reported an induction period for the b-value of roasted peanuts at initial stages of roasting followed by an increase but Özdemir and Devres (2000) did not observe any proper trend in the b-value of roasted hazelnuts.

The browning index (BI) represents purity of brown color (Maskan, 2001). The variation in the BI value of seeds during roasting was presented in Figure 3.4. The BI plot provides better possibility to determine roasting time at which darkening began. The BI value of sesame remained nearly constant during roasting at 120°C up to end of roasting. However, at 150 and 180°C, it was constant up to 90 minute, then, BI increased sharply.

The common problem with the processing of sesame paste is the formation of dark color. If sesame seeds were over-roasted, consumers may not accept sesame paste. Therefore, the color formation during roasting should be properly controlled. The kinetics of color formation is the important elements for the control models. Two kinetic models (zero and first) and two polynomials (quadratic and cubic) models were evaluated for modeling the color changes of sesame seeds during roasting operation. The L-, a-, and b-values were selected for modeling analyses. The results of fitting criteria and equation coefficients for all models were shown in Table 3.6.

Although commonly the changes in color as affected by heat treatment followed zero- or first-order kinetics (Avila and Silva, 1999), the best fits were obtained with cubic model over the temperature and time range of this study. The cubic polynomial

model gave the high coefficient of determination ( $r^2$ ) and small standard error of estimate (SEE) for fitting of all color values. As similar to our results, Özdemir and Devres (2000a) used a cubic model in describing L-, a, and b- values of the color in hazelnut roasting. Moss and Otten (1989) also reported that changes in the L-, and a-values of peanut during roasting could be described by quadratic model, and cubic model for b-value.

To divide the sesame roasting into two periods as lightening and darkening provided detail investigation of color formation during roasting. To represent the adequacy of kinetic models to describe changes up to 90 min of roasting, zero and first order kinetics were applied to experimental L-value data. The results of this fitting were given in Table 3.7. The high coefficient of determination ( $r^2 > 0.977$ ) and small standard error of estimate ( $SEE < 0.45$ ) of fitting showed that the lightening period during roasting of sesame could be modeled by zero- and first-order kinetics. The values of the kinetic constants  $k$  increased with the roasting temperature. Hence, it was argued that the kinetic models could be used for only modeling of lightening period but cubic models could be more suitable to describe conditions of entire roasting operation including over-roasting (darkening period).

The one-step nonlinear regression analysis was carried out to relate the color models with roasting temperature. The results of this regression are given in Table 3.8. Initially, the Arrhenius-type relationship was tested, but it was failed due to its low  $r^2$  (0.15-0.40). Then the linear relationship was found between coefficients of cubic model and roasting temperature.

The form of generalized model as a function of temperature and time was obtained as follow by cubic polynomial model;

$$P = (a + bT) + (c + dT)t + (e + fT)t^2 + (g + hT)t^3 \quad (3.21)$$

For the a-value, coefficient of determination and SEE were better than those of L-value. The model for the b-value had nearly the same fitting criteria as a-value. Figures 3.5-3.7 show the experimental and predicted values of L-, a-, and b-values, respectively.

Table 3.6 Parameters and fitting criteria of zero-, first-order, quadratic and cubic models for the color values of sesame seed during conventional roasting operation

Model	Parameter and criteria	L-value			a-value			b-value		
		Roasting Temperature (°C)			Roasting Temperature (°C)			Roasting Temperature (°C)		
		120	150	180	120	150	180	120	150	180
Zero order	P <sub>o</sub>	51.65	53.61	58.72	1.97	0.80	-0.70	14.93	14.06	13.65
	k	0.0575	0.0243	-0.1171	0.0075	0.0470	0.0892	0.0113	0.0422	0.0561
	r <sup>2</sup>	0.917	0.114	0.314	0.825	0.621	0.553	0.856	0.641	0.719
	SEE	0.766	3.002	7.686	0.1535	1.6331	3.5630	0.2053	1.404	1.559
First order	P <sub>o</sub>	51.68	53.67	58.30	1.98	0.83	0.84	14.93	14.03	13.64
	k	0.0011	0.0004	-0.0021	0.0032	0.0190	0.0437	0.0007	0.0027	0.0035
	r <sup>2</sup>	0.925	0.108	0.269	0.857	0.858	0.929	0.863	0.687	0.773
	SEE	0.731	3.007	7.839	0.140	1.1119	1.64	0.201	1.334	1.433
Quadratic	P <sub>o</sub>	52.56	50.79	48.96	2.14	2.84	3.57	15.14	15.80	15.69
	s	0.0066	0.1815	0.4261	-0.0020	-0.0667	0.1488	-0.0004	-0.0547	-0.0571
	b	0.0004	-0.0013	-0.0044	0.0001	0.0009	0.0019	0.0001	0.0008	0.0009
	r <sup>2</sup>	0.970	0.466	0.810	0.923	0.887	0.842	0.924	0.888	0.933
	SEE	0.498	2.518	4.364	0.1097	0.9608	2.287	0.161	0.8446	0.818
Cubic	P <sub>o</sub>	52.12	52.80	52.64	2.16	1.98	1.56	15.01	14.97	14.94
	a	0.0776	-0.1406	-0.161	-0.0046	0.0717	0.1716	0.0192	0.0777	0.0615
	b	-0.0012	0.0059	0.0087	0.0001	-0.0022	-0.0052	-0.0003	-0.0022	-0.0017
	c	0.0000	-0.0000	-0.0001	-0.0000	0.0000	0.0000	0.0000	0.0000	0.0000
	r <sup>2</sup>	0.994	0.8160	0.948	0.925	0.981	0.966	0.969	0.998	0.989
	SEE	0.235	1.619	2.499	0.118	0.431	1.156	0.111	0.113	0.356

Table 3.7 Parameters and fitting criteria of zero- and first-order kinetics for modeling of L-value in the lightening period of roasting of sesame seed

Model	Parameters and criteria	Roasting temperatures (°C)		
		120	150	180
Zero order	P <sub>o</sub>	52.24	51.86	52.10
	k	0.040	0.0715	0.0785
	r <sup>2</sup>	0.978	0.977	0.995
	SEE	0.2182	0.4415	0.1960
First order	P <sub>o</sub>	52.26	51.91	52.21
	k	0.0007	0.0013	0.0014
	r <sup>2</sup>	0.978	0.977	0.994
	SEE	0.2170	0.4045	0.2152

Table 3.8 Constants and fitting criteria obtained from generalized model (Eq. (3.21)) for color parameters of sesame seed during conventional roasting operation

Model constants and fitting criteria	Color parameters		
	L-value	a-value	b-value
a	48.84922	6.085946	15.47153
b	0.008688	-0.00988	-0.00116
c	1.610834	-1.1626	-0.2452
d	-0.00398	0.002937	0.000705
e	-0.06501	0.03526	0.008322
f	0.000164	-8.9x10 <sup>-5</sup>	-2.3x10 <sup>-5</sup>
g	0.000542	-0.00026	-7.5x10 <sup>-5</sup>
h	-1.4x10 <sup>-6</sup>	6.69x10 <sup>-7</sup>	2.05x10 <sup>-7</sup>
r <sup>2</sup>	0.878	0.971	0.969
SEE	23.318	0.6521	0.4335

L-values of sesame seeds during roasting were over estimated at 120°C at later stages of roasting but under estimated at initial and later stages of roasting at 180°C (Figure 3.5). This result suggested that as the roasting temperature increased, the success of model for description of whole roasting period decreased. Hence, at higher roasting



temperatures for sesame, the development of control model based on the measurement of the L-value may cause some difficulties.

As it can be seen from Figure 3.6 the predicted a-values were mostly the same as experimental values except for a few points. Hence, the stability and development of redness of sesame during roasting could be estimated satisfactorily by developed model over all the temperature and time ranges used in this study. L-value has been used to monitor color formation for hazelnut roasting (Ozdemir and Devres, 2000). However, it was found that the a-value could be used to monitor the color formation and control the roasting process of sesame seeds. Similarly b-values were adequately estimated by generalized model (Figure 3.7). Thus, to calculate the activation energy values ( $E_a$ ) for color changes, a- and b- value were selected, a zero-order kinetic equation was assumed based on Arrhenius-type relation (Eq. (3.6)) between temperature and parameters a- and b-value.

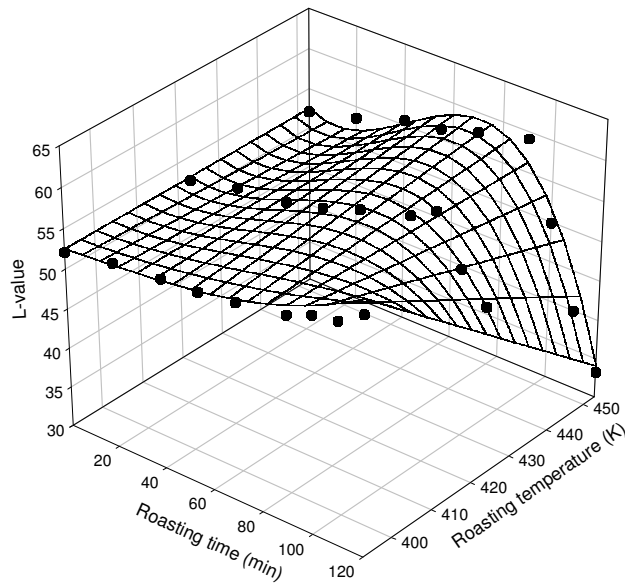


Figure 3.5 Changes in the L-values of sesame seed conventionally roasted at different temperatures studied. Symbols show the actual data points. Mesh lines represent the fitted line by Eq. (3.21)

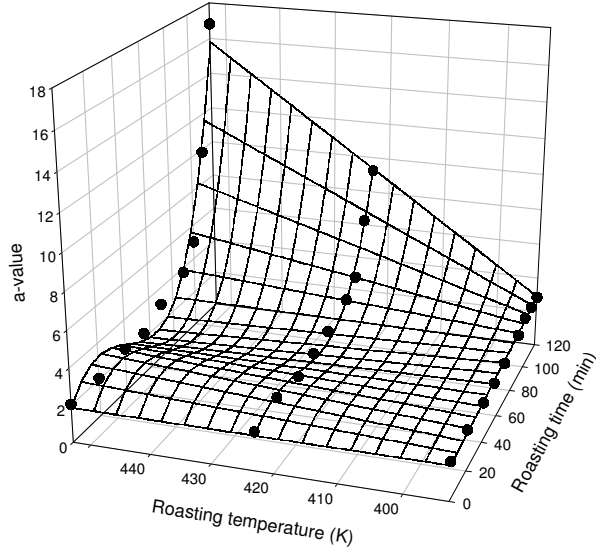


Figure 3.6 Changes in the a-values of sesame seed conventionally roasted at different temperatures studied. Symbols show the actual data points. Mesh lines represent the fitted line by Eq. (3.21)

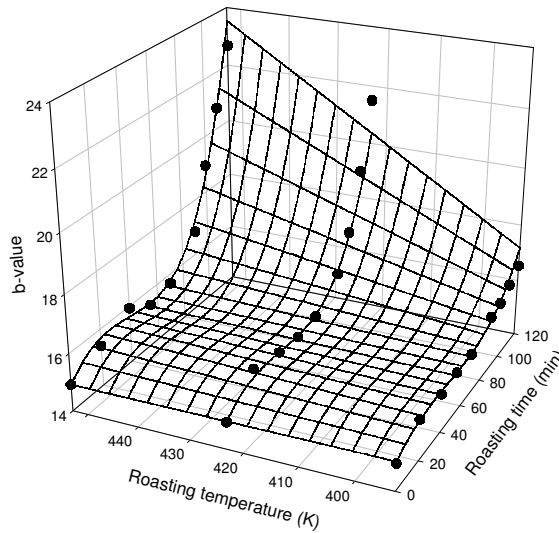


Figure 3.7 Changes in the b-values of sesame seed that conventionally roasted at different temperatures studied. Symbols show the actual data points. Mesh lines represent the fitted line by Eq. (3.21)

The one-step nonlinear regression analysis was used for determination of activation energies because two-step regression produced high standard deviation and

confidence interval of  $E_a$ . Activation energies of a- and b-values for sesame seeds were calculated as 25.4 and 14.18  $\text{kJmol}^{-1}$ , respectively. These values also showed that a-value is more sensitive to temperature change than b-value. These values are also lower than  $E_a$  values of color changes in foods (41-125  $\text{kJmol}^{-1}$ ) reported in literature (Saguy and Karel, 1980). The lower  $E_a$  is most probably due to high roasting temperatures (120-180°C), and also  $E_a$  may change according to heating system and product type.

Texture is the other important control parameter for sesame roasting. The decrease of hardness and fracturability (first fracture force) of sesame during roasting process are shown in Figures 3.8-3.9, respectively. Regardless of the roasting temperature, the trend of textural parameters as a function of the corresponding time was almost similar, showing a progressive and significant decrease ( $P<0.01$ ) as exposure time increased, indicating a progressive reduction in the strength of the seed.

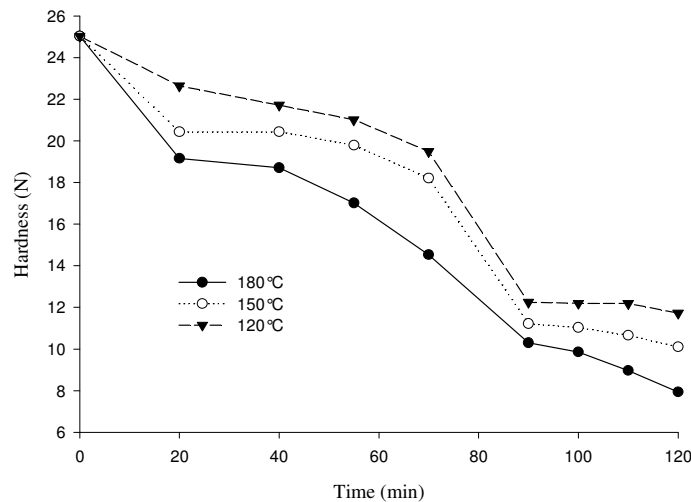


Figure 3.8 Effect of roasting temperature and time on the hardness of sesame seeds

The decrease in the hardness shows that the required force to break the seed decreased with an increase in roasting time and temperatures (Figure 3.8). Similarly, in all cases, as the roasting time increased, the first fracturability decreased, reaching similar and very low values at the end of the process (Figure 3.9). Saklar et al. (1999) also observed a decrease in the first fracture point during roasting of hazelnuts.

The kinetic and polynomial models were evaluated for description of textural changes during roasting. The overall fit of all models to hardness and fracturability were applicable except first-order model (Table 3.9). Due to simplicity, zero-order kinetic model could be used to monitor the textural changes in sesame seed during roasting.

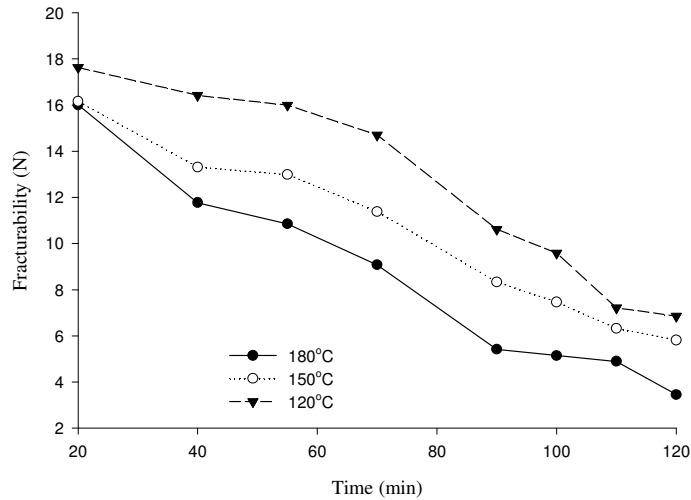


Figure 3.9 Effect of roasting temperature and time on the fracturability of sesame seeds

The reaction rate constants ( $k$ ) increased, as the roasting temperature was augmented. The temperature dependence of rate constants was evaluated using Arrhenius type equation (Eq. 3.6). The zero-order reaction rate constants, obtained from hardness data, followed the Arrhenius type equation well, giving an  $r^2$  value of 0.935 and SEE of 1.466. The activation energy and frequency term for hardness were determined as  $6.92 \text{ kJmol}^{-1}$ , and  $0.93 \text{ min}^{-1}$ , respectively. For the fracturability data, the activation energy and frequency term were found as  $9.82 \text{ kJmol}^{-1}$ , and  $1.87 \text{ min}^{-1}$ , respectively with an  $r^2$  value of 0.945 and SEE of 1.056. The activation energy values determined for both textural parameters are lower than reported in literature, a range of 40-125  $\text{kJmol}^{-1}$  has been suggested as being typical for loss of texture (Alvarez and Canet, 2002). When the activation energies of textural changes are compared to those of color changes, it can be seen that textural changes had lower activation energy values

than color changes. This result suggests that textural changes were less sensitive than color changes to the temperature variance during sesame roasting.

Table 3.9 Parameters and fitting criteria of zero-, first-order, quadratic and cubic models for the textural change of sesame seed during conventional roasting operation

Model	Parameters and criteria	Hardness (N)			First fracture force (N)		
		Roasting temperature (°C)			Roasting temperature (°C)		
		120	150	180	120	150	180
Zero order	P <sub>o</sub>	25.95	25.00	23.84	21.34	18.21	17.46
	k	0.1246	0.1291	0.1374	0.1186	0.1058	0.1208
	r <sup>2</sup>	0.917	0.923	0.971	0.944	0.985	0.970
	SEE	1.659	1.651	1.054	1.096	0.490	0.802
First order	P <sub>o</sub>	26.49	25.67	25.00	22.89	20.24	21.34
	k	0.0066	0.0073	0.0089	0.0086	0.0097	0.0138
	r <sup>2</sup>	0.878	0.887	0.9606	0.877	0.961	0.976
	SEE	1.972	1.9633	1.2140	1.5775	0.7802	0.707
Quadratic	P <sub>o</sub>	25.09	24.36	24.21	18.05	18.00	19.41
	a	-0.0766	-0.0936	-0.1578	0.0004	-0.0982	-0.1916
	b	-0.0004	-0.0003	0.0002	-0.0008	-0.0001	0.0005
	r <sup>2</sup>	0.927	0.928	0.972	0.980	0.985	0.983
	SEE	1.680	1.723	1.107	0.712	0.533	0.665
Cubic	P <sub>o</sub>	24.30	24.04	24.29	15.59	17.18	19.51
	a	0.0492	-0.0419	-0.1711	0.1524	-0.0477	-0.1975
	b	-0.0032	-0.0014	0.0005	-0.0033	-0.0009	0.0006
	c	0.0000	0.0000	-0.0000	0.0000	0.0000	-0.0000
	r <sup>2</sup>	0.943	0.931	0.972	0.986	0.986	0.983
	SEE	1.620	1.853	1.209	0.668	0.579	0.7434

### 3.5.2 Hot air roasting (HAR)

RSM is an approach used in optimization studies and the aim of this part study was the utilization of such an approach in hot-air roasting. The experimental data for the color parameters (L-, a-, b-values and BI), textural properties (hardness, fracturability) and moisture content values of roasted seeds are given in Table A.1. The results of ANOVA and lack of fit tests with  $r^2$  (coefficient of determination) are presented in Table A.2.

The moisture content change was adequately described by the quadratic model ( $r^2 = 0.92$ ) in the design points. However, significant lack-of-fit makes it difficult to use as a predictive model. The result of statistical analysis showed that the roasting temperature was the main factor affecting the moisture content (Table A.2) The application of response surface methodology for developing a predictive model that described the moisture changes during roasting of sesame was not successful.

Color can be used for process control; especially roasting operations are controlled by degree of color formation because the brown pigments increase as the browning and caramelization reactions progress (Saklar et al. 2001). The coefficient of determinations of regression equations changed from 0.88 to 0.96 for color parameters of the sesame seed samples with no lack-of-fit (Table A.2). These models could be adequately used as predictor models. The lack-of-fit compares the residual error and pure error. The lack-of-fit error significantly larger than the pure error indicate that something remain in the residuals can be removed by an appropriate model. If a model has a significant lack-of-fit, it is not a good indicator of the response and should not be used for prediction. Hence, it can be concluded that the proposed model approximates the response surfaces and can be used suitably for prediction at any values of the parameters within experimental domain (Montgomery, 2001; Hebbar and Ramesh, 2005).

It was observed that the linear and quadratic terms of roasting temperature significantly affected all color parameters of the roasted sesame seeds. On the other hand for b- value, cross-product term was also found as significant ( $P < 0.05$ ). Demir et al. (2002) reported that among the color parameters of L-, a-, and b-values, L-values of hazelnuts had highest sensitivity for the air roasting time and temperature. In a similar manner, in this study it was observed that quadratic term of the time was

significant for L-value model. These results show that the roasting temperature could be accepted as the main factor governing a-, b- and BI-values in sesame seeds during hot air roasting operation. But for L-value, besides the roasting air temperature, the roasting time is also significant ( $P < 0.05$ ). In contrast to our results, Özdemir and Devres (2000b) stated that roasting time was insignificant for color attributes of hazelnut.

The regression equations (Table 3.10) were used to generate response surfaces for all responses. The response surfaces of color values are shown in Figures 3.10-3.13. The shape of response surfaces was found different for L-value than other color values. The response surface for the L-value showed saddle shape (Figure 3.10). The L-value ranged from 61.45 to 64.44 that was very narrow range. The saddle shape of response and the narrow range of L-value were probably due to lightening period. The initial lightening and main browning period during roasting were also previously reported for peanuts by Moss and Otten (1989) and for hazelnuts by Özdemir and Devres (2000a).

Table 3.10 Regression equation coefficients for response parameters of sesame seed roasted in the hot air in terms of coded terms<sup>a</sup>

Regression constants	L- value	a-value	b-value	BI-value	Hardness (N)	Fracturability (N)	MC (g/kg, db)
$b_0$	63.00	2.68	16.21	32.29	9.87	8.91	3.75
$b_1$	0.42 (S)	0.61 (S)	1.06 (S)	2.77 (S)	-2.02 (S)	-2.63 (S)	-1.53 (S)
$b_2$	0.05 (NS)	0.17 (NS)	0.19 (NS)	0.58 (NS)	-0.60 (NS)	-0.46 (NS)	-1.06 (S)
$b_3$	0.13 (NS)	-0.01 (NS)	-0.38 (S)	-0.91 (NS)			
$b_4$	-0.64 (S)	0.45 (S)	0.70 (S)	2.46 (S)			
$b_5$	0.50 (S)	0.10 (NS)	0.04 (NS)	-0.10 (NS)			

<sup>a</sup> $Y = b_0 + b_1x_1 + b_2x_2 + b_3x_1x_2 + b_4x_1^2 + b_5x_2^2$  where  $x_1$ = air temperature, °C,  $x_2$ = roasting time, min, S: Significant at  $P < 0.05$ ; NS: not significant

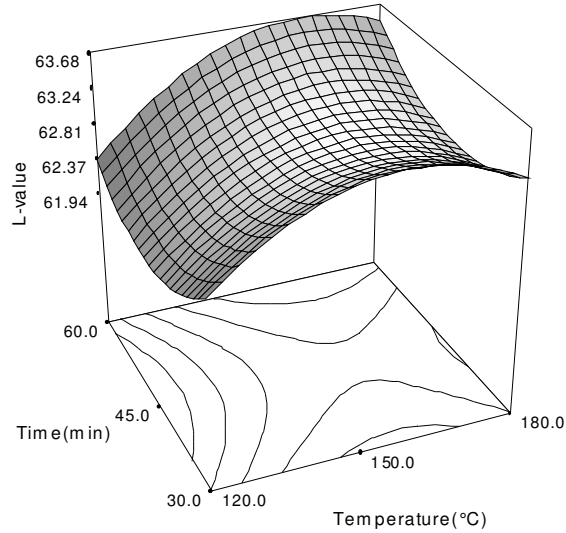


Figure 3.10 Response surface for color whiteness (L-value) of sesame seeds roasted in a hot air roaster

Higher roasting temperature and longer exposure time resulted in an increase in the a- and b-values. The response surface of a- and b-values showed rising ridge behavior (Figures 3.11-3.12). Sharp increases in these values were observed during roasting. The higher a- and b-values related to an increase in redness and yellowness, respectively, are indication of browning. Only the roasting temperature was found as main parameter that affects these values (Table 3.10).

The BI represents purity of brown color (Maskan, 2001). The shape of the response surface of BI was similar to that of a- and b-values (Figure 3.13). As roasting temperature and time increased the BI value remained constant for a short time period then increased and this effect pronounced at higher temperature and time. The result of RSM analysis showed that all color parameters should be considered to monitor the color changes during roasting of sesame seeds in hot air roaster.



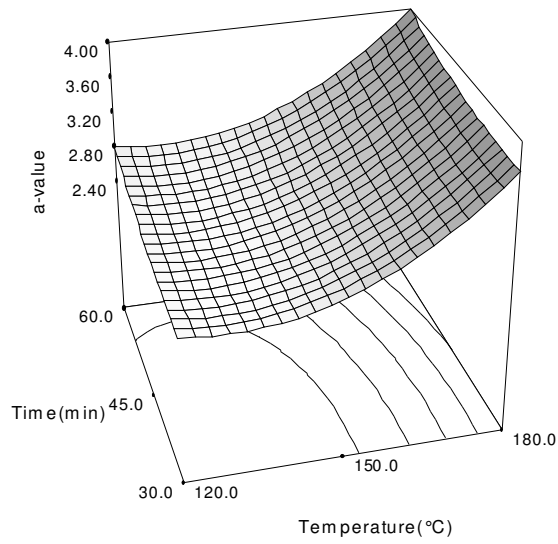


Figure 3.11 Response surface for redness (a-value) of sesame seeds roasted in a hot air roaster

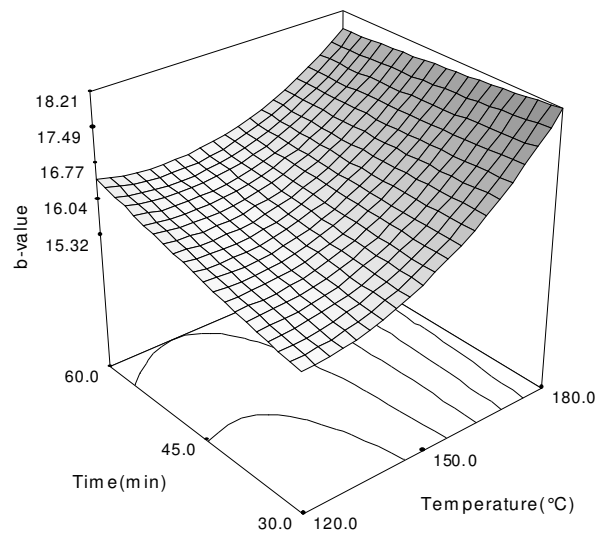


Figure 3.12 Response surface for yellowness (b-value) of sesame seeds roasted in a hot air roaster

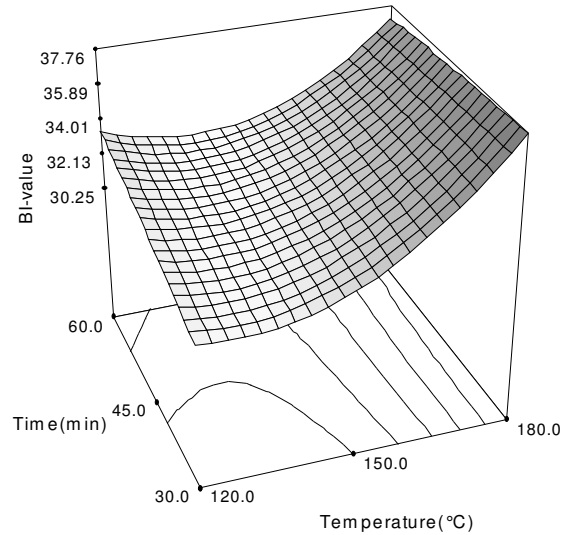


Figure 3.13 Response surface for browning index (BI) of sesame seeds roasted in a hot air roaster

The decrease of hardness and fracturability of sesame during roasting process are shown in Figure 3.14. Regardless of the roasting temperatures, the trend of textural parameters as a function of the corresponding time was almost similar, showing a progressive and significant decrease ( $P < 0.05$ ) as exposure time increased, indicating a progressive reduction in the strength of the seed.

The decrease in hardness shows that at the same deformation, the required force to break the seed decreased with an increase in roasting time and temperature. Similarly, in all cases, as the roasting time increased, the fracturability decreased. Saklar et al. (1999) also observed the decrease in the fracturability during the roasting of hazelnuts. The coefficient of determinations of the proposed models that described the textural changes during roasting process were found lower than color parameters ones. Model fitting showed no lack-of-fit, regardless of low coefficient of determinations. Therefore models could be used for the prediction of textural parameters through the experimental design space. The significant linear temperature effects were found for hardness and fracturability models (Table 3.10). The linear regression equation could be used for both textural parameters.

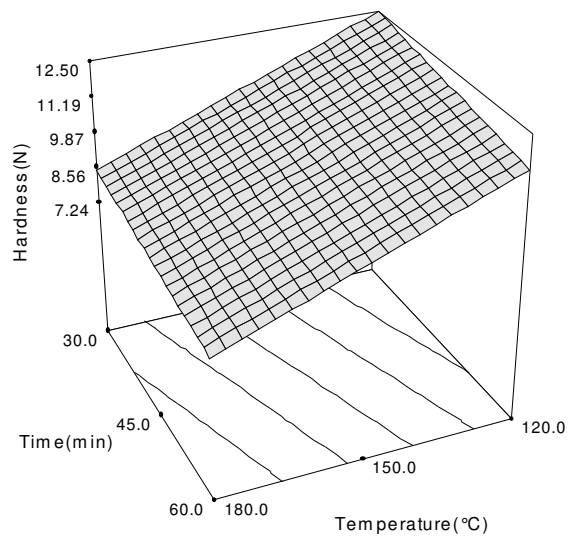
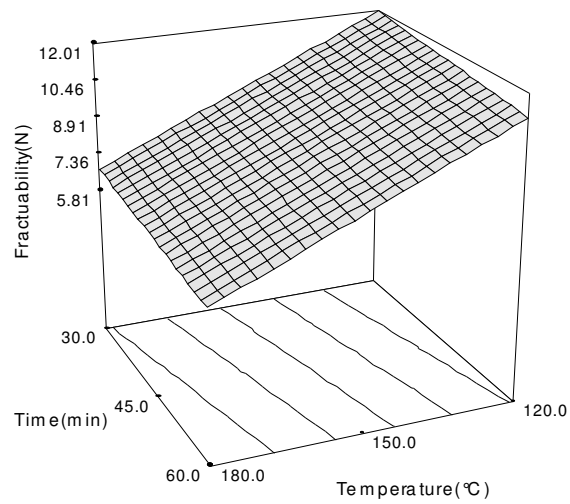


Figure 3.14 Response surface for textural parameters of sesame seeds roasted in a hot air roaster

The hardness values of sesame seeds during hot air roasting changed from 7.27 (193°C-45 min) to 15.63 N (108°C-45 min). This was similar to the values obtained from conventionally roasted sesame at rotary drum roaster. The linear shape of

response surface was observed for textural properties. As roasting temperature and time increased the textural responses of the seeds decreased.

One of the main purposes of RSM design is to find the optimum conditions for a process. For roasted sesame seeds, color and textural properties are the main responses that determine the degree of roasting. Since multiple responses exist for quality determination, desirability functions were used for optimization.

The determination of an optimum operating range for the roasting process only in terms of the roasting time and temperature is not highly reproducible procedure, because the data will vary according to the type of roaster and the scale of process (Simal et al. 2005). However, color and textural properties of sesame seeds during the process can be used as reference standards to characterize the range of an optimum roasting degree for a given type of seed. Therefore, to characterize the optimum operating conditions for hot air roasting process, the target properties of roasted sesame seed for paste production were selected as; L-value: 61-64, a-value: 2.5-3.5, b-value: 16-18, hardness: 7-12 N and fracturability: 5-8 by considering the commercially produced samples.

Desirability function response surface is shown in Figure 3.15 for obtaining target values for roasted sesame seed. The region at which the highest possible desirability functions could be acceptable as the optimum operating conditions for hot air roasting of sesame seeds to produce sesame paste. The optimum roasting range for production of sesame paste from dehulled brown sesame seeds was found to be 155-170°C for temperature and 40-60 min for time. According to the desired product type (e.g. light roasted, dark roasted sesame), the optimum operating conditions could be determined using desirability function for further process and product optimization.

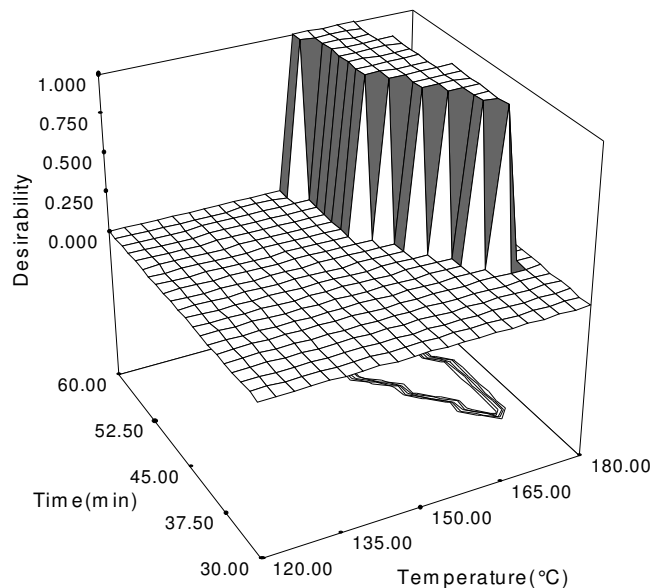


Figure 3.15 Desirability function response surface for the sesame seeds roasted in a hot air roaster

### 3.5.3 Electric oven roasting (EOR)

The experimental data for the color parameters (L-, a-, b, and BI-values), textural properties (hardness, fracturability) and moisture content are given in Table A.3. The result of sum of squares of sequential models and lack of fit tests with  $r^2$  are also shown in Table A.4. The results indicated that the quadratic model would be suggested to describe the response parameters except the fracturability that was described by linear model.

The coefficients of determination ranged from 0.97 to 0.98 for color parameters except b-value, which is 0.80. These values may be acceptable as satisfactory for adequacy of proposed models. But when lack of fit test results was investigated, it was seen that suggested models had significant lack-of-fit value that is not desirable.

The regressions coefficients are given in Table 3.11. Roasting temperature and time generally affect the color of the product. It was observed that the linear terms of roasting temperature and roasting time significantly affected L-, a-, and BI-value of the roasted sesame seeds. But only the quadratic term of temperature was found

important for L-, a- and BI-values. On the other hand for b-value only linear term of roasting temperature was found significant.

Table 3.11 Regression equation coefficients for response parameters of sesame seed that roasted in an electrical oven in terms of coded terms<sup>a</sup>

Regression constants	L-value	a-value	b-value	BI	Hardness (N)	Fracturability (N)	MC (g/kg, db)
$b_0$	61.92	4.48	18.92	41.11	6.50	5.63	5.75
$b_1$	-3.76 (S)	1.54 (S)	0.36 (S)	6.40 (S)	-0.50 (S)	-0.61(S)	-0.66 (S)
$b_2$	-1.01 (S)	0.37 (S)	-0.03 (NS)	1.40 (S)	-0.35 (S)	-0.15(NS)	-0.06 (NS)
$b_3$	-2.51 (S)	0.60 (S)	-0.57 (S)	2.17 (S)	0.38 (S)		-0.53 (S)
$b_4$	-0.48 (NS)	0.27 (S)	0.18 (NS)	1.07 (NS)	0.21 (NS)		-0.05 (NS)
$b_5$	-1.52 (S)	0.63 (S)	0.02 (NS)	2.35 (S)	0.15 (NS)		0.12 (NS)

<sup>a</sup>  $Y = b_0 + b_1x_1 + b_2x_2 + b_3x_1x_2 + b_4x_1^2 + b_5x_2^2$  where  $x_1$ = roasting temperature, °C,  $x_2$ = roasting time, min, S: Significant at  $P < 0.05$ ; NS: not significant

The regression equations were used to generate response surfaces for all responses. The response surface plots of color values are shown in Figure 3.16-3.19. The shape of response surfaces differed between color values. The shape of response surface for the L-value seemed as decreasing ridge when temperature and time increased (Figure 3.16). The L-value ranged from 49.25 to 63.45. As it was observed in conventional roasting process, the changes in the L-value could be divided into two part; initial lightening and main browning period. The initial lightening and main browning period during roasting were previously reported for peanuts by Moss and Otten (1989) and for hazelnuts by Özdemir and Devres (2000). In electrical oven roasting process, as temperature increased, these two periods could be detected easily.

The response surface of a-value of sesame seeds showed rising ridge shape (Figure 3.17). The a-value ranged from 3.06 to 8.27. These values were higher than that obtained from conventional roasting process. This difference may result from the difference in temperature and moisture distribution. The higher a-values related to an increase in redness are indication of browning.

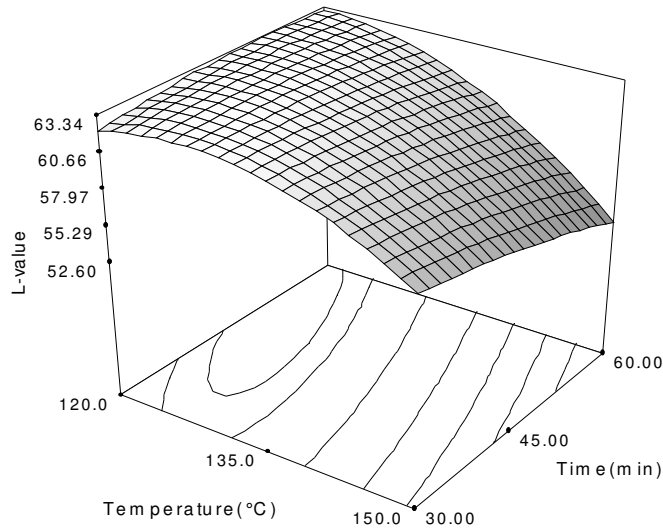


Figure 3.16 Response surface plots for L-value of sesame seeds that roasted in an electrical oven

The response surface of b-value showed saddle shape. The only roasting temperature was found as main parameter that affects the b-value. The range of b-values (17-19) was lower than that obtained from conventional roasting. The shape of response surface of BI was similar to that of a-value (Figure 3.19). As roasting temperature and time increased the BI value remained constant for a short period of time and then increased and this effect pronounced at higher temperature and time.

The results of RSM showed that the roasting time and temperature are the main factors that governing color changes except b-value. In contrast to our results, Özdemir and Devres (2000b) stated that roasting time was insignificant for color attributes of hazelnut.

Among the color values of roasted sesame seeds, the b-value is not suitable for monitoring sesame seed roasting that was accomplished in electrical oven since it is not affected by roasting time. The L- and a-values and BI are significantly affected by roasting conditions; hence, all of them should be considered to monitor the color changes during electrical oven roasting of sesame seeds. Since there are two main periods for color changes, more narrow temperature and time range should be studied to improve better predictive models.

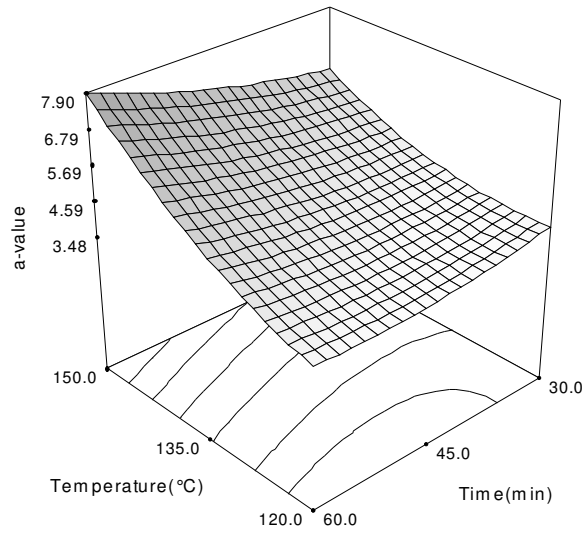


Figure 3.17 Response surface plots for a-value of sesame seeds that roasted in an electrical oven

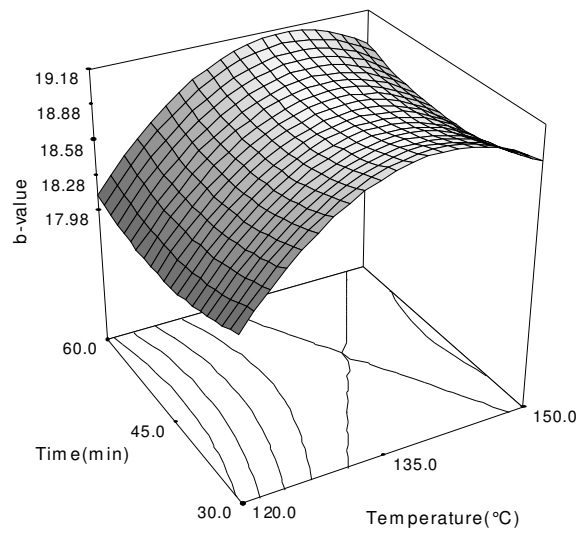


Figure 3.18 Response surface plots for b-value of sesame seeds that roasted in an electrical oven



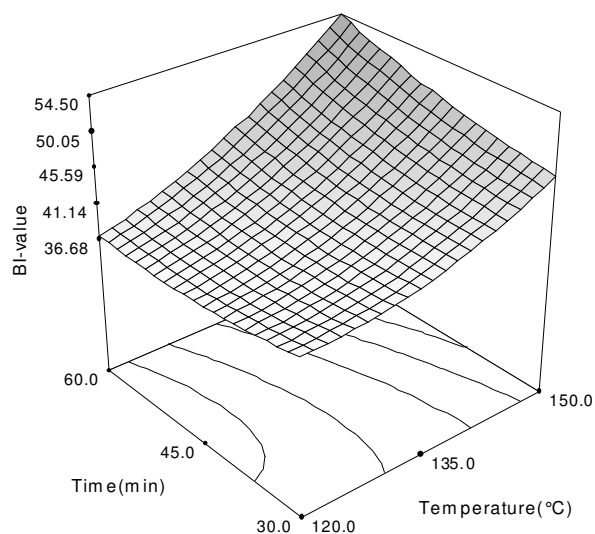


Figure 3.19 Response surface for browning index (BI) of sesame seeds roasted in an electrical oven

The coefficient of determinations of the proposed models that described the textural changes during roasting process were found lower than color parameters ones. Model fitting showed no lack-of-fit, although their low coefficient of determinations, they might be used for prediction of response parameters through the experimental design space. The significant linear temperature effects were found for hardness and fracturability models. The roasting time was also important for hardness but it was found insignificant for fracturability (Table 3.11). The linear regression equation could be used for both parameters. The quadratic model also could be suggested for hardness changes.

The response surface of instrumental hardness and fracturability are shown in Figures 3.20-3.21. The shape of response surface for hardness like decreasing ridge, as roasting temperature and time increased the hardness of the seeds decreased. The response surface of fracturability showed linear changes with temperatures.

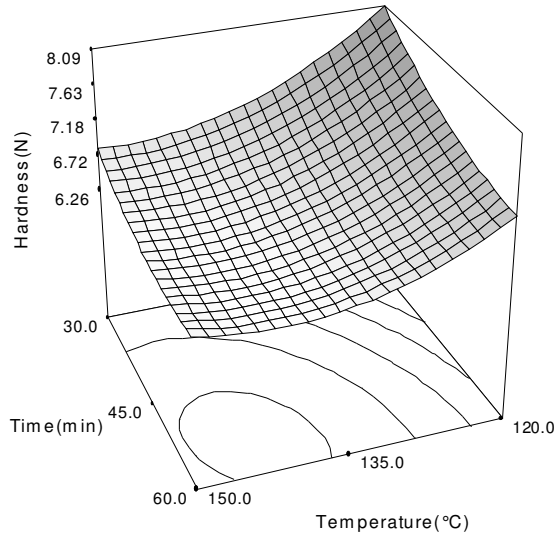


Figure 3.20 Response surface plots for hardness of sesame seeds that roasted in an electrical oven

The results RSM showed that hardness would be satisfactorily described by quadratic model but any model of RSM would not describe fracturability changes. The moisture content change was adequately described by quadratic model ( $r^2 = 0.94$ ) in the design points (Figure 3.22). But significant lack-of-fit makes it difficult to use as a predictive model. The result of statistical analysis showed that roasting temperature was the main factor that affects the moisture content.

One of the main purposes of RSM design is to find the optimum condition for a process. For roasted sesame seeds, color and textural properties are the main responses that determine roast degree. Since multiple responses exist, desirability functions were used for optimization. In EOR process the selection of L-, and a-values and hardness might be more suitable to monitor the roasting process. The optimum conditions for production of sesame paste, if the properties of roasted sesame were selected as: L-value: 60, a-value: 4-5 and hardness: 6-7. The optimum operating region found as shown in Figure 3.23.

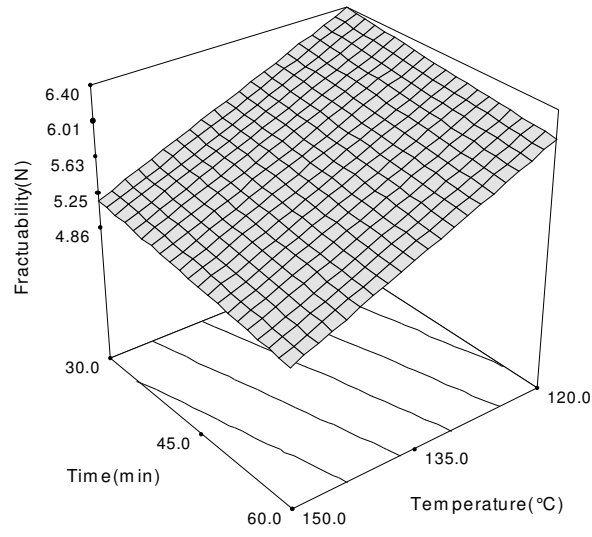


Figure 3.21 Response surface plots for fracturability of sesame seeds that roasted in an electrical oven

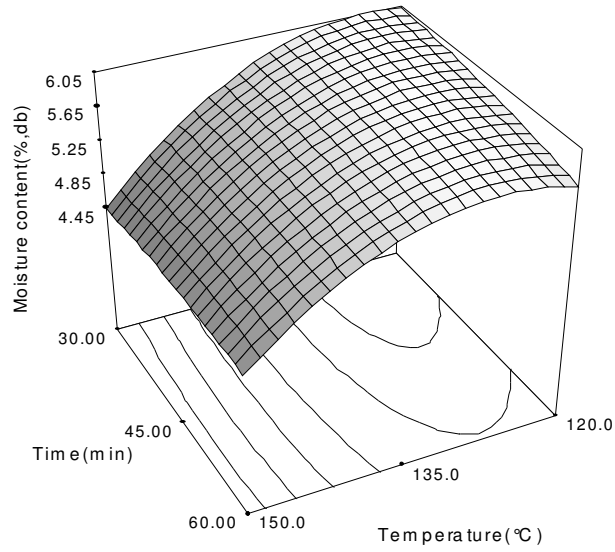


Figure 3.22 Response surface plots for moisture content of sesame seeds that roasted in an electrical oven

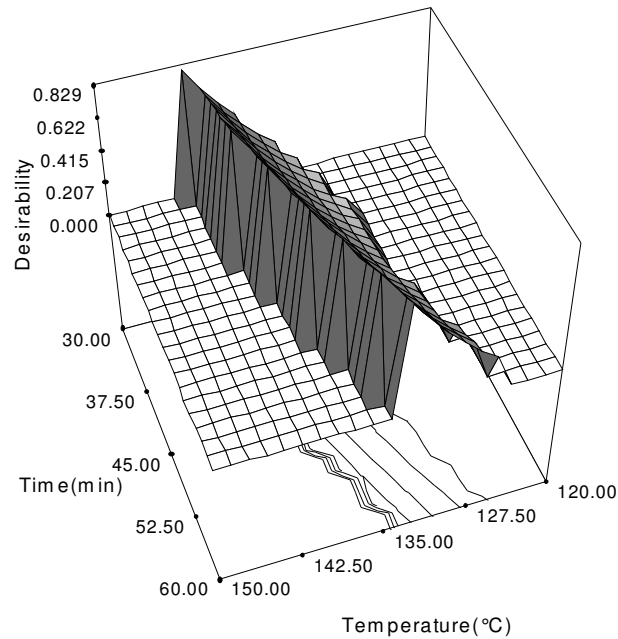


Figure 3.23 Desirability function response surface plot for the sesame seeds that roasted in an electrical oven

### 3.5.4 Vacuum Oven Roasting (VOR)

The experimental data for the color parameters ( $L$ -,  $a$ -,  $b$ -, and BI-value), textural properties (hardness, fracturability) and changes in moisture content for vacuum oven roasted samples are given in Table A.5. A summary of the linear, cross-product and quadratic terms for all responses are given in Table A.6. The coefficient of determinations ranged from 0.68 to 0.96 for color parameters with no lack-of-fit except BI. The  $L$ - and  $a$ -value models could be adequately used as the predictor models.

The regressions coefficients are given in Table 3.12. It was observed that the linear and quadratic terms of roasting temperature significantly affect  $L$ -value of the roasted sesame seeds. On the other hand for  $b$ -values only the linear terms of temperature and time were found as significant ( $P < 0.05$ ). The roasting temperature was also found important factor that affects  $a$ -value. Similar to HAR method, it was observed that quadratic term of the time was also significant for  $L$ -value model. These results show that the roasting temperature and exposure time could be accepted as the main factors governing the  $L$ -,  $b$ - and BI-values in sesame seeds

during the VOR process. The a-value is only significantly affected only by roasting temperature.

Table 3.12 Regression equation coefficients for response parameters of sesame seed that roasted in the vacuum oven in terms of coded terms<sup>a</sup>

Regression constants	L-value	a-value	b-value	BI	Hardness (N)	Fracturability (N)	MC (g/kg, db)
$b_0$	64.94	2.34	10.80	31.08	12.35	9.56	2.93
$b_1$	-0.91 (S)	0.42 (S)	0.03 (S)	2.12 (S)	-2.92 (S)	-2.28 (S)	-0.19(S)
$b_2$	-0.54 (S)	0.11	0.02 (S)	1.19 (S)	-1.34 (NS)	-0.94 (S)	-0.17(S)
$b_3$	-1.31 (S)			1.11 (S)	2.39 (S)		
$b_4$	-1.25 (S)			0.24 (NS)	0.19 (NS)		
$b_5$	0.32 (NS)			0.56 (NS)	-0.46 (NS)		

<sup>a</sup> $Y = b_0 + b_1x_1 + b_2x_2 + b_3x_1x_2 + b_4x_1^2 + b_5x_2^2$  where  $x_1$ = roasting temperature, °C,  $x_2$ = roasting time, min, S: Significant at  $P < 0.05$ ; NS: not significant

The regression equations were used to generate response surfaces for all responses. The response surface plots of color values are shown in Figures 3.24-3.26. The shape of response surfaces differed between color values. The L-value ranged from 60.44 to 65.52. These values were higher than that obtained from EOR, CR and similar to HAR process (Figure 3.24).

The response surface of a-value showed linear raising behavior (Figure 3.25). The range of a-values was 1.83-3.2 that was lower than that obtained from all other roasting plots. The b-value showed similar responses surface shape with a-value (Figure 3.26). The b-values obtained from VOR were lower than that of EOR and CR and similar to HAR values. On the other hand similar BI value obtained with EOR and HAR process (Figure 3.27). The result of RSM analysis showed that L-value should be considered to monitor the color changes during roasting of sesame seed in vacuum oven.

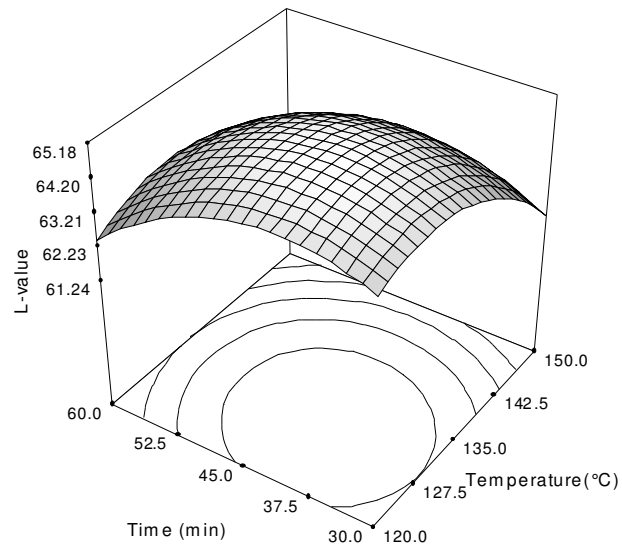


Figure 3.24 Response surface plots for L-value of sesame seeds that roasted in a vacuum oven

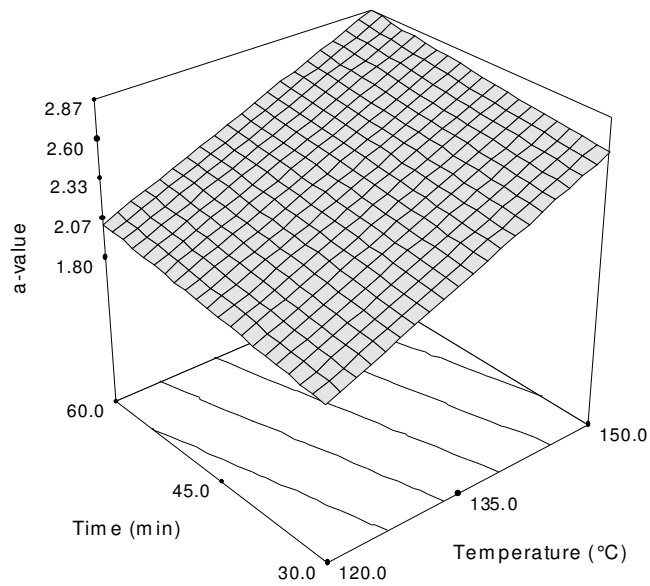


Figure 3.25 Response surface plots for a-value of sesame seeds that roasted in a vacuum oven

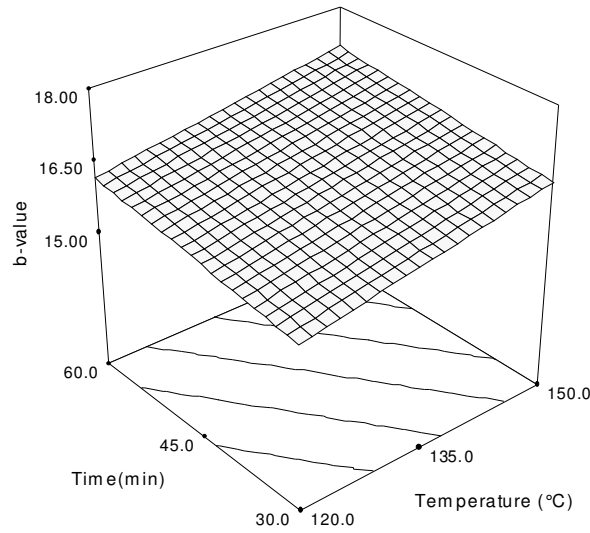


Figure 3.26 Response surface plots for b-value of sesame seeds that roasted in a vacuum oven

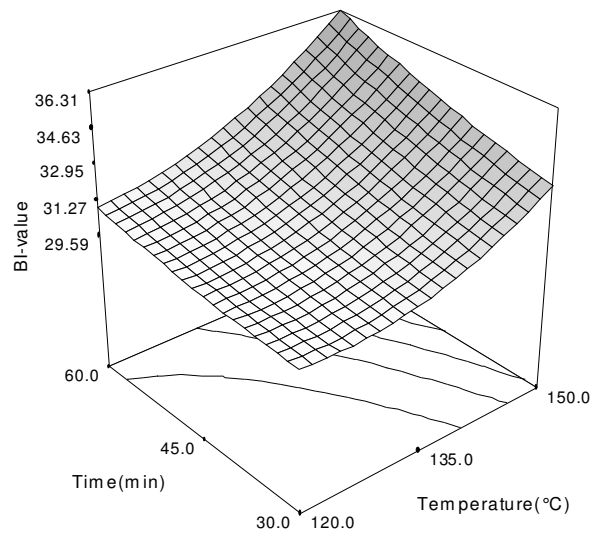


Figure 3.27 Response surface plots for BI-value of sesame seeds that roasted in vacuum oven

The high hardness values of sesame seeds were observed in VOR method (7-20 N). Those values were higher than the values of all other roasting methods. Similar fracturability values were obtained with HAR method. These results suggested that vacuum roasting is not so effective on the reduction of textural degradation. The

response surface of instrumental hardness and fracturability are shown in Figures 3.28-3.29, respectively. The linear shape of response surface was observed for fracturability, as roasting temperature and time increased the textural responses of the seeds decreased.

The moisture content change was not adequately described by linear model ( $r^2 = 0.71$ ). The shape of response surface of moisture content changes was given in Figure 3.30. The result of statistical analysis showed that roasting temperature was the main factor that affects the moisture content. The application of response surface methodology, to develop a predictive model that described the moisture changes during roasting of sesame was not successful.

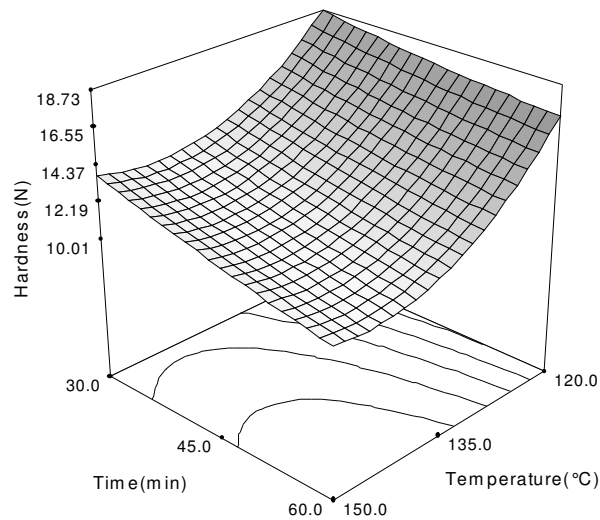


Figure 3.28 Response surface plots for hardness of sesame seeds that roasted in a vacuum oven



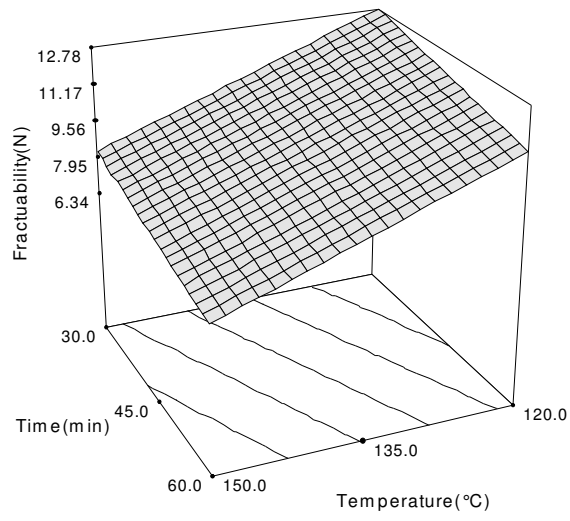


Figure 3.29 Response surface plots for fracturability of sesame seeds that roasted in a vacuum oven

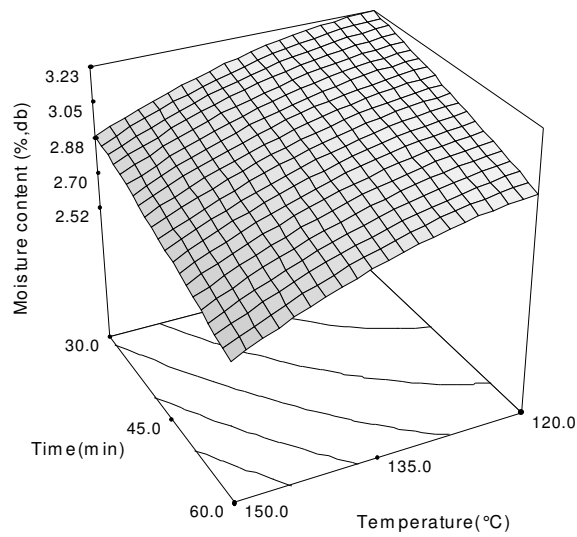


Figure 3.30 Response surface plots for moisture content of sesame seeds that roasted in a vacuum oven

In VOR process the selection of L-, a- , b- values and fracturability might be suitable to monitor the roasting process. The optimum operating region found as shown in Figure 3.31, if the properties of roasted sesame were selected as; L-value: 61-65, a-value: 2.5-3.0, b-value: 16-17, and fracturability: 6-10 N.

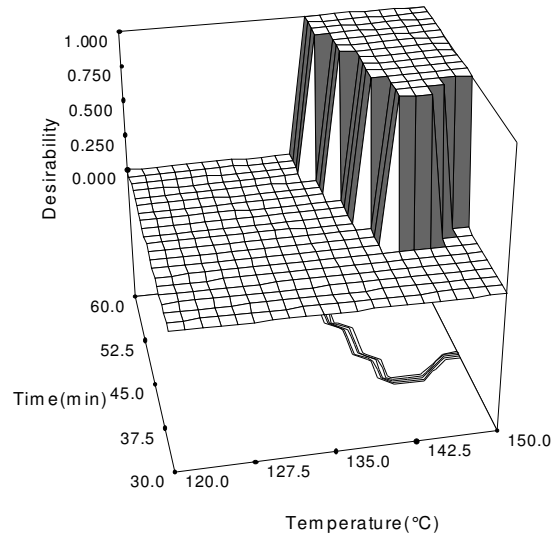


Figure 3.31 Desirability function response surface plot for the sesame seeds that roasted in vacuum oven

### 3.6 Conclusions

Roasting is one of the most important step of the sesame seed processing. In this study, some of the physical changes of sesame seeds occurred during roasting process were investigated and described using mathematical models. The sesame seeds were roasted using conventional, hot air, electrical oven, and vacuum oven methods. The conclusions of the study were listed below:

1. As the roasting temperature and time were increased the moisture content of sesame seeds decreased for all roasting methods. The whiteness of seeds initially increased and then decreased during the roasting process. The increase in the redness and yellowness of sesame seeds were observed by increasing temperature and exposure time. Sesame seeds become more fracture and less hard with the effect of roasting that might be evidence of crisp texture.

2. It was found that roasting/drying characteristic of sesame seeds in conventional roasting process was satisfactorily described by empirical two-parameter exponential model and Page model. The temperature dependence of moisture content changes was described by linear function relationship.

3. The kinetics of color changes during conventional roasting of sesame seeds were adequately defined by cubic polynomial models. The linear relationship was found between coefficients of cubic model and roasting temperature by using the one-step nonlinear regression analysis. The generalized models (functions of temperature and time) can be used to predict the color changes during roasting of sesame. The reduction in hardness and fracturability of sesame seeds during conventional roasting was satisfactorily described by zero-order kinetic model. The temperature dependence of these models was evaluated by Arrhenius type model.

4. As a result of this study, it is possible to estimate the optimum process conditions for obtaining desired sesame seed characteristics using the parameters of the derived models.

5. The study revealed that the response surface methodology could be used to develop adequate prediction models for describing color and texture changes in sesame seeds during hot air roasting. The changes in the color values and textural parameters were adequately described by quadratic and linear models, respectively. The roasting temperature was found as the main factor affecting the color development and texture degradation of sesame seeds during roasting. The successful optimization for sesame roasting process can also be made using desirability functions in response surface methodology.

6. The optimum roasting conditions to product sesame paste were determined for each method using RSM. The results of response surface analysis showed that roasting temperature and time were the main factors for color changes in electrical oven roasting process. Prediction models derived from quadratic equation, described color parameters. Hardness satisfactorily described by quadratic model but fracturability by linear model.

7. The a-value was only significantly affected only by roasting temperature of the vacuum oven. The linear models satisfactorily described most of the roasting

parameters, but quadratic models described L-value and hardness. The L-, a-, b-values and fracturability could be used for optimization of vacuum roasting process.

8. The application of response surface analysis showed that, the prediction models for each physical parameters of roasted sesame depends on the roasting method. For each method, different models and parameters should be used to control the roasting.

Further research about the effect of initial composition of sesame is necessary for developing more sensitive predictive control models.

## CHAPTER 4

### INFLUENCE OF DEHULLING AND ROASTING PROCESS ON THE THERMODYNAMICS OF MOISTURE ADSORPTION IN SESAME SEED

#### 4.1 Introduction

Water activity has long been considered as one of the most important quality factors in food systems especially for long-term storage, drying and roasting operations. The determination of water activity and moisture content relation is described by moisture sorption isotherms (MSI). Several empirical and semi-empirical equations have been proposed to correlate equilibrium moisture content, temperature and  $a_w$  (Chirife and Iglesias, 1978). The Guggenheim-Anderson-de Boer (GAB) and Halsey models were mostly applied to describe the sorption isotherms of foods (McMinn and Magee, 2003).

The application of thermodynamic principles to sorption isotherm data has been used to obtain more information about the dehydration process energy requirement, the properties of water, food microstructure, and physical phenomena on the food surfaces, and sorption kinetic parameters. The net isosteric heat of adsorption ( $q_{st}$ ), differential entropy ( $S_d$ ), spreading pressure ( $\Phi$ ), net integral enthalpy ( $Q_{in}$ ) and net integral entropy ( $S_{in}$ ) are used as thermodynamic functions for analysis of sorption isotherms (Rizvi and Benado, 1984; Aviara and Ajibola, 2002; McMinn and Magee, 2003; Aviara et al. 2004; Kaya and Kahyaoglu, 2005). The changes in integral enthalpy may provide a measure of the energy changes occurring upon mixing of water molecules with sorbent during sorption processes (Telis et al. 2000). The differential entropy ( $S_d$ ) of a material may be related to the number of available sorption sites at a specific energy level (Madamba, et al. 1996b).

The changes in entropy could be used in exergy balance giving valuable information about energy utilization in food processing (Rotstein, 1983). Also, the order/disorder concept, useful for the interpretation of processes that take place during moisture sorption such as dissolution, crystallization and swelling, is related with entropy variation (Aviara et al. 2002). The spreading pressure ( $\Phi$ ), or surface potential, represents the surface free energy of adsorption and can be regarded as the difference in the surface tension between bare sorption sites in the solid and sorbed molecules (Al-Muhtaseb et al. 2004).

Whole sesame seeds (WS) are generally used for oil production and some types of bakery foods. Dehulled seeds (DS) also have been consumed in baked goods such as breads, hamburger buns, cakes, cookies, confections and snack foods. In many countries (Middle-East, Mediterranean and Oriental) dehulled roasted sesame seeds (DRS) are used for producing sesame paste (called tahin, tehina, tahina or matahina) (El-Adawy and Mansour, 2000; Lokumcu and Ak, 2005). The effective design of roasting, drying and storage systems for both three forms of sesame seeds (whole, dehulled and dehulled-roasted) needs knowledge of their energy requirements and the state and mode of the moisture sorption with them (Aviara and Ajibola, 2002).

The objectives of this study were to obtain MSI data of the WS, DS, and DRS samples, to evaluate the best MSI equation to fit the experimental data, and to determine the effect of dehulling and roasting on the thermodynamic parameters of sesame seed (net isosteric heat of adsorption, differential entropy, spreading pressure, net integral enthalpy, and net integral entropy) in relation to moisture adsorption.

#### **4.2 Isotherm Models**

There are many equations to define MSI. For the purpose of this work, two isotherm models were chosen to fit the experimental sorption data; three-parameter GAB model GAB (Eq. (4.1); Van den Berg, 1985) and two-parameter Halsey model (Eq. (4.2); Halsey, 1948). The GAB model application is preferred to determine not only the MSI relation but also to define  $m_0$ . Halsey model has been reported as the best equation for the sesame seed sorption data (Ajibola and Dairo, 1998).

$$m = \left( \frac{m_o C k a_w}{(1 - k a_w)(1 - k a_w + k C a_w)} \right) \quad (4.1)$$

$$m = \left( \frac{-a}{\ln(a_w)} \right) l/r \quad (4.2)$$

The parameters of the models used were estimated by the nonlinear regression procedure of SigmaPlot (SPSS Inc.). The criterion used to evaluate goodness of fit of experimental sorption data was defined as the mean deviation modulus (Tolaba et al. 1995):

$$\% E = \frac{100}{n} \sum_{i=1}^n \frac{|M_i - M_{pi}|}{M_i} \quad (4.3)$$

A model is considered acceptable if values for E are below 10% (Arslan and Toğrul, 2005).

### 4.3 Net Isotheric Heat of Adsorption

The net isotheric heat of adsorption ( $q_{st}$ ) is obtained by subtraction of heat of water vaporization from the isotheric heat of adsorption ( $Q_{st}$ ). The  $q_{st}$  could be determined by applying the Clausius-Clayperon equation to data from the best fitting equation (Rizvi, 1986):

$$\left[ \frac{\partial \ln(a_w)}{\partial \left( \frac{1}{T} \right)} \right]_m = - \frac{Q_{st} - \lambda}{R} = - \frac{q_{st}}{R} \quad (4.4)$$

The net isotheric heat of adsorption was determined from the slope after plotting the  $\ln(a_w)$  from the best fitting equation *versus*  $1/T$ , for specific moisture content. This approach assumes that isotheric heat of adsorption does not change with temperature.

#### 4.4 Differential Entropy

The differential entropy ( $S_d$ ) of adsorption can be calculated from Gibbs-Helmholtz equation as follows:

$$S_d = \frac{Q_{st} - G}{T} \quad (4.5)$$

where free Gibbs energy is calculated as

$$G = -RT \ln a_w \quad (4.6)$$

Substituting Eq. (4.6) into Eq. (4.5), and after rearranging, the final form is (McMinn and Magee, 2003):

$$-\ln(a_w) \Big|_m = \frac{Q_{st}}{RT} - \frac{S_d}{R} \quad (4.7)$$

By plotting  $\ln(a_w)$  versus  $1/T$ , for a constant moisture content ( $m$ ), the  $S_d$  can be determined from the intercept ( $S_d/R$ ). The  $S_d$  values at different moisture contents were used to determine the relation between  $S_d$  and moisture content.

#### 4.5 Spreading Pressure

The spreading pressure is the two-dimensional analog of pressure, having units of force per unit length, akin to surface tension. It can be viewed as the force in the plane of the surface that must be exerted perpendicular to each unit length of edge to keep the surface from spreading (Smith et al. 2001). Skaar and Babiak (1982) used the spreading pressure concept as the driving force in developing transport models during diffusion in porous solid. The spreading pressure is not subject to direct experimental measurement; it can be estimated using an analytical procedure such as described by (Fasina et al. 1999) from the relationship:

$$\varphi = \frac{KT}{A_m} \int_0^{a_w} \frac{\theta}{a_w} d(a_w) \quad (4.8)$$

where  $\theta = m/m_0$ .



The value of the spreading pressure will be indeterminate at a value for  $a_w = 0$ . Therefore, the lower limit was taken as  $a_w = 0.05$  in Eq. (4.8). The computed values of spreading pressure is adjusted by adding the value corresponding to the interval  $a_w = 0-0.05$ , which was calculated by assuming that there is a linear relationship (Henry's law) between  $m$  and  $a_w$  (Fasina et al. 1999).

The spreading pressure was estimated using analytical procedures that use the empirical relationship between moisture content and water activity. The Halsey equation was used to describe the  $m$  and  $a_w$  relation (Aviara et al. 2002; McMinn and Magee, 2003). Substituting the Halsey equation into Eq. (4.8), and rearranging, final form is;

$$\varphi = \frac{KT}{A_m} a_w^{1/r} \left[ \frac{I}{\left(\frac{I}{r} - 1\right) (-\ln(a_w))^{1-r}} \right]_{0.05}^{a_w} \quad (4.9)$$

#### 4.6 Net integral enthalpy and entropy

The net integral enthalpy is analogous to isosteric heat of sorption. However, while isosteric heat of sorption is a reversible process at a constant pressure, the equilibrium heat of sorption refers to constant pressure and constant spreading pressure as obtained from the Gibbs equation (Hill and Rizvi, 1982). The equation given below is used for calculation of the net integral enthalpy,  $Q_{in}$  :

$$\left. \frac{[\partial \ln a_w]}{\partial \left(\frac{1}{T}\right)} \right|_{\varphi} \approx -\frac{Q_{in}}{R} \quad (4.10)$$

A plot of  $\ln(a_w)$  versus  $1/T$  at constant spreading pressure gives the net integral enthalpy from the slope of straight line obtained. The changes in net integral enthalpy with moisture content represent the level to which water/substrate interaction is greater than interaction of water molecules (Fasina et al. 1999).

The net integral entropy (molar entropy) for a thermodynamic system is calculated from the following equation (Benado and Rizvi, 1985):

$$S_{in} = \frac{-Q_{in}}{T} - R \ln(a_w^*) \quad (4.11)$$

where  $a_w^*$  is the geometric mean water activity obtained at constant spreading pressure at different temperatures.

## **4.7 Materials and Methods**

### **4.7.1 Preparation of the sesame seed samples**

Turkish cultivars brown sesame seeds (Gaziantep region, season 2003), were used in this study. Mechanically dehulled sesame seeds are generally used in the production of sesame paste, therefore sesame seeds were dehulled as follows; firstly seeds were sieved and then soaked in water ( $T = 18 \pm 2^\circ\text{C}$ ) for 12 h. The soaked seed were strained off and passed through a mechanical peeler for removing of hulls from seed. The hulls and other foreign materials were separated from seed by using salt solutions (first 18% and then 15% NaCl solutions). The seeds were taken from surface of solution batches and then washed with water many times to remove the salt. The cleaned sesame seeds were centrifuged (at 1400 rpm for 20 min) to reduce the water content from the surface of seeds (wet dehulled sesame seeds).

The wet dehulled sesame seeds (25 kg) were roasted using a temperature-controlled rotary roasting machine (Gürmaksan Co., Turkey) at roasting temperature of  $150^\circ\text{C}$  for 100 min. The final characteristics of roasted sesame seed were determined in previous study as L-, a-, b-values and moisture content were 60.1, 4.1, 17.5 and 1.5% (db), respectively. The different sesame seeds are coded as WS, DS, and DRS, which correspond to whole, dehulled and dehulled-roasted sesame seeds respectively.

### **4.7.2 Moisture sorption measurements**

Moisture adsorption isotherms of WS, DS and DRS samples were determined according to the gravimetric static method as described by Labuza (1984). The samples were dried completely in a vacuum oven at  $40 \pm 2^\circ\text{C}$  (40 Torr). Nine saturated solutions (KAc,  $\text{MgCl}_2$ ,  $\text{K}_2\text{CO}_3$ ,  $\text{MgNO}_3$ , KI, KCl,  $\text{KNO}_3$ , and NaCl and

NaOH) were used to provide water activities ranging from 0.06 to 0.98. Saturated solutions were prepared at each temperature studied. They were placed into separate jars in an amount to occupy a space of about 1 cm deep at the bottom. A small amount of solid salt was added to make sure that solutions remain saturated. A tripod was also placed in each jar. Duplicate samples of  $0.5\pm 0.03$  g of the sesame seeds were weighed into small crucibles of aluminum foil and placed on tripods in the jars, which were then tightly closed. The samples were kept in ovens at 15, 25 and  $35\pm 1^\circ\text{C}$  for equilibration. This required about 4 weeks. At high water activities ( $a_w > 0.75$ ), a small amount of toluene was placed in a capillary tube fixed in the jar to prevent microbial spoilage of the samples (Labuza, 1984). Moisture content of the samples was determined using the vacuum oven method at a temperature of  $70\pm 1^\circ\text{C}$  for 6 h (Tsami et al. 1990). The equilibrium moisture content of the samples was given as g/100 g dry solids.

## **4.8 Results and Discussion**

### **4.8.1 Adsorption isotherms**

The experimental adsorption isotherms of WS, DS, and DRS seed samples obtained at 15, 25, and  $35^\circ\text{C}$  are shown in Figure 4.1. As expected, the equilibrium moisture contents increased with an increase in the water activity at any particular temperature and decreased with increase in temperature at constant water activity. The increased temperature activated the water molecules to a higher energy levels and this allows them break away from their sorption sites, thus decreasing the equilibrium moisture content (Arslan and Toğrul, 2005).

The adsorption isotherms of all sesame seeds samples showed type II behavior according to the BET classification. At a constant water activity, WS samples had higher equilibrium moisture content than the DS and DRS samples. This might be due to the separation of hulls from sesame seeds, since dehulling process reduces the fiber content, which absorbs more water. It was determined that change of temperature was not significant on sorption characteristics of all sesame seed samples in the studied range ( $P > 0.05$ ).

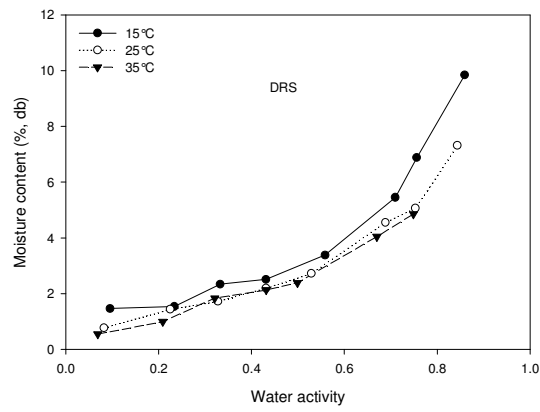
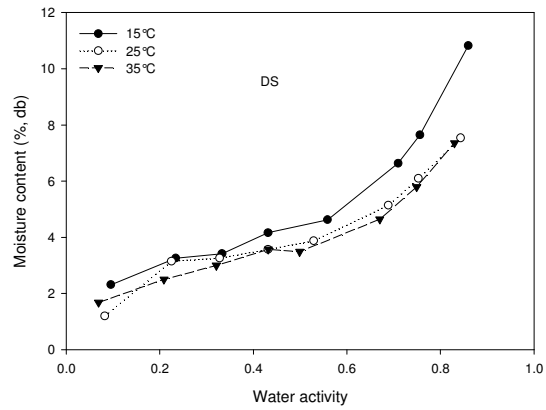
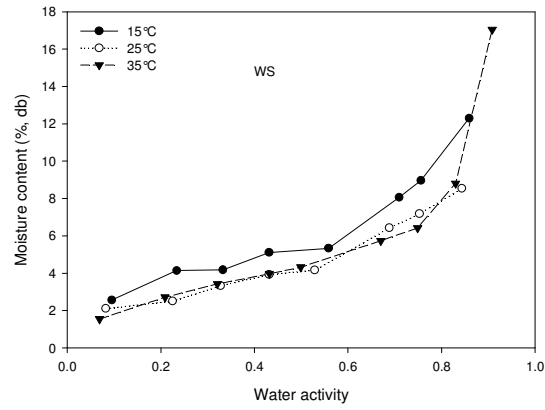


Figure 4.1 Sorption isotherms of whole sesame seed (WS), dehulled sesame seed (DS), and dehulled-roasted sesame seed (DRS) at different temperatures studied

#### 4.8.2 Isotherm equations

The results of nonlinear regression analysis for fitting the GAB and Halsey models to experimental data are shown in Table 4.1 and 4.2, respectively. The models tested were found to be acceptable for predicting the equilibrium moisture content of the seed samples according to the mean deviation modulus (E%) values, except WS samples at 35°C. However, it is possible to state that Halsey and GAB models gave acceptable fit for WS and DRS, respectively. The GAB model gave the important information (monolayer moisture content) for the sesame seed samples, since it is well known that defining  $m_0$  and its respective water activity are important to define storage conditions. Roasting process reduced monolayer moisture content of sesame seeds. The DRS samples had lower monolayer moisture content value than WS and DS samples. The monolayer moisture content shows the amount of water that adsorbed by a single layer to binding sites in the material.

Table 4.1 Estimated parameters and criteria of GAB model for the sesame seed samples

Samples	Constants and criteria	Temperature (°C)		
		15	25	35
WS (whole sesame seed)	$m_0$	3.094	2.656	1.866
	C	53.281	27.802	776.532
	k	0.872	0.832	0.978
	$r^2$	0.9894	0.9864	0.9793
	E	5.006	5.404	13.672
DS (dehulled sesame seed)	$m_0$	2.442	2.623	2.151
	C	104.987	19.0635	54.809
	k	0.901	0.777	0.849
	$r^2$	0.9963	0.9740	0.9899
DRS (dehulled-roasted sesame seed)	E	3.296	9.006	4.426
	$m_0$	1.821	1.645	1.738
	C	12.599	7.494	4.916
	k	0.955	0.929	0.904
	$r^2$	0.9895	0.9957	0.9916
	E	9.178	4.817	7.981

$m_0$ , C, k are the regression constants of GAB model

The water binding properties of active points in roasted seeds were probably reduced; hence, some water sorption active points disappeared (Martinez and Chiralt, 1996). Halsey equation has been widely used to describe the sorption data in literature and also to evaluate the thermodynamic properties of the food products.

Figure 4.2 represents the fitting ability of both equations to adsorption data of DS samples, as an example. Similar results were obtained for the WS and DRS samples.

Table 4.2 Estimated parameters and criteria of Halsey model for the sesame seed samples

Samples	Constants and criteria	Temperature (°C)		
		15	25	35
WS (whole sesame seed)	a	15.933	10.884	4.499
	r	1.854	1.899	1.378
	r <sup>2</sup>	0.9890	0.9799	0.9746
	E	5.261	5.471	11.790
HS (dehulled sesame seed)	a	9.699	10.386	8.459
	r	1.751	2.019	1.924
	r <sup>2</sup>	0.9953	0.9598	0.9912
DRS (dehulled-roasted sesame seed)	E	3.408	13.060	4.476
	a	3.182	2.465	1.991
	r	1.318	1.33	1.196
	r <sup>2</sup>	0.9908	0.9926	0.9829
	E	7.944	6.352	13.253

a and r are the regression constants of Halsey model

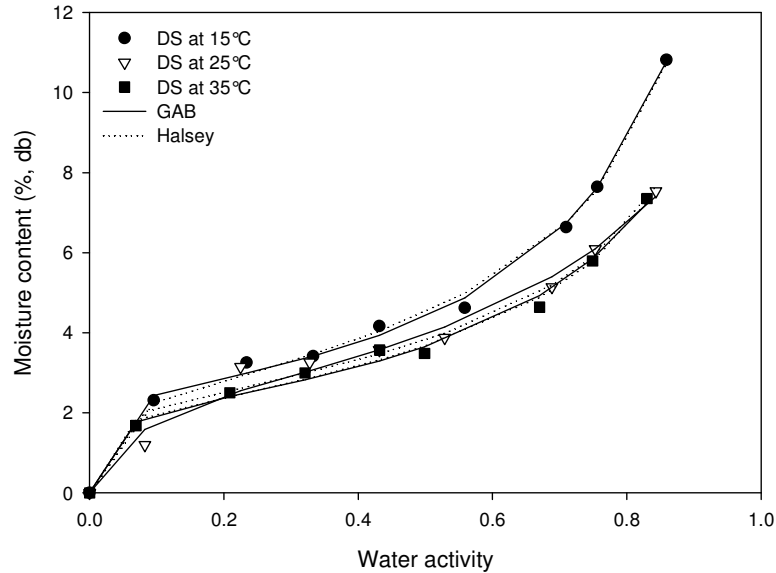


Figure 4.2 Application of GAB and Halsey models to adsorption data of dehusled sesame seed at all temperature range studied

### 4.8.3 Net isosteric heat of adsorption

In order to define effect of temperature, net isosteric heat of sorption ( $q_{st}$ ), a measure of the interaction between water vapor and the adsorbent food material, should be determined. At constant moisture content, water activity values at each studied temperature were determined using Halsey model (since it fitted the experimental data satisfactorily). The net isosteric heats of sorption values were calculated by applying Eq. (4.4) and represented with respect to equilibrium moisture content in Figure 4.3. At low moisture content the heat of sorption is high, indicating the highest binding energy for removal of water. Increasing moisture content decreased the heat of sorption due to reduced water interactions. Roasting process reduced the  $q_{st}$  values of seed samples. The net isosteric heats of sorption of DRS were lower than those of DS and WS samples for all moisture content values.

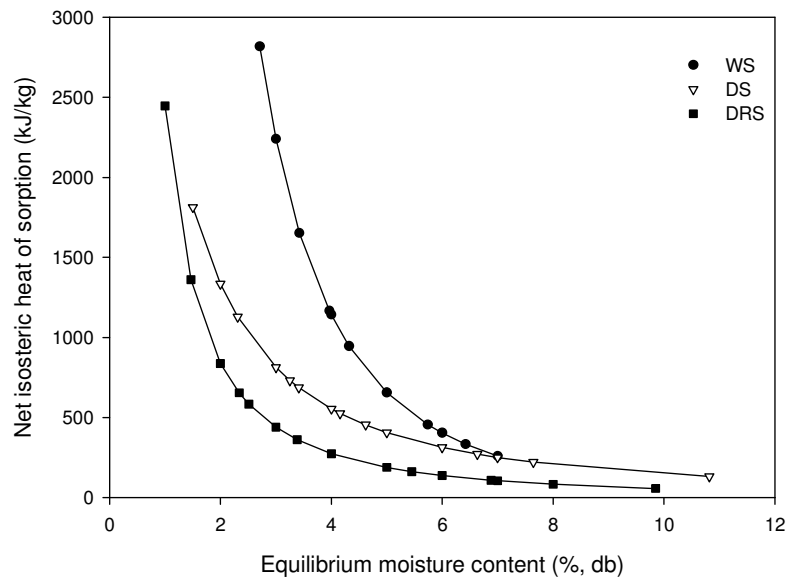


Figure 4.3 Net isosteric heat values of sesame seed samples (WS: whole sesame seed, DS: dehulled sesame seed, and DRS: dehulled-roasted sesame seed) as a function of equilibrium moisture content

These results are in a good agreement with literature, Martinez et al. (1996) reported that the roasting process decreased the heat of sorption values of hazelnut, almond and peanut samples. They suggested that this event might be due to enhancement of lipid-lipid interaction that increases the hydrophobicity of cellular components of seeds. On the other hand, WS, DS and DRS samples also had different  $q_{st}$  in the range of moisture content 2-6% (db), but after 6% moisture content the WS and DS

seeds possessed similar trends of heat of sorption. The knowledge of value of the heat of sorption, at a specific moisture content, enables an indication of the state of sorbed water and hence, a measure of the physical, chemical and microbiological stability of the food material under given storage conditions (McMinn and Magee, 2003).

The net isosteric heat of sorption with respect to equilibrium moisture content was adequately described by the power law relation of the form:

$$\text{For whole sesame seed (WS)} \quad q_{st} = 30768.7m^{-2.39} \quad (r^2 = 0.9997)$$

$$\text{For dehulled sesame seed (DS)} \quad q_{st} = 3071.1m^{-1.24} \quad (r^2 = 0.9969)$$

$$\text{For dehulled-roasted sesame seed (DRS)} \quad q_{st} = 2525.8m^{-1.57} \quad (r^2 = 0.9997)$$

McMinn and Magee (2003) also reported that a power law model was sufficient to express the relationship between net isosteric heat of sorption and moisture content of potato.

#### 4.8.4 Differential entropy

An entropy change takes place in each amount of water that is absorbed. The size of the change varies with the relative vapor pressure at which water is adsorbed. This is the differential entropy of adsorption. Together with the differential enthalpy, it describes the change in Gibbs energy of the water. The experimental and predicted differential entropy and moisture content relations, determined using Eq. (4.7), are shown in Figure 4.4. The differential entropy showed strong dependence on the moisture content. Similar trends were observed for potato starch powder, highly amylose, and highly amylopectin starch powders (Al-Muhtaseb et al. 2004). The power-law model was used to interpret the data and following equation was found;

$$\text{For WS sample} \quad S_d = 101.7m^{-2.46} \quad (r^2 = 0.9989)$$

$$\text{For DS sample} \quad S_d = 6.57m^{-1.05} \quad (r^2 = 0.9872)$$

$$\text{For DRS sample} \quad S_d = 7.07m^{-1.62} \quad (r^2 = 0.9995)$$

#### 4.8.5 Spreading pressure

Eq. (4.9) was used to determine the spreading pressures at studied temperatures. The constants (a and r) were evaluated from the Halsey equation. The spreading pressures



of sesame seed samples are given in Figure 4.5. The results show that the spreading pressure increases with increasing water activity. As temperature increased, spreading pressure values decreased. It was also found that the effect of temperature on the spreading pressure values for WS was significant ( $P < 0.05$ ), however, for the DS and DRS were not. On the other hand, Aviara et al. (2002) found that temperature effect was not significant on spreading pressure of dried sesame seed.

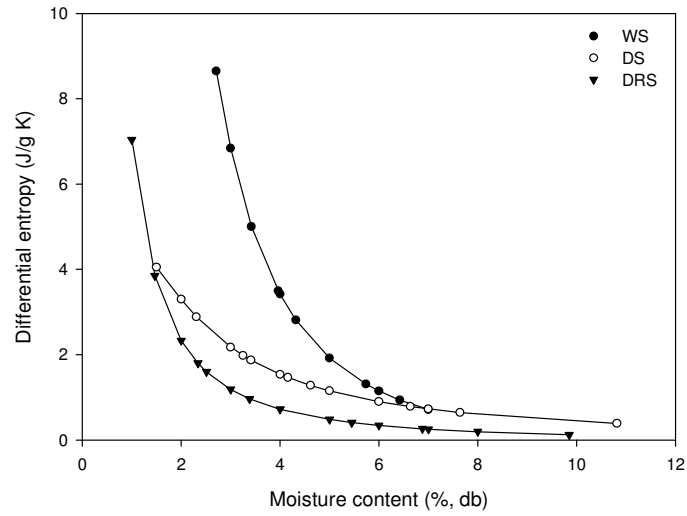


Figure 4.4 Differential entropy of sesame seed sesame seed samples (WS: whole sesame seed, RS: dehulled sesame seed, and DRS: dehulled-roasted sesame seed) as a function of equilibrium moisture content

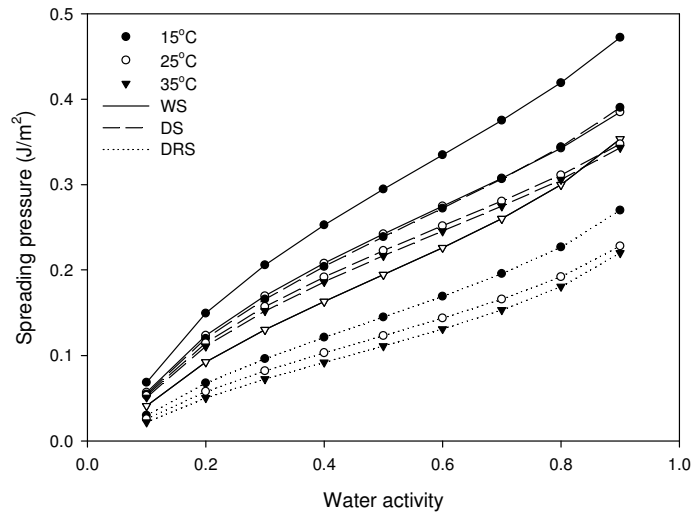


Figure 4.5 Spreading pressure adsorption isotherms for whole sesame seed (WS), dehulled sesame seed (DS), and dehulled-roasted sesame seed (DRS) at different temperatures studied

#### 4.8.6 Net integral enthalpy and entropy

The changes of net integral enthalpy values with the moisture content for all sesame seed samples (WS, DS, and DRS) are presented in Figure 4.6. The net equilibrium heat values of whole sesame increased sharply to a maxima (1088 kJ/kg) with increasing moisture content up to a certain point ( $m = 4.7\%$ ), and then gradually decreased in magnitude with further increase in moisture content. Similarly the net integral enthalpy of dehulled sesame samples increased sharply to a maxima (305 kJ/kg) up to nearly same moisture content ( $m = 4.6\%$ ) of WS sample. However, DRS sample reached maxima (712 kJ/kg) around moisture content of 2 %. Increasing trend at low moisture content can be explained by the location of the bound water, and the greater water-solid interaction compared to the interaction of the water molecules. At low moisture content, the low enthalpy values indicate the occupation of highly accessible sites on the exterior surface of the solid. Increasing moisture content swells the material and increases the availability of the new high-energy sites, which binds the water to obtain the greatest water-solid interaction. Covering less propitious locations and forming multiple layers of sorbed water are the factors for the decrease in the net enthalpy values (Kaya and Kahyaoglu, 2005). Although the order in the magnitude of isosteric heat of sorption was determined as  $WS > DS > DRS$ , the order in the magnitude of integral enthalpy became as  $WS > DRS > DS$ . This difference is surely due to the changes in the spreading pressures, since while isosteric heat of sorption is a reversible process at a constant pressure; the integral enthalpy refers to constant pressure and constant spreading pressure. The determination of integral enthalpy is two-dimensional approach based on surface area; therefore the differences in the surface areas of roasted, dehulled and whole sesame seeds probably caused the changes in the integral enthalpy values.

Integral entropy values of the sesame seeds were plotted with respect to moisture content (Figure 4.7). A sharp decline in the entropy values with increasing moisture content up to a certain points were observed for all forms of sesame seeds. Further increase in moisture content caused a gradual increase in the net entropy values. Similar to the changes in the order of net integral enthalpy values of samples, the order in the magnitude of net integral entropy was found as  $DS > DRS > WS$ , however, it was as  $WS > DS > DRS$  for differential entropy.

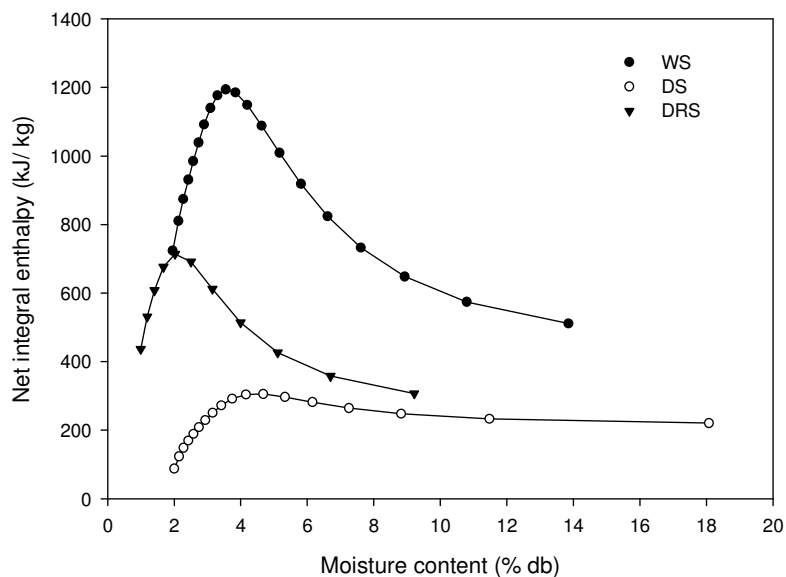


Figure 4.6 Net integral enthalpy values of sesame seed samples (WS: whole sesame seed, DS: dehulled sesame seed, and DRS: dehulled-roasted sesame seed) as a function of equilibrium moisture content

Most of the net integral entropy values of dehulled sesame seed and all of the other seeds are negative. It is interesting to note that the results of the sesame seed are in a good agreement with the reported data for dried sesame seed with a similar trend (decreasing and then increasing) but all of its net integral entropy values have been positive (Aviara et al. 2002). Another similarity is the equilibrium moisture content (3.3% db in this study and 3.7% for the reported datum) at which minimum net integral entropy values have been obtained. Similar trends have been reported in literature for winged bean and gari (Fasina et al. 1999), soya bean (Aviara et al. 2002), and cassava (Aviara and Ajibola, 2002). At low water activity range, a decrease in the net integral entropy values is possibly caused by localization of water (loss of rotational freedom and degree of randomness) due to the strongest binding sites with water molecules and solid as suggested by McMinn and Magee (2003).

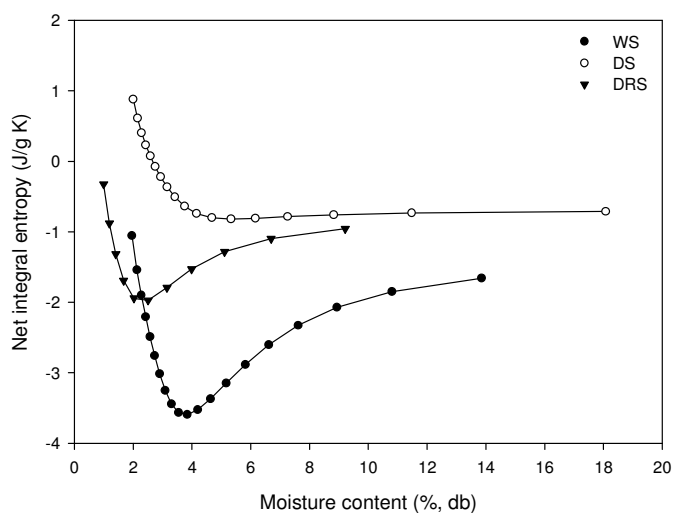


Figure 4.7 Net integral entropy values of sesame seed samples (WS: whole sesame seed, DS: dehulled sesame seed, and DRS: dehulled-roasted sesame seed) as a function of equilibrium moisture content

#### 4.9 Conclusions

1. Moisture adsorption isotherms of whole sesame seed, dehulled sesame seed and dehulled-roasted sesame seed were evaluated using the isopiestic method at 15, 25, and 35°C. Changing temperature was not significant for sorption isotherms of all samples ( $P > 0.05$ ). The order in the magnitude of equilibrium moisture contents at each water activity values was found as whole sesame (WS) > dehulled sesame (DS) > dehulled-roasted sesame.

2. GAB and Halsey equations were applied to adsorption data. Both models gave an acceptable fit of the experimental data. The Halsey equation has been used for predicting the water activity of samples for thermodynamic calculations.

3. The isosteric heat of adsorption of all samples, calculated using the Clausius-Clapeyron equation, showed power relations with moisture content; whole sesame seed has higher net isosteric heat of sorption than that of the others. The power-law model can also characterize differential entropy of adsorption for all sesame seed samples.

4. Spreading pressure increased with increasing water activity. Except WS samples, effect of temperature on spreading pressure was found as non-significant for DS and DRS. The order of spreading pressure was changed with increasing temperature (WS>DS>DRS at 15 and 25°C but WS>DRS>DS at 35°C).

5. Net integral enthalpy increases with moisture content to a maximum value and thereafter decreases. In a reverse manner, net integral entropy decreases with increasing moisture content to a minimum value and then increases.

## **CHAPTER 5**

### **STEADY AND OSCILLATORY FLOW PROPERTIES OF SESAME PASTE WITH DIFFERENT GUMS**

#### **5.1. Introduction**

A better understanding the rheological properties of the foods is important for their processing and new product formulation. Concentrated suspensions are extensively encountered in the food industry and include many foods such as cream, fruit juices, purees, dough, sauces, mayonnaise, and yogurts (Citerne 2001; McKenna 2003). Sesame paste is one of the concentrated colloidal suspension basically contains protein and oil. Sesame paste is used as an ingredient for helva (sweetened sesame paste with saponin extract) and many local sauces. Besides, there has been great interest in the production of sesame seed containing commercial creamy product. In order to achieve that, gums are used widely as thickening and gelling agents. Because of the difference in gum structure and extrinsic condition with fluid food system the rheological, particularly thixotropic, behavior is quite different and complex, and varies from one gum to another. The research could help to food manufacturer in selecting the suitable gums for required process and storage condition.

The determination of the thixotropic and shear-thinning behavior is important from commercial and industrial perspective (flowing, mixing, and texture). For example, as the thixotropic fluid enters a long pipe from a large vessel where it has been allowed to rest, the development of the velocity and pressure fields in the pipe is very complicated. Moreover, since viscosity decreases with shear rate and shearing time during mixing, this will lead to less power consumption (Abu-Jdayil, 2004). The other important parameter related with thixotropy is spreadability because a food product should gain its viscosity to prevent drainage after spreading and this affects directly the consumer acceptance. Therefore a good understanding of the thixotropic and shear-thinning behavior of sesame paste/gum mixture is useful for

food manufacturer. This study is aimed to gain a better and wider understanding of the rheological behavior, creamy structure of sesame paste with some types of gums that are used widely.

## **5.2 Food Rheology**

Rheology is the science of deformation and flow of matter. It investigates the consequent behavior of sample when a force applied on it. So all materials have rheological properties and many areas are related with rheological data such as geology, bioengineering, chemical engineering, and tribology as well as food science and technology. Food industry and food scientists require the rheological data of foods for many purposes (Steffe, 1992; Rao, 1999 and McKenna, 2003):

- Plant and process design: At the plant design stage, pumps, pipes, heat exchangers, mixers, extruders, etc. need to be selected. The rate of process (e.g. flow of liquid) is highly dependent on the rheological properties of matters. An alternative interpretation is that for a given flow rate of a given liquid, a particular pressure drop will be needed along the length of the pipe. This, in turn, will influence the quantity delivered by the pump chosen for the system. The nature of the process itself may lead to further effects (McKenna, 2003).
- Quality control: Intermediate and final product quality control, determination of ingredient functionality and shelf-life testing could be accomplished by using rheological properties of foods. The correlation between rheological data and other quality parameters of foods have been developed over many years.
- Evaluation of sensory attributes: quantitative measurement of consumer acceptance is determined by correlating rheology measurements with sensory data.
- Analysis of food structure and conformation of molecular constituents.

Foods can be classified in different manners, including solids, gels, homogenous liquids, suspension of solids in liquids, and emulsions. Food rheology is often confined to the behavior of liquid foodstuffs. However, there is an increasing tendency to consider the response of both solid and liquid materials to applied stress

and strains as being two extremes of same science. There are in fact same foods that will exhibit either behavior depending on stress applied; molten chocolate, fat-based spreads, mashed potato and some salad dressings will exhibit solid-like behavior at low stresses and a liquid-like behavior at high stress (Mitchell, 1984). This tendency is increasing as more food products are developed that would be classed by the consumer as being semi-solid or semi-liquid. A more exact definition would therefore be the study of both the elastic and plastic properties of foods (McKenna, 2003). A large group of foods such as pastes, sauces, purees and concentrates are called semi-solid and semi-liquid foods.

### **5.3 Basic rheology and its terms**

The purpose of rheological measurements is to assess the force system necessary to cause a given deformation or flow in a body, or conversely, to predict the deformation or flow resulting from the application of a given force system to a body. The advantage of using rheology term to describe this phenomenon is that many of the concepts associated with fluid flow can be utilized in the description of suspension flow, the flow of granular products or powders and, solid food products, which are of considerable importance when discussing food texture. Under external force food materials exhibit ability of flow or accumulate recoverable deformations or both. According to the extent of recoverable deformation the basic rheology concepts can be classified into viscous flow, elastic deformation and viscoelasticity (Barbosa-Canovas et al. 1996).

Many fluid foods can be described by viscous behavior. In this case, the shear stress developed in the fluid is directly proportional to the rate of deformation or the rate of strain. In such cases, the liquid is said to be Newtonian and obey the relationship:

$$\tau = \mu \dot{\gamma} \quad (5.1)$$

where  $\tau$  is the shear stress and  $\dot{\gamma}$  is the shear rate. Shear stress is the stress component applied tangentially. It is equal to the force vector divided by the area of application and expresses in the units of force per unit area (Pa). Shear rate is the velocity gradient established in a fluid as a result of applied shear stress. It is expressed in the units of reciprocal seconds,  $s^{-1}$ . The constant of proportionality  $\mu$



(Pa.s) between the shear stress and shear rate is termed the coefficient of viscosity of fluid. The major types of fluid flow behavior can be described by means of basic shear diagrams of shear rate versus shear stress (Figure 5.1).

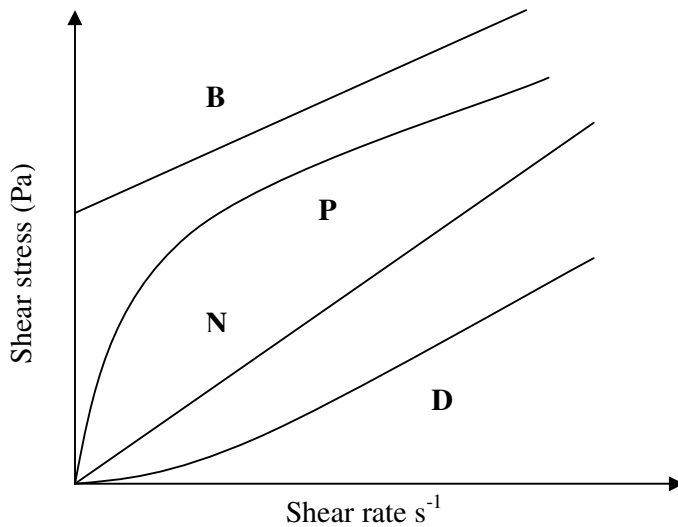


Figure 5.1 Basic shear diagram of shear rate versus shear stress for classification of time independent flow behavior of fluid foods: Newtonian (N), Pseudoplastic (P), Bingham (B), and Dilatant (D)

With Newtonian fluids, the shear rate is directly proportional to the shear stress. Typical foods are those containing compounds of low molecular weights and do not contain large concentrations of either dissolved polymers (e.g. pectin, proteins, starches) or insoluble solids. However only a few liquid foods are Newtonian such as water, milk, edible oils, filtered juices and carbonated beverages (Rao, 1999).

Most foods can be classified as non-Newtonian, which means that the shear stress-shear rate plot is not linear and/or the plot does not begin at the origin or that the material exhibits time dependent rheological behavior as a result of structural changes. Flow behavior may depend only on the shear rate and not on the duration of shear (time-independent) or may depend also on the duration of shear (time-dependent).

Many foods are termed ‘pseudoplastic’ and their response to an applied deformation varies with the rate of application of deformation. The more general term that describes this type of flow also is called as shear-thinning fluids. Shear-thinning may be thought of being due to structural breakdown in a food due to hydrodynamic forces generated during shear. Most non-Newtonian foods exhibit pseudoplastic behavior, including many salads dressings, concentrated milk, solution of concentrated molecules and several fruit juices. Of lesser importance in the food industry are the foods with curves type of (D) “dilatant” or “shear-thickening”. Shear-thickening behavior of foods only rarely observed in partially gelatinized starch dispersions and then over shear rate ranges normally not observed in practice (Van Vliet, 1999). Shear-thickening should be due to increase in the size of the structural units as a result of shear (Rao, 1999).

The power-law model is generally used to describe the data of shear-thinning and shear thickening-fluids:

$$\tau = K \dot{\gamma}^n \quad (5.2)$$

where  $K$ , the consistency index or apparent viscosity ( $\text{Pa}\cdot\text{s}^n$ ),  $n$  is the exponent, the flow behavior index, is dimensionless that also reflects the closeness to Newtonian flow. A Newtonian fluid would of course have an  $n$  value of 1.0 and  $K$  is identically equal to the viscosity of the fluid. For pseudoplastic fluids,  $0 < n < 1.0$ , while for dilatant liquid the value will be greater than 1.0. Since power-law model contains only two parameters ( $K$  and  $n$ ) that describe shear rate-shear stress data, it has been extensively used to characterize the flow behavior of fluid foods.

Finally, some materials do not flow until a threshold value of stress is exceeded (e.g. Bingham (B) in Figure 5.1). For certain food products (e.g. tomato ketchup, mustard, chocolate and other coatings) the existence of a yield stress in the food is essential for application of technology. There are two popular models that describe such products mathematically:

Herschel-Bulkey:

$$\tau = \tau_y + K_H (\dot{\gamma})^n \quad (5.3)$$

Casson:

$$\tau^{0.5} = (\tau_y)^{0.5} + K_C (\dot{\gamma})^{0.5} \quad (5.4)$$

Where  $\tau_y$  is the yield stress and  $K_H$  and  $K_C$  are constants. The Casson model is widely used particularly in the chocolate industry, The International Office of Cocoa and Chocolate has adopted this model as the official method for interpretation of flow data on chocolates. The Herschel-Buckley equation is only modified form of power – law model including yield stress.

### 5.3.1 Thixotropy

Two types of time-dependent flow behavior that could be observed in foods, are those of thixotropic and antithixotropic (rheopectic). The time-dependent shear-thinning behavior is called as thixotropic behavior. The opposite of thixotropy is antithixotropy, where shear-thickening flow behavior is observed during shearing time at constant shear rate (Figure 5.2).

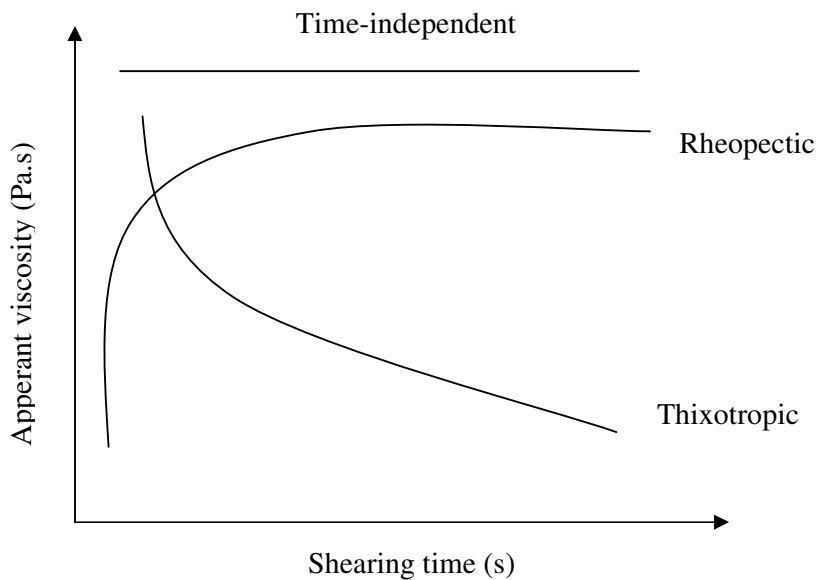


Figure 5.2 Time-dependent flow behaviors of fluids

The term thixotropy comes from the Greek word thixis (stirring or shaking) and trepo (turning and changing). The definition thixotropy is given in the Polymer Science

Dictionary as follows; “Time-dependent flow behavior in which the apparent viscosity decreases with the time of shearing and which the viscosity recovers to, or close to, its original value when shearing ceases. The recovery may take place over a considerable time.”

All liquids with microstructure can show thixotropy, because thixotropy only reflects the finite time taken to move from any one state of microstructure to another and back again, whether from different states of flow or from rest (Barnes, 1997).

Shear thinning can occur for many reasons, e.g.

- Alignment of rod-like particles in the flow direction;
- Loss of junctions in polymer solutions;
- Rearrangement of microstructure in suspension and emulsion flow;
- Breakdown of flocs.

Since changes in any of these states take some time to come about, thixotropy is always to be expected from any shear-thinning mechanism. Difficulties then arise in mixing and handling thixotropic materials due to the progressive breakdown of structures on shearing and slowly rebuild at rest.

Many food products are well known examples of thixotropy. For instance, stirring the yogurt makes them thinner, but leave them to rest thereafter thickens them again (Barnes, 1997). Mayonnaise is also well-known thixotropic material. Rheological characterization of flow time-dependent fluids is not easy (Tiu and Boger, 1974). Experimentally the flow time dependence is clearly shown by performing a loop test, that linearly increasing the shear rate from zero to maximum value, and then return at the same rate to zero. The hysteresis area between up and down curve will give an estimate of magnitude of the thixotropy (Abu-Jdayil, 2004; Tarrega et al. 2004; Altan et al. 2005).

### 5.3.1.1 Mathematical theories for thixotropy

Thixotropy is caused by time-consuming structural changes in colloidal suspensions at a given shear rate. Thus the structural kinetic models (SKM) based on the previous structural theory proposed by Cheng and Evans (1965) has been used to model the thixotropic behavior of foods (Tiu and Boger, 1974; Nyugen and Boger, 1985; Nguyen, Jensen, and Kristeninsen, 1998, Abu-Jdayil, 2003; Tarrega et al. 2004). This model is analogues to that used for chemical reaction, and according to this theory the rate of breakdown in food structure is associated with the destruction by shearing of its internal structure.

The structured state of matter at any time  $t$  and under applied shear rate, can be represented by a dimensionless parameter

$$\Psi = \Psi(t, \dot{\gamma}) \quad (5.5)$$

and

$$\Psi(t, \dot{\gamma}) = \frac{(\eta - \eta_e)}{(\eta_0 - \eta_e)} \quad (5.6)$$

where  $\eta_0$  is the initial apparent viscosity at  $t=0$  and  $\eta_e$  is the equilibrium apparent viscosity at  $t \rightarrow \infty$ .

The rate of structural breakdown as general reaction form given as:

$$\frac{d\Psi}{dt} = k(\Psi - \Psi_e)^m \quad (5.7)$$

where  $k = k(\dot{\gamma})$  is the rate constant, and  $m$  is the kinetic order

At a constant shear rate, integrating Eq.5.7:

$$(\Psi - \Psi_e)^{1-m} = (m-1)kt + (\Psi_0 - \Psi_e) \quad (5.8)$$

and then substituting Eq.5.6 into Eq.5.8, final form is given in Eq. 5.9

$$\left[ \frac{(\eta - \eta_e)}{\eta_0 - \eta_e} \right]^{1-m} = (m-1)kt + 1 \quad (5.9)$$

Some empirical mathematical models are also used to characterize the time-dependent flow properties of foods. The famous ones for describing relation between shear stress and shearing time are Weltman's model (1943) (Eq.5.10), first-order stress decay with a zero (Eq.5.11) or non-zero (Eq.5.12) equilibrium stress value (Abu-Jdayil, 2003):

$$\tau = A + B \ln t \quad (5.10)$$

$$\tau = \tau_0 e^{-kt} \quad (5.11)$$

$$\tau - \tau_{eq} = (\tau_0 - \tau_{eq})^{-kt} \quad (5.12)$$

where  $A$  is the initial shear stress value,  $B$  is the time coefficient of the breakdown,  $\tau_0$  is the initial shear stress value,  $\tau_{eq}$  is the equilibrium shear stress value,  $t$  is the shearing time, and  $k$  is the breakdown rate constant.

In literature some studies had been reported for modeling of thixotropic behavior of foods such as for starch pastes (Nguyen, 1998), pure sesame paste (Abu-Jdayil, 2002), natillas (semi-solid dairy desert) (Tarrega et al. 2004), starch-milk-sugar paste (Abu-Jdayil, 2004) and gilaboru juices (Altan et al. 2005).

### 5.3.2 Dynamic Rheological Methods

Dynamic rheological experiments, also called small amplitude oscillatory shear (SAOS) can be used to determine viscoelastic and gel characteristics of food. In oscillatory instruments, a sinusoidal oscillating stress or strain with a frequency  $\omega$  is applied to the material, and the phase difference between the oscillating stress or strain, as well as the amplitude ratio, is measured (Steffe, 1999). The parameters obtained from SAOS experiments are given in Table 5.1.

The  $G'$  (storage modulus) is a measure of energy stored and subsequently released:  $G''$  (loss modulus) of the energy dissipated per cycle of deformation. Therefore, for a perfectly elastic solid, all the energy is stored; that is,  $G''$  is zero and the stress and

the strain will be in phase. In contrast, for a liquid with no elastic properties, all the energy is dissipated as heat, that is  $G'$  is zero and the stress and the strain will be out of phase by  $90^\circ$ . The loss tangent is the ratio of dissipated to that stored per cycle of deformation. These viscoelastic functions have been found to play important roles in the rheology of polysaccharide and proteins (Ferry, 1980; Rao, 1999).

Table 5.1 Material functions used to describe viscoelastic behavior

Material Functions	Equations
Shear storage modulus	$G' = (\sigma_0/\gamma_0) \cos(\delta)$
Shear loss modulus	$G'' = (\sigma_0/\gamma_0) \sin(\delta)$
Complex modulus	$G^* = (\sigma_0/\gamma_0) = (G'^2 + G''^2)^{1/2}$
Complex viscosity	$\eta^* = G^*/\omega = (\eta'^2 + \eta''^2)^{1/2}$
Dynamic viscosity	$\eta' = G'/\omega$
Out of phase component of the complex viscosity	$\eta'' = G''/\omega$
Complex compliance	$J^* = 1/G^*$
Storage compliance	$J' = G' / (G')^2 + (G'')^2$
Loss compliance	$J'' = G'' / (G')^2 + (G'')^2$
Tan delta ( loss tangent, phase angle)	$Tan(\delta) = G''/G'$

Frequency sweep and temperature sweep test are generally conducted as SAOS test to the food materials. The frequency sweep is probably the most common mode of oscillatory testing because it shows how the viscous and elastic behavior of the material changes with the rate of application of strain and stress. In this test the frequency is increased while the amplitude of the input signal (stress or strain) is held constant. Frequency sweeps are very useful in comparing, sometimes called “finger printing” different food products or in comparing the effects of various ingredients and processing treatments on viscoelasticity.

Based on the frequency sweep data, one can designate “true gels” when the molecular rearrangements within the network are much reduced over the time scales analyzed, such that  $G'$  is higher than  $G''$  through out the frequency range and is almost independent of frequency. In contrast, for “weak gels” the is higher dependence on frequency for the dynamic moduli, suggesting the existence of relaxation processes occurring even at short time scales, and lower difference

between moduli values. Additionally (Ross-Murphy, 1995), with a dilute polymer solution,  $G''$  is larger than  $G'$  over the entire frequency range, but at high frequencies they approach each other. For a concentrated biopolymer solution,  $G''$  is larger than  $G'$  at lower frequencies but the  $G'$  and  $G''$  curves intersect at a cross over frequency; at frequencies higher than the crossover frequency, values of  $G'$  are the higher than those of  $G''$ .

The characterization of food samples at elevated temperatures is important for prediction of its behavior during heating and also temperature dependency of materials. With the temperature sweep study,  $G'$  and  $G''$  are determined as a function of temperature at fixed frequency.

#### **5.4 Use of gums in improving food texture**

The term 'hydrocolloid' is commonly used to describe a group of water-soluble gums naturally occurring polymers found in nature abundantly and used in foods. They have evolved to perform many different functions, e.g. act as structural agents and energy reserves in plants and animals, to facilitate cell recognition and adhesion process, to provide lubrication in bone joints, to act as ion exchangers and blood anticoagulants (Williams and Philipps, 2003). Their key function in food products is to impart viscosity, gelling and film formation. Even at concentration of 1 wt% or less some hydrocolloids are capable of producing highly viscous solutions or of forming gels with varying textures. Their thickening ability has led to their use as suspension and emulsion stabilizers where they function by retarding particle sedimentation and droplet creaming caused by bulk viscosity effects.

Food gums are obtained from a variety of sources. Details of some of the commercially used types of gums are given in Table 5.2. As a consequence of the increasing consumer demand for convenience foods and modern trend towards healthier high-fiber and low-fat diets, hydrocolloids are finding ever-increasing application in food products to improve product texture and quality. This is evident from the fact that the worldwide market volume increased from 720 000 tones with a value of \$690 million in 1990 to 1420 000 tones at a value of \$3.2 billion in 2001 (Williams and Philipps, 2003).



Table 5.2 Source, function and main applications of some types of gums (Williams et al., 2003)

Gum	Source	Function	Application areas
<b>Botanical</b>			
Carboxymethyl cellulose	Trees and cotton	Thickener	Dairy and deserts, ready-to-eat meals, bakery products
Guar gum	Seed endosperm <i>Cyamopsis tetragonoloba</i>	Thickener	Dairy and deserts, ready-to-eat meals, bakery products,
Modified starches	Corn, potato etc.	Thickener and gelling agent	Dairy and deserts, ready-to-eat meals, soups, sugar confectionary,
Locust bean gum	Seed endosperm <i>Ceratonia siliqua</i>	Thickener	Dairy and deserts
<b>Algal</b>			
<b>Red seaweeds</b>			
Agar	<i>Gelidium, Gelidiella Pterocladia</i>	Gelling agent	Confectionary, and dairy and deserts
Carrageen <i>Kappa type</i>	<i>Euchema cottonii</i> and <i>chondus crispus</i>	Gelling agent	Dairy and deserts, meat products
<b>Microbial</b>			
Xanthan gum	<i>Xanthomonas campestris</i>	Thickener	Dairy and deserts, ready-to-eat meals, sauces and dressing
<b>Animal</b>			
Gelatin	Cattle, pigs, fish	Gelling agent	Sugar confectionary, Meat products, dairy and deserts

Textural modification and control are an integral part of food processing. The demand for fast food and ready-to-eat meals is also increasing. Hence, the use of hydrocolloids probably will continue to increase considerably in the future.

As the gums are dissolved or dispersed in the food systems the change in the viscosity occurs due to the high molecular weight polymeric nature of gums and their interactions between polymer chains. Gum solutions normally exhibit Newtonian behavior at the concentrations well below critical concentration  $C^*$ , however, above  $C^*$  non-Newtonian behavior is usually observed. Among the hydrocolloid thickeners, the most striking features are the profile for xanthan gum, a well-known extracellular microbial polysaccharide. This gum has a very large low-shear viscosity, and hence

it is good at suspending particles and oil droplets. In addition, however, it is also extremely shear thinning and, therefore, it readily flows on simple shaking. These characteristics have led to its widespread use in many food applications, notably, mayonnaise, dressing and sauces. The shear-thinning character of xanthan gum is more pronounced than those of other polysaccharide gums (guar gum, locust bean gum etc.) due to unique rigid, rod-like conformation of xanthan gum which is more responsive to shear than a random-coil conformation (Urlacher and Noble, 1997).

Due to the diversity of gums and their modified derivatives, food companies may have a difficult time making decisions regarding the choice of gums for addition to their food formulations (Yaseen et al. 2005). The researches on the comparative viscoelastic properties of gums in food systems may help for selection of proper gum.

The present study is aimed at measuring the rheological properties of sesame paste mixtures with varying gums by using two different rheological methods, (1) steady flow measurements (2) small amplitude oscillatory measurements.

## **5.5 Materials and Methods**

The mechanically dehulled sesame seeds were roasted (150°C for 100 min) and then milled by a commercial miller (Gürmaksan, Co, Turkey) in a local company. Locust bean gum (LBG), xanthan gum (XG), guar gum (GG), kappa-carrageen gum (KG) were obtained from INCOM (Incom Co, Mersin, Turkey).

### **5.5.1 Preparation of gum and paste mixture**

To prepare the sesame paste/gum mixture at 1% (wt), 1 g of gum prepared with 99 g of sesame paste and in similar manner blends with 5% (wt) were made. Samples were stirred by a 4-bladed propeller stirrer. Sesame paste/gum mixture contained 1% LBG and 5% LBG were coded as LBG1 and LBG5 respectively. By the same way, GG1, GG5, KG1, KG5, XG1, and XG5 are the codes for guar gum, kappa-carrageen gum, and xanthan gum, respectively.

### **5.5.2 Rheological measurements**

Rheological measurements were performed by a rheometer HAAKE RheoStress RS coupled with a Peltier/Plate TCP/P temperature control unit (HAAKE GmbH,

Karlsruhe) using cone and plate system (d: 35 mm  $\alpha$ : 2°). Circulator DC10 unit was used to control temperature within range 5-70°C.

### 5.5.3 Hysteresis loop

The samples were allowed to rest 5 min after loading, before measurement. The hysteresis loop was obtained by registering shear stress at shear rates from 0.08 to 500 s<sup>-1</sup> in 120 s and down in 120 s. Areas under the upstream data points ( $A_{up}$ ) and under the downstream data points ( $A_{down}$ ) as well as the hysteresis (thixotropic) area ( $A_{up}-A_{down}$ ) were obtained using Rheowin Pro software (version 2.64, Haake). The percentage of relative hysteresis area was calculated using Eq. (5.13)

$$A_r=(A_{up}-A_{down})/A_{up}\times 100 \quad (5.13)$$

### 5.5.4 Shear stress decay with recovery test

The time dependent rheological properties were investigated by shearing samples at constant shear rates at 5 and 25°C. Then the shear stress was measured as a function of shearing time. The shear stress decay was determined by applying a shear rate of 200 s<sup>-1</sup> during 1200 s. Experimental data were fitted to structural kinetic models (Eq.5.9) and Weltman's model (1943) (Eq.5.10), first-order stress decay model with a zero (Eq.5.11) or non-zero (Eq.5.12) equilibrium stress value (Abu-Jdayil, 2003).

After shearing for 1200 s, recovery test were performed by registering the shear stress at shear rates from 0.08 to 200 s<sup>-1</sup> in 60 s and down in 60 s. The hysteresis loop measurements were also performed again after shearing for 1200 s to observe the ability of samples in rebuilding of their structure. All samples were subjected to the same standard routine and measurements were performed at least twice.

### 5.5.5 Frequency sweep tests

In frequency sweep, the storage ( $G'$ ) and the loss ( $G''$ ) moduli were recorded versus frequency. Before performing these frequency spectra, the linear viscoelastic region was determined and an appropriate stress was selected (1 Pa).  $G'$ ,  $G''$  were recorded between 0.01-10 Hz at 25°C.

### **5.5.6 Temperature sweep tests**

The rheological changes during heating from 5 to 70°C were measured by temperature sweep test. Sesame paste samples were equilibrated at 5°C for 5 min and subjected to a harmonic low amplitude shear stress at 200 Pa and 1 Hz frequency. The temperature was increased to 70°C at a rate of 3°C min<sup>-1</sup>. Data were analyzed using a RheoWin Data Manager ( RheoWin Pro V.2.64, Haake).

## **5.6 Results and Discussions**

### **5.6.1 Steady-shear flow measurements**

#### **5.6.1.1 Flow curve tests**

Pure sesame paste (control) showed pseudoplastic behavior at 5° and 25°C (Figures 5.3-5.4). The flow curves of pure sesame paste and sesame/guar gum systems at temperatures 5°C and 25°C in the forward direction is shown in Figure 5.3. All samples exhibited pseudoplastic (shear-thinning) behavior for both temperatures, where the apparent viscosity decreased with increasing shear rate (Figure 5.4). Sesame paste is a colloidal solution basically composed of protein suspended in sesame oil (Abu-Jdayil, 2004). Since, the addition of gum also results the formation of new aggregates and clusters, the shear-thinning behavior is probably due to the breakdown of proteins, fats, gummy materials and aggregates by the effect of shearing.

The samples with guar gum revealed higher shear stress values than pure sesame paste and these effects enhanced with increasing the gum concentration at 5°C. On the other hand, the effect of gum addition on the flow behavior of pastes decreased as the testing temperature was increased. At 25°C, GG1 and control samples had nearly same apparent viscosity within studied shear rate range (Figure 5.4)

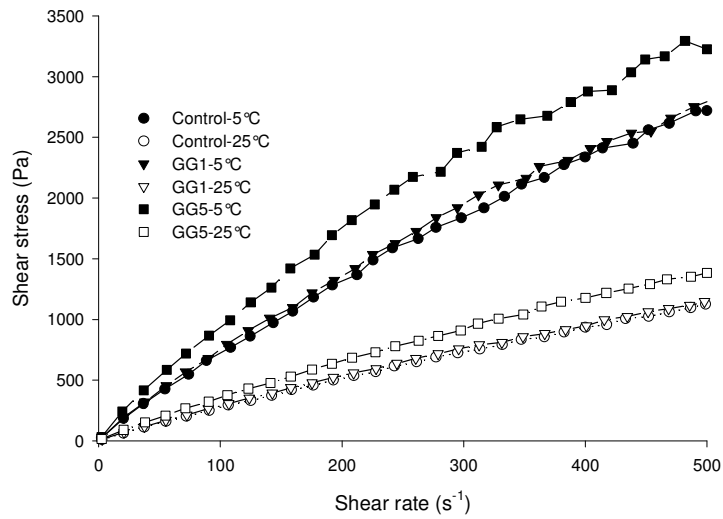


Figure 5.3 Flow curves of pure sesame paste (control) and paste containing guar gum 1% (wt) (GG1) or 5% (wt) (GG5) at 5° and 25°C

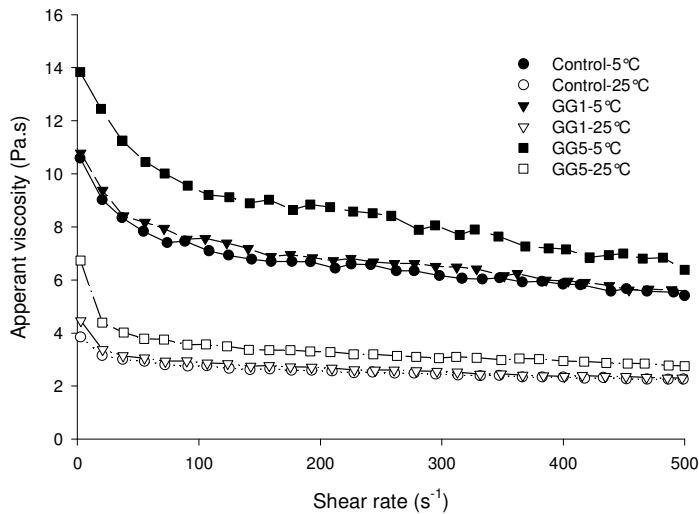


Figure 5.4 Apparent viscosity versus shear rate for pure sesame paste (control) and paste containing guar gum 1% (wt) (GG1) or 5% (wt) (GG5) at 5° and 25°C

The increasing temperatures may cause the breakdown of structural units and probably reduce the volume and size of the proteins, fats and hydrocolloids, resulting in a decrease in the apparent viscosity.

Flow behavior of the other studied sesame paste/gum mixtures was similar to that of sesame paste/guar gum mixture. They increased the apparent viscosity of sesame

paste. To compare and discuss the effect of each gum on the flow behaviors of pastes more clearly, the flow curves (shear stress vs. shear rate) were fitted to power-law model. The coefficients ( $K$  and  $n$ ) of the applied model for each sample are reported in Table 5.3. The power-law model adequately described the shear stress-shear rate data for all samples ( $r^2 > 0.998$ ). The consistency coefficient ( $K$ ), increased with the addition of gum, and this effect was pronounced at high concentration of gum especially at lower temperatures. As the temperature increased, the range of ( $K$ ) values for the samples become very narrow (Table 5.3). Hence, it is possible to claim that there is not any considerable effect of the gum addition on the consistency of sesame paste at high temperatures for selected gums and concentrations in this study. The maximum  $K$  value (43.08) obtained for sesame paste/xanthan gum mixture (5% w/w) at 5°C. The order of  $K$  values for pastes was determined as XG5>KG5>LBG5>GG5 at 5°C. However, at 25° this order changed as XG5>LBG5>GG5>KG5.

It was also interestingly found that the order of  $K$  values changed for the samples containing 1% gum as KG1>LBG1>GG1>XG1 at 5°C. The xanthan gum was superior to others at 5% but it was not at 1%. This is probably due to the critical polymer concentration of xanthan gum. This concentration corresponds to the transition from dilute region, where the polymer molecules are free to move independently in a mixture without touching, to the semi-dilute region, where molecular crowding gives rise to overlap of other polymer coils (e.g. proteins) and interpenetration occurs (McKenna, 2003). When compared to the other gums, xanthan gum produces low viscosity below critical concentration but above critical concentration vice versa at 5°C. At high temperature, there are no considerable differences between the  $K$  values of the sesame paste that contained 1% gum.

The flow behavior index,  $n$ , decreased with gum addition and increased with increasing the temperature (Table 5.3). The reduction in the  $n$  value shows the deviation from Newtonian behavior to non-Newtonian one. The flow behavior index value of pure sesame paste was reported as 0.91-0.95 for temperature range of 5-45°C by Abu-Jdayil, 2002. However, according to the results of Lokumcu and Ak, (2005), the value of  $n$  for sesame paste was nearly constant (~0.87) up to 50°C. In comparison, the  $n$  values in our study for all samples were lower (0.70-0.86) up to

25°C. On the other hand Abu-Jdayil (2004) also reported in the presence of sugar component in sesame paste resulted a remarkable deviation from Newtonian behavior ( $n = 0.44$ ). These results are important for calculation of power consumption in mixing of sesame paste. The flow behavior knowledge of the gums with sesame paste also required for the production of different types of sesame paste containing creams and sauces, those popularities are ever increasing.

Table 5.3 Coefficients of power law-model for forward measurements of sesame paste/ gum mixtures at studied temperatures (5 and 25°C)

Sample	5°C			25°C		
	K (Pa.s <sup>n</sup> )	n	r <sup>2</sup>	K(Pa.s <sup>n</sup> )	n	r <sup>2</sup>
Control	16.68	0.824	0.999	5.19	0.866	0.999
GG1	20.03	0.797	0.998	5.99	0.846	0.999
GG5	30.39	0.757	0.997	7.45	0.844	0.999
XG1	17.24	0.821	0.999	6.15	0.841	0.999
XG5	43.08	0.708	0.996	8.32	0.838	0.999
KG1	21.48	0.791	0.998	5.72	0.858	0.999
KG5	41.78	0.715	0.999	7.42	0.878	0.999
LBG1	21.00	0.787	0.998	5.38	0.865	0.999
LBG5	33.29	0.741	0.996	7.77	0.830	0.999

The most common way of measuring thixotropy is to apply the loop test. In this test, material is sheared at increasing rates (ascending) and then decreasing shear rate (descending), the area between ascending and descending flow curves is called as the thixotropic area (hysteresis area), which gives an idea about the magnitude of the thixotropy in a qualitative manner. All samples in the present study showed observable thixotropy at both temperatures tested, 5°C and 25°C. For clarity, only the hysteresis areas for control and XG5 samples were shown in Figure 5.5.

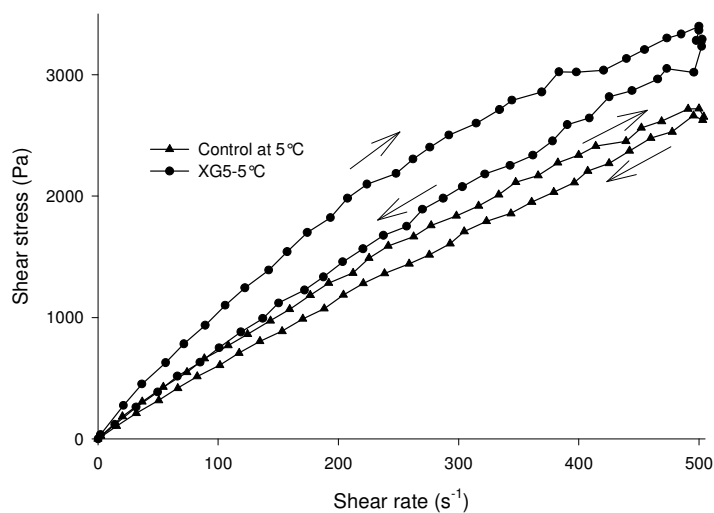


Figure 5.5 Flow curves of pure sesame paste (control) and sesame paste/xanthan gum mixture

The higher values of hysteresis area found for all samples with gum when compared to pure sesame paste means that they are more prone to thixotropic behavior. Also the thixotropy of the sesame paste/gum mixtures increased at rising gum concentration except sesame paste/guar gum mixture (Table 5.4). In the reverse manner, increasing the guar gum concentration decreased the thixotropy of paste. This behavior is probably due to the strong flocs at high concentration of guar gum since usually strong flocculated emulsions show much less thixotropy than weakly flocculated systems (Tadros, 2004). Similarly, Koru et al. (2004) reported that increasing gum concentration decreased the thixotropy of starch/guar gum and starch/Arabic gum systems. The magnitude of hysteresis area for all samples became lower as the temperature increased from 5 to 25°C. The hindered flocculation and breakdown of the aggregates due to accelerated motions of solid particle with effect of high temperature and shearing probably caused the reduction in the thixotropic behavior of pastes. In literature, Tarrega et al. (2003) and Lokumcu and Ak, (2005) reported similar results for natillas and pure sesame paste respectively, but Abu-Jdayil (2004) concluded that the increasing temperature increased the thixotropy of the sesame paste/sugar mixture. The temperature effect for each paste-gum mixture were found different in this study probably due to the variability of thermo-physical properties of gums; such as KG1 and GG5 samples showed lower thixotropy than control sample at 25°C.



The hysteresis area depends on the loop contour; shearing time, ranges of shear applied, and shear resistance of the sample (Tadros, 2004). The relative thixotropic area could be used as an alternative approach for discussing the extension of time, which is defined as the ratio of the ‘absolute’ hysteresis area to the area under the ascending flow curve (Tarrega et al. 2003). The differences between the samples were not the same as the relative areas were compared. As the relative thixotropic area was used, the order of thixotropy between samples was changed at 25°C (e.g. LBG1 showed higher thixotropy than KG5) (Table 5.4).

Table 5.4 Thixotropic and relative thixotropic area values of sesame paste/gum mixtures at 5 and 25°C

Sample	Thixotropic area (Pa/s) $\times 10^{-4}$		Relative thixotropic area (%)	
	5°C	25°C	5°C	25°C
Control	6.06	2.11	8.20	7.04
GG1	11.42	2.14	14.30	9.50
GG5	10.36	1.89	11.42	5.19
XG1	9.27	2.84	12.04	9.19
XG5	20.70	4.85	20.00	11.81
KG1	10.63	1.39	12.78	4.52
KG5	17.66	3.33	18.92	8.58
LBG1	8.88	3.31	11.44	10.61
LBG5	10.30	4.27	12.82	11.41

### 5.6.1.2 Shear stress decay test

The prepared sesame paste/gum samples were sheared at a shear rate  $200 \text{ s}^{-1}$  and at testing temperatures of 5 and 25°C for 1200 s. The rate and extent of shear stress decay changed according to the gum type and concentration of samples and testing temperatures and typical behavior of samples were shown in Figures 5.6-5.7 as examples. The observed time dependent flow behaviors of samples were described using four models; structural kinetic model (Eq. 5.9), Weltman model (Eq. 5.10), first-order stress decay with a zero equilibrium (Eq. 5.11), and first-order stress decay model with a non-zero equilibrium (Eq. 5.12).

The structural kinetics model assumes that the change in the time dependent flow properties is related with shear induced breakdown of the internal fluid structure and that the rate of this breakdown during shearing depends on the kinetics of this breakdown process as in the case of chemical reactions (Abu-Jdayil, 2003). For most samples studied, the transient apparent viscosity data at shear rate of  $200 \text{ s}^{-1}$  during 1200 s of shearing time could be modeled with a second-order structural kinetic model ( $m = 2$ ) (Table 5.5).

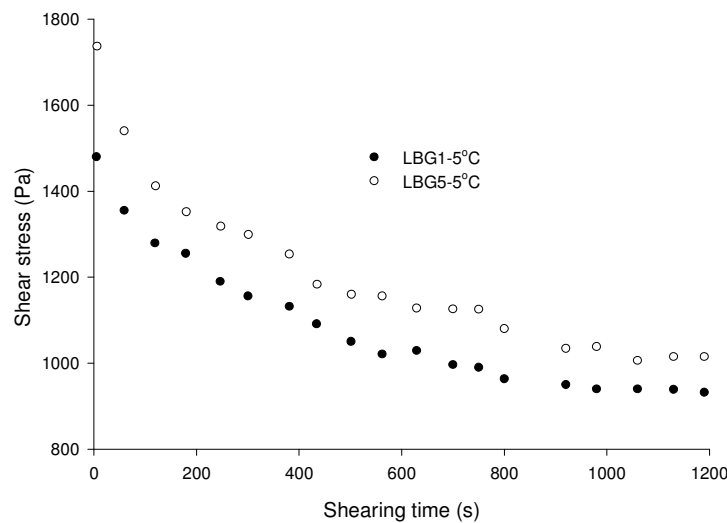


Figure 5.6 Effect of locust bean gum concentration on the thixotropic behavior of the sesame paste

The  $k$  value is a measure of the rate of thixotropic breakdown, and a ratio of the initial to equilibrium viscosity ( $\eta_0/\eta_e$ ), can be considered to be relative measure of the extent of thixotropy. The addition of gum increased the  $k$  values of the samples. This means that increasing the amount of biopolymer (fat, protein and gum), the rate of breakdown of this cross-linked structures increased. As expected,  $k$  increased with increasing temperature. This shows that the rate of breakdown of protein, fat and other biopolymer aggregates increased with increasing temperature. The same behavior was reported for sweetened sesame paste by Abu-Jdayil (2004) and for natillas by Tarrega et al. (2004).

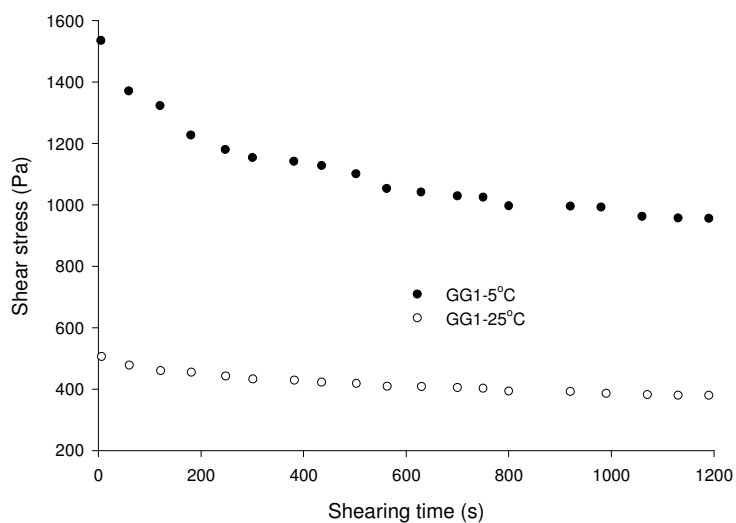


Figure 5.7 Effect of temperature on the thixotropic behavior of the sesame paste/guar gum mixture

The amount of structural breakdown also was shown in Table 5.5, as the gum concentration increased, the extent of thixotropy ( $\eta_o/\eta_e$ ) also enhanced. The maximum amount of structural breakdown was obtained for KG5 sample. The value of ( $\eta_o/\eta_e$ ) decreased with the effect of temperature. These results showed that probably more aggregates exist due to unmelted fat particle at low temperature than at high temperatures. If the high  $k$  value is considered at high temperatures also, it could be concluded that at high temperature, the little amount of aggregates were broken-down faster.

Table 5.5 Viscosity ratio and structural breakdown rate constant for second order kinetic model for the sesame pastes with varying gums

Sample	$\eta_o/\eta_e$	5°C			25°C		
		$k \times 10^4$ (1/s)	$r^2$	$\eta_o/\eta_e$	$k \times 10^4$ (1/s)	$r^2$	
Control	5.42	4.81	0.897	2.22	5.63	0.916	
GG1	6.85	5.60	0.893	2.39	5.83	0.955	
GG5	7.09	6.80	0.871	2.66	8.05	0.929	
XG1	7.19	6.22	0.865	2.89	6.69	0.884	
XG5	7.63	6.31	0.893	3.68	7.87	0.936	
KG1	7.01	5.78	0.861	2.60	6.37	0.878	
KG5	8.61	5.89	0.916	3.30	7.83	0.910	
LBG1	6.79	5.82	0.883	2.84	7.41	0.872	
LBG5	7.64	6.44	0.920	3.13	8.45	0.905	

In the Weltman model, parameters *A* represent the initial shear stress, and parameter *B*, the time coefficient of thixotropic breakdown (extent of thixotropy), is the product of rate in breakdown of thixotropic structure and time of agitation at constant rate of shear (Weltman, 1943).

Table 5.6 shows the parameters of Weltman models. The experimental data of all samples fitted well ( $r^2 = 0.939-0.985$ ) to the Weltman model. The *B* value increased with increasing gum concentration. The increasing temperature also decreased *B* value. As an example, it can be seen in Fig 5.5 that the effect of temperature on the time depend flow properties of sesame paste/guar gum mixture. As the temperature was increased the thixotropic behavior of samples decreased. The KG5 sample had maximum *B* value at 5°C but at 25°C the LBG5 had maximum value.

The order of samples according to their extent of thixotropy that obtained from Weltman model did not followed similar pattern as the thixotropic area values. However, Altan et al. (2005) reported the correlation between the *B* value of Weltman model and thixotropic area for gilaboru juice. This difference might be explained as the *B* value indicates the rate of structural breakdown but thixotropic area is a function of rebuilding mechanisms of structured aggregates of biopolymers.

Abu-Jdayil et al., 2002 reported that the first order stress decay model with a zero-equilibrium stress value adequately describe the time dependent flow properties of pure sesame paste. The first order stress decay model with zero equilibrium (Eq.5.10) was tested to describe the time dependent flow behavior of samples (Table 5.7).

Table 5.6 Weltman model parameters for the sesame pastes with varying gums

Sample	5°C			25°C		
	A (Pa)	B (Pa)	$r^2$	A (Pa)	B (Pa)	$r^2$
Control	1657	-83.4	0.963	328	-12.3	0.958
GG1	1940	-138.7	0.960	606	-31.9	0.947
GG5	2089	-163.5	0.984	720	-47.1	0.941
XG1	2058	-153.1	0.960	719	-44.1	0.948
XG5	2004	-166.6	0.951	788	-52.7	0.939
KG1	2020	-148.6	0.965	687	-40.8	0.943
KG5	2460	-181.5	0.946	919	-64.6	0.963
LBG1	1946	-137.3	0.947	782	-51.9	0.969
LBG5	2194	-165.6	0.964	875	-148.6	0.965

The other first-order stress decay model (Eq. 5.11) was used to search the existence of a non-zero, equilibrium shear stress value. The parameters of this model are shown in Table 5.8. This model was found more successful than structural kinetic, Weltman and first-order stress decay model with zero equilibrium for fitting the time dependent flow properties of all sesame paste/gum mixtures, except XG5 sample as in the case of Weltman model. The equilibrium shear stress value increased with increasing gum concentration for all samples. The equilibrium stress values represent the final stress values that obtained after shearing for infinite time, further structural breakdown of aggregates occurs beyond that value. The increasing temperature decreased the equilibrium stress value as expected. The constant  $k$  represents how fast the sample, under the action of shearing, reaches the equilibrium value (Abu-Jdayil, 2002).

Table 5.7 Coefficients of first-order stress decay with zero-equilibrium stress value, for a shearing time of 1200 s for the sesame pastes with varying gums

Sample	5°C			25°C		
	$\tau_0$ (Pa)	$k \times 10^4$ (s <sup>-1</sup> )	r <sup>2</sup>	$\tau_0$ (Pa)	$k \times 10^4$ (s <sup>-1</sup> )	r <sup>2</sup>
Control	981	2.96	0.906	403	1.69	0.884
GG1	1333	3.39	0.873	469	2.05	0.930
GG5	1366	3.88	0.833	512	2.91	0.894
XG1	1386	3.61	0.832	523	2.59	0.849
XG5	1392	3.84	0.858	557	3.07	0.905
KG1	1363	3.47	0.823	506	2.45	0.840
KG5	1674	3.68	0.901	634	3.26	0.967
LBG1	1316	3.41	0.852	547	2.83	0.827
LBG5	1474	3.78	0.898	600	3.30	0.853

After shearing the samples for 1200 s, the recover tests were performed to measure the rebuilding ability of the samples. In this test, the shear stress values were measured as a function of shear rate for both forward (1-200 s<sup>-1</sup>) and backward (200-1 s<sup>-1</sup>). The thixotropic and relative thixotropic areas for sesame paste/gum mixtures are shown in Table 5.9.

As the thixotropic areas values were compared for qualitative purposes, the XG5 sample had the maximum thixotropic area than the others. On the other hand, the thixotropic area value for XG1 was negative. This result also is convenient that obtained from initial flow curve test (Table 5.3). The negative areas of samples were obtained at 25°C except XG5.

Table 5.8 Parameters of the first-order stress decay model with non-zero equilibrium for the sesame pastes with varying gums

Sample	5°C				25°C			
	$\tau_e$ (Pa)	$\tau_0$ (Pa)	$k \times 10^3$ (s <sup>-1</sup> )	$r^2$	$\tau_e$ (Pa)	$\tau_0$ (Pa)	$k \times 10^3$ (s <sup>-1</sup> )	$r^2$
Control	761	1053	4.52	0.973	293	451	3.84	0.967
GG1	944	1470	2.81	0.976	367	490	1.89	0.984
GG5	945	1561	3.43	0.966	370	548	2.24	0.963
XG1	983	1578	3.42	0.985	402	567	2.76	0.950
XG5	1131	1989	3.78	0.952	395	596	2.14	0.968
KG1	983	1558	3.59	0.978	396	550	2.93	0.955
KG5	1129	1826	2.45	0.982	455	697	2.76	0.964
LBG1	940	1471	3.10	0.982	417	610	3.31	0.956
LBG5	986	1612	2.49	0.977	433	667	3.06	0.965

Table 5.9 Thixotropic and relative thixotropic areas of the sesame paste/gum mixtures after shearing 1200 s for 200 s<sup>-1</sup>

Sample	Thixotropic area (Pa/s)		Relative thixotropic area (%)	
	5°C	25°C	5°C	25°C
Control	641	-392	1.02	-0.26
GG1	2670	-2158	2.62	-0.005
GG5	3968	-2044	3.91	-0.005
XG1	-636	-2028	-0.005	-0.04
XG5	6510	1352	6.07	3.14
KG1	2108	-7028	5.11	-6.73
KG5	5266	-1887	4.71	-3.80
LBG1	518	-1260	0.56	-2.88
LBG5	5179	-1117	2.51	-2.42

## 5.6.2 Dynamic small oscillatory tests

The flow behavior of a food sample can not always be expressed only as viscous flow behavior. The SAOS tests are extensively used to obtain more information about elasticity of the materials in recent years. In this study, frequency sweep and temperature sweep tests were conducted to investigate the viscoelastic behavior of these same paste/gum mixtures.

### 5.6.2.1 Frequency sweep tests

Frequency sweep tests were performed to study viscoelastic behavior of sesame paste/ gum mixtures. The storage modulus ( $G'$ ) and loss modulus ( $G''$ ) as function of frequency (Hz) for pure sesame paste is shown in Figure 5.8.  $G''$  was greater than  $G'$  in the studied range of frequency that shows the material behavior is liquid-like. The energy used to deform sesame paste/gum mixtures was dissipated viscously. This

behavior did not change with gum addition for both concentrations (Figure 5.9). All mixtures showed liquid-like behavior.

They shows similar characteristics with dilute polymer solutions for that  $G''$  is larger than  $G'$  over the entire frequency range, but at high frequencies they approach each other. Such trend was also reported for corn starch-locust bean gum mixtures (Alloncle and Doublier, 1991). In general, at low frequencies, the flow behavior is controlled by transitional motion of macromolecules, and  $G''$  is usually higher than  $G'$  (Da Silva and Rao, 1992). At high frequencies, on the other hand, the value of  $G'$  increases due to the macromolecular distortion and it is higher than that of  $G''$ . This was most probably due to the high oil content and biopolymer structures of proteins and gums.

The low phase angles at low frequencies indicate primarily elastic behavior, but as frequency was increased the phase angles also increased (Figure 5.10). The gum addition decreased slightly viscous character of sesame paste (control) except the sesame paste/xanthan gum mixture which showed more viscous character than other samples at studied frequency ranges. This could be due to that as xanthan gum added to fluid foods, it increases low shear rate viscosity while having little effect on the viscosity of the food at high shear rate (Speers and Tung, 1986)

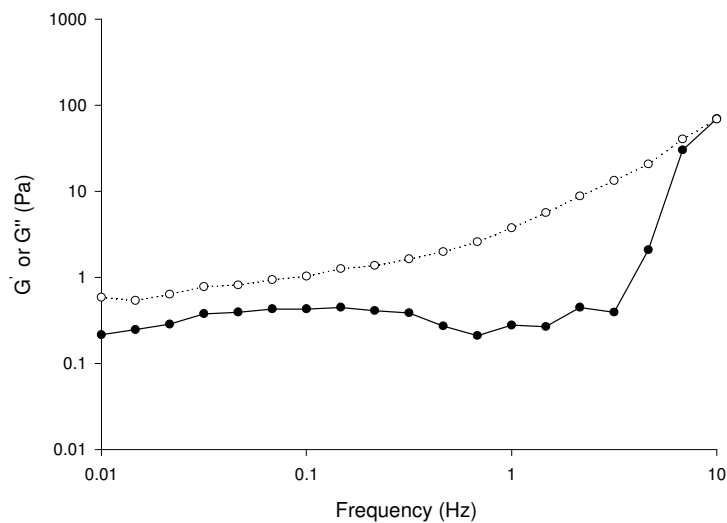


Figure 5.8 Storage modulus ( $G'$ : solid line) and loss modulus ( $G''$ : dotted line) of the pure sesame paste

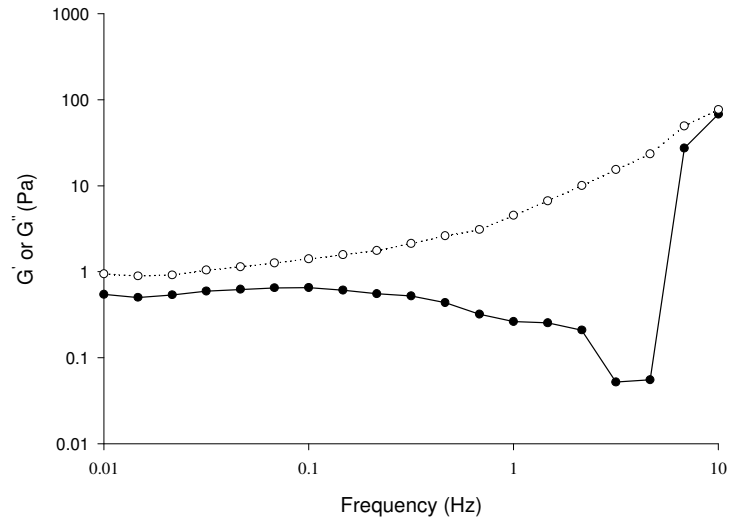


Figure 5.9 Storage modulus ( $G'$ : solid line) and loss modulus ( $G''$ : dotted line) of the sesame paste/locust bean gum mixture (1% wt)

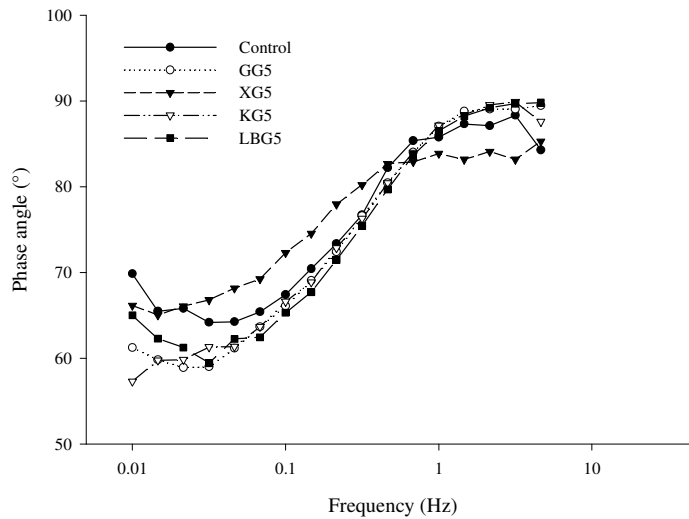


Figure 5.10 Phase angle values of sesame paste/gum mixtures (GG5, XG5, KG5 and LBG5 contains 5% wt of guar gum, xanthan gum, kappa-carrageen gum, and locust bean gum respectively)

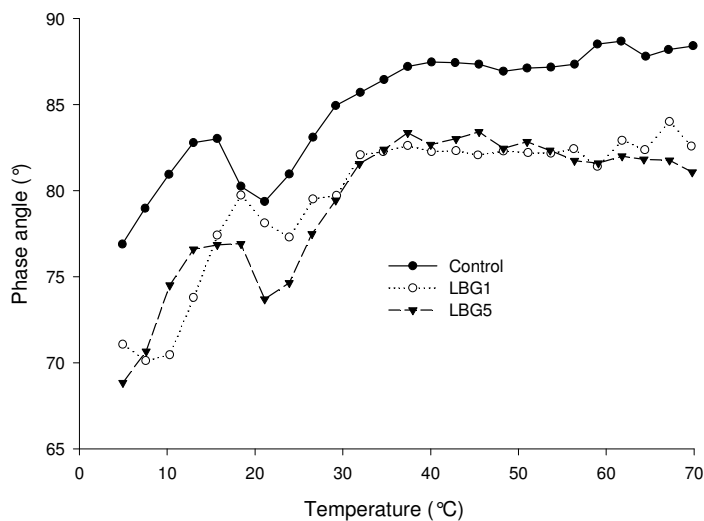
### 5.6.2.2 Temperature sweep tests

The effects of temperature on the viscoelastic properties of sesame paste/gum mixture were analyzed by temperatures sweep tests. Figure 5.11 shows the temperature dependency of the phase angles during heating at 5 to 70°C of LBG1



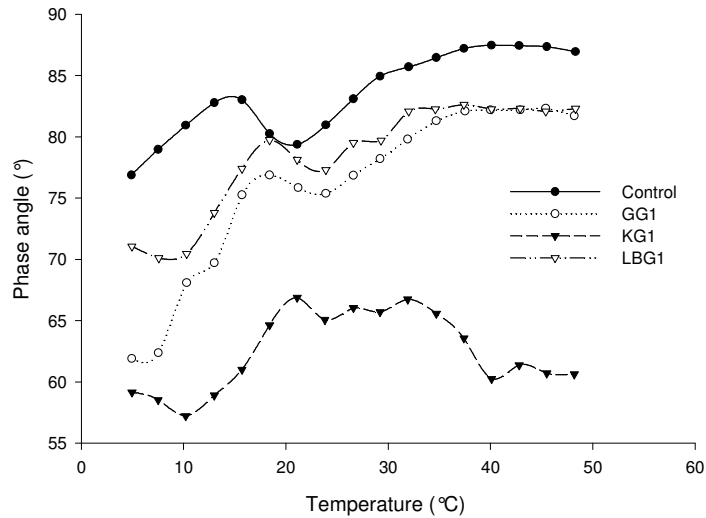
and LBG5 with control. During heating process, phase angle initially increased sharply at lower temperatures (5-15°C) and subsequently decreased suddenly around 20-25°C, thereafter increased again and become nearly constant. This trend was almost observed for all samples.

The initial increasing in the phase angle values was probably due to the melting of fat particles in the sesame paste. At low temperature fat particles are in the solid state and then with the effect of temperature, melting occurred and viscous character of the control and mixtures increased. The sudden reduction in the phase angle values around 20-25°C was probably due to the aggregation of proteins. The second step increase in phase angle may be induced by the melting of stronger junction zones formed by the aggregated protein and gum helices (Norziah et al. 2006). This phenomenon can be explained by Zipper model. In terms of a Zipper model approach, the appearance of two steps in melting in the mixtures suggests that the zippers with different bonding energies or different rotational freedoms may be formed in the presence of gums. The lower melting process is attributed to the melting of zippers with lower bonding energies or with higher rotational freedoms while the higher melting process corresponds to the melting of zippers with higher bonding energies or lower rotational freedoms (Norziah et al. 2006).

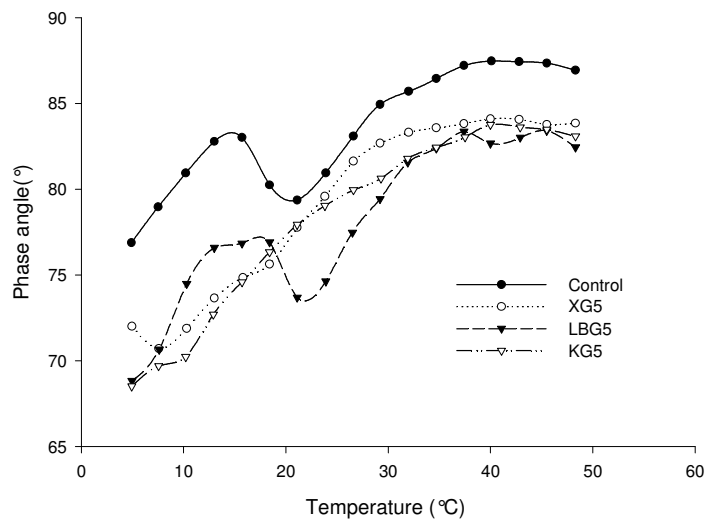


5.11 Temperature dependency of phase angle of pure sesame paste (control), sesame paste/locust bean gum mixtures (LBG1 and LBG5 contains 1 and 5% wt of locust bean gum respectively).

The sesame paste samples that contain gum materials had lower phase angle values than pure sesame paste (Figure 5.11). The increasing gum addition also decreased phase angle values paste/gum mixtures. In addition to this, the temperature dependency paste/gum mixture varied according to gum type and concentration (Figure 5.12-5.13) such as the KG1 sample had low viscous than the others (Figure 5.12) but KG5 had similar values with others (Figure 5.13).



5.12 Temperature dependency of phase angle of pure sesame paste (control), sesame paste/gum mixtures (GG1, KG1 and LBG1 contains 1%wt of guar gum, kappa-carrageen gum and locust bean gum respectively)



5.13 Temperature dependency of phase angle of pure sesame paste (control), sesame paste/gum mixtures (XG5, KG5 and LBG5 contains 5%wt of xanthan gum, kappa-carrageen gum and locust bean gum respectively)

## 5.7 Conclusions

The sesame paste/gum mixtures exhibited shear-thinning and thixotropic behavior. The power law models adequately described the shear stress-shear rate data. Magnitudes of  $K$  and  $n$  parameters of power law models were strongly influenced by gum type (locust bean gum, xanthan gum, guar gum, and kappa-carrageen gum), gum concentration (1 and 5%) and temperature (5 and 25°C). Xanthan and kappa carrageen gums had more pronounced effects on the thixotropic behavior of sesame paste than the others. The effect of temperature on the rheological properties of pastes varied according to gum type; locust bean gum showed higher thermal stability.

The effects of shearing time on the thixotropic characteristic of samples were evaluated. The structural kinetic, Weltman, and first-order shear stress decay with or without zero equilibrium models were applied to characterize the time dependent behavior. The first-order shear stress decay with non-zero equilibrium was determined as the most successful model. Sesame paste/ locust bean gum showed high recovery ability after shearing period at 5 and 25°C.

Small amplitude oscillatory shear tests showed that sesame paste samples were primarily viscous with frequency dependence. Gum addition to the sesame paste did not changed this behavior, all sesame paste/gum mixtures represents similar behavior with pure sesame paste.

The changes in viscoelastic properties of sesame paste/gum mixture during temperature sweep occurred in three different temperature zones. The addition of various gums decreased viscous characters of the sesame paste sample. The temperature dependency of viscoelastic properties of sesame paste/gum mixtures differed with gum type, concentration and studied temperatures zones.

## **CHAPTER 6**

### **CONCLUSIONS**

The present study investigates the roasting process for sesame seeds and rheological characterization of sesame paste with gums. The different mathematical models were developed for descriptions of physical changes in sesame during roasting. The developed color and textural models could be useful for controlling roasting of sesame. The prediction models for each physical parameters of roasted sesame depend on the roasting method. The optimization of roasting process can be carried out successfully by response surface methodology.

The sorption isotherms and thermodynamic parameters for different types of sesame were determined. The whole sesame has higher equilibrium moisture contents at each water activity values than that of dehulled sesame and dehulled-roasted sesame. Roasting process reduced monolayer moisture content of sesame seeds. The Halsey equation is used for predicting the water activity of sesames for thermodynamic calculations.

The sesame paste has a thixotropic behavior. The addition of gums increases the thixotropy of the paste. The first-order shear stress decay with non-zero equilibrium is the most successful model for modeling of thixotropic behavior. The each gum has distinct effect at each concentration and temperature. Locust bean gum, xanthan, and kappa carrageen could be used in new product formulation of sesame paste. From viscoelastic perspective, sesame paste primarily viscous material and addition of gum does not promote so much elasticity.

### **6.1 Further Recommendations**

Food processes are largely rely on the operator's rules of thumb and are not fully automated. For computer automation, good control models are necessary. Sesame roasting is also controlled by operators. Thus developed models in this study could

be used for controlling purposes. On the other hand, precise models are required to use instead of operator decision. Future work about sesame roasting can be focused on the development of more precise control models. This could be achieved using intelligent models e.g. fuzzy logic, neural networks and genetic algorithms. The further studies could be focused on these subjects.

The research on the design of new sesame paste products will help enhancing the use of the sesame. The good rheological behavior could be obtained with more detailed study about gums with sesame paste. Since sesame paste has a good nutritional effect, the alternative products may also be useful for child diets.

## REFERENCES

- Abu-Jdayil, B. (2003). Modeling the time-dependent rheological behavior of semisolid foodstuffs. *Journal of Food Engineering*, **57**, 97–102.
- Abu-Jdayil, B., Al-Malah, K., and Asoud, H. (2002). Rheological characterization of milled sesame (tehineh). *Food Hydrocolloids*, **16**, 55–61.
- Abu-Jdayil, B., (2004). Flow properties of sweetened sesame paste (halawa tehineh). *European Food Research Technology*, **219**, 265-272.
- Abu-Jdayil, B., and Mohammed, H.A. (2004). Time-dependent flow properties of starch-milk-sugar pastes. *European Food Research Technology*, **218**, 123-127.
- Ajibola, O.O., and Dairo, U.O. (1998). The relationship between equilibrium relative humidity and moisture content of sesame seed using the vapor manometric method. *Ife Journal of Technology*, **8**, 61-67.
- Alloncle, M., Lefebvre, J., Llamas, G., and Doublier, J.L. (1989). Rheology of starch–galactomannan gels. *Cereal Chemistry*, **66**, 90–93. 1200–1207
- Al-Muhtaseb, A.H., McMinn, W.A.M., and Magee, T.R.A. (2004). Water sorption isotherms of starch powders. Part 2: Thermodynamic characteristics. *Journal of Food Engineering*, **62**, 135-142.
- Alobo, A.P. (2001). Effect of sesame flour on millet biscuit characteristics. *Plant Foods For Human Nutrition*, **56**, 195–202.
- Altan A., Kuş, S., and Kaya, A., (2005). Rheological behavior and time dependent characterisation of Gilaboru juices (*Viburnum opulus* L.). *Food Science and Technology International*, **11**,129-137.
- Alvarez, M.D., and Canet, W. (2002). A comparison of various rheological properties for modeling the kinetics of thermal softening of tissue (c.v. *Monalisa*) by water cooking and pressure steaming. *International Journal of Food Science and Technology*, **37**, 41-55.
- Annussek, G. 2001. Sesame oil. In: *Gale encyclopedia of alternative medicine*. Gale Group and Looksmart.
- AOAC. 1990. *Official Methods of Analysis of the Association of Official Analytical Chemists*. (15<sup>th</sup> ed). pp 837, 999-1000. Association of Official Analytical Chemists.
- Arslan, N., and Toğrul, H. (2005). Moisture sorption isotherms for crushed chillies. *Biosystems Engineering*, **90**, 47-61.
- Aviara, N.A., Ajibola, O.O., and Dairo, U.O. (2002). Thermodynamics of moisture sorption in sesame seed, *Biosystems Engineering*, **83**, 423-431.
- Aviara, N.A., Ajibola, O.O., and Oni, S.A. (2004). Sorption equilibrium and thermodynamic characteristics of soya bean. *Biosystems Engineering*, **87**, 179-190.
- Aviara, N.A., and Ajibola, O.O. (2002). Thermodynamics of moisture sorption in melon seed and cassava. *Journal of Food Engineering*, **55**, 107-113.

- Avila, I. M.L.B., and Silva, C.L.M. (1999). Modeling kinetics of thermal degradation of colour in peach puree. *Journal of Food Engineering*, **39**, 161-166.
- Barbosa-Canovas, G.V., Kokini, J.L., Ma, L., and Ibarz, A. (1996). The rheology of semiliquid foods. *Advanced Food and Nutrition Research*, **29**, 1-69.
- Barnes, H.A. (1997). Thixotropy a review. *Journal of Non-Newtonian Fluid Mechanics*, **70**, 1-33.
- Benado, A.L., and Rizvi, S.S.H. (1985). Thermodynamic properties of water on rice as calculated from the reversible and irreversible isotherms. *Journal of Food Science*, **50**, 101-105.
- Bourne, M.C. (1982). Food Texture and Viscosity: Concept and Measurement In G.F. Stewart, B.S. Schweigert and J. Hawtorn (Eds), *Principles of objective texture measurement* Academic Press, New York.
- Budowski, P. (1962) Recent research on sesamin, sesamol and related compounds. *Journal of American Oil Chemistry*, **41**, 280-285.
- Can A., (1964). Susam (*Sesamum indicum*). *Tarım Bakanlığı Ziraat İşleri Gen. Müd. Teknik Neşriyat Şub.*, Ankara.
- Cheng, D.C.H. and Evans, F. 1965. Phenomenological characterisation of the rheological behaviour of inelastic reversible thixotropic and antithixotropic fluids. *British Journal of Applied Physics*, **16**, 599-617.
- Chirife, J., and Iglesias, H.A. (1978). Equations for fitting water sorption isotherms of foods. *Journal of Food Technology*, **13**, 159-174.
- Citerne, G.P., Carreau, P.J., and Moan, M. (2001). Rheological properties of peanut butter. *Rheologica Acta*, **40**, 86-96.
- Da Silva, J.A.L., and Rao, M.A. (1992). Viscoelastic properties of food hydrocolloid dispersions. In M.A. Rao and J.F. Steffe (Eds.), *Viscoelastic properties of foods*. London, UK: Elsevier, 285-316.
- Demir A.D, Celayeta, J., Cronin K., and Abodayeh, K. (2002). Modeling of the kinetics of colour change in hazelnuts during air roasting. *Journal of Food Engineering*, **55**, 283-29.
- Doymaz, I. (2004). Convective air-drying characteristics of thin layer carrots. *Journal of Food Engineering*, **61**, 359-364.
- Egbekun, M.K., & Eiheze, M.U. (1987). Proximate composition and functional properties of fullfat and defatted beniseed (*Sesamum indicum* L.) flour. *Plant Foods For Human Nutrition*, **51**, 35-41.
- El-Adawy, T.A., and Mansour, E.H. (2000). Nutritional and physicochemical evaluations of tahina (sesame butter) prepared from heat-treated sesame seeds. *Journal of Science of Food and Agriculture*, **80**, 2005-2011.
- El-Adawy, T.A. (1997). Effect of sesame seed proteins supplementation on the nutritional, physical, chemical and sensory properties of wheat four bread. *Food Chemistry*, **59**, 7-14.
- Eleazar, M.S., Salvador, H.G.M., and Alicia, C.M. (2003). Simplified process for the production of sesame protein concentrate. Differential scanning calorimetry and

nutritional, physicochemical and functional properties. *Journal of Science and Food Agriculture*, **83**, 972–979.

Fasina, O., Ajibola, O.O., and Tyler, R. (1999). Thermodynamics of moisture sorption of winged bean seed and Gari. *Journal of Food Process Engineering*, **22**, 405-418.

Fukuda, Y., Nagata, M., Osawa, T., and Namiki, M. (1986). Chemical aspects of the antioxidative activity of roasted sesame seed oil and the effect of using the oil for frying. *Agricultural and Biological Chemistry*, **50**, 857–862.

Halsey, G. (1948). Physical adsorption on non-uniform surfaces. *Journal of Chemical Physics*, **16**, 931-937.

Hebbar, H.U., and Ramesh, M.N. (2005). Optimisation of processing conditions for infrared drying of cashew kernels with testa. *Journal of Science and Food Agriculture*, **85**, 865-871.

Hill, P.E., and Rizvi, S.S.H. (1982). Thermodynamic parameters and storage stability of drum dried peanut flakes. *Lebensmittel-Wissenschaft und-Technologie*, **15**, 185-190.

<http://faostat.fao.org>

Hussain, S.R., Terao, J., and Mathuushita, S. (1986). Effect of browning products of phospholipids on autoxidation of methyl lioenete. *Journal of American oil Chemist Society*, **63**, 1457-1560.

İbanoglu, Ş. (2005). Effect of dilute lactic acid hydrolysis on the cooked viscosity of a fermented white wheat flour–yogurt mixture. *Journal of Food Engineering* **64**, 343-346.

Johnson, L.A., Suleiman, T.M., and Lusa, E.W. (1979). Sesame protein: A review and prospectus. *Journal of American oil Chemist Society*, **56**, 463-468.

Kahyaoglu, T., and Kaya, S. (2005). Modeling of moisture, color and texture changes in sesame seeds during the conventional roasting. *Journal of Food Engineering*, (in press).

Kamal-Eldin, A., and Appelqvist, L. A. (1994). Variation in fatty acid composition of the different acyl lipids in seed oils from four sesamum species. *Journal of American Oil Chemistry*, **71**, 135–139.

Kaya, S., and Kahyaoglu, T. (2005). Thermodynamic properties and sorption equilibrium of Pestil (grape leather). *Journal of Food Engineering*, **71**, 200-207

Kikugawa, K., Arai M., and Kurechi, T. (1983). Participation of sesamol in stability of sesame oil. *Journal of American oil Chemist Society*, **60**, 1528-1533.

Korus, J., Juszczak, L., Witczak, M., and Achremowicz, B. (2004). Influence of selected hydrocolloids on triticale starch rheological properties. *International Journal of Food Science and Technology*, **39**, 641-652.

Labuza, T.P. (1984). *Practical aspects of isotherm measurement and use*. Am. Assoc. Cereal Chem., St. Paul, MN.

Labuza, T.P. (1980). Enthalpy/Entropy compensation in food reactions. *Food Technology*, **37**, 67-77.



- Lokumcu A.F., and Ak, M.M. (2005). Effects of temperature, shear rate and constituents on rheological properties of tahin (sesame paste). *Journal Food Science and Agriculture*, **85**, 105-11.
- Madamba, P.S., Discroll, R.H., and Buckle, K.A. (1996a). Thin layer drying characteristics of garlic slices. *Journal of Food Engineering*, **29**, 75-97.
- Madamba, P.S., Driscoll, R.H., and Buckle, K.A. (1996b). Enthalpy-entropy compensation models for sorption and browning of garlic. *Journal of Food Engineering*, **28**, 109-119.
- Martinez N.N, and Chiralt, A. (1996). Influence of roasting on the water sorption isotherms of nuts. *Food Science and Technology International*, **2** (6), 399-404.
- Maskan, M. (2001). Kinetics of colour change of kiwifruit during hot air and microwave drying. *Journal of Food Engineering*, **48**, 169-175.
- McKenna, B.M. (2003). Texture in Food Vol.1- Semi solid Foods. In McKenna B.M (Ed), *Introduction to food rheology and its measurement*. Cambridge, Woodhead.
- McMinn, W.A.M., and Magee, T.R.A. (2003). Thermodynamic properties of moisture sorption of potato. *Journal of Food Engineering*, **60**, 157-155.
- Mitchell, J.R. (1984). Food Analysis-Principles and Techniques Vol. 1. In Gruenwedel, D.W. and Wihtear, J.R., (Eds), *Rheological techniques*. New York, Marcel Dekker.
- Montgomery, D.C. (2001). *Design and Analysis of Experiments*, (5<sup>th</sup> ed.), John Wiley and Sons.
- Morris, J.B. (2002). Food, Industrial, Nutraceutical, and Pharmaceutical uses of sesame genetic resources. In J. Janick and A. Whipkey (Eds.), *Trends in new crops and new uses*. ASHS Press, Alexandria, VA.
- Moss, J.R., and Otten, L. (1989). A relationship between color development and moisture content during roasting of peanuts. *Canadian Institute of Food Science and Technology*, **22**, 34-39.
- Nagata, M., Osawa, T., Namiki, M., Fukuda, Y., & Ozaki, T. (1987) Stereochemical structures of antioxidative bisepoxylignans, sesaminol and its isomers transformed from sesamol. *Agricultural and Biological Chemistry*, **51**, 1285-1289.
- Namiki, M. (1995). The chemistry and physiological functions of sesame. *Food Review International*, **11**, 281-329.
- Nguyen, Q.D., and Boger, D.V. (1985). Thixotropic behavior of concentrated bauxite residue suspensions. *Rheologica Acta*, **24**, 427-437.
- Nguyen, Q.D., Jensen, C.T.B. and Kristensen, P.G. (1998). Experimental and modeling studies of the flow properties of maize and waxy maize starch pastes. *Chemical Engineering Journal*, **70**, 165-171
- Nixon, R., and Peleg, M. (1995). Effect of sample volume on the compressive force-deformation curves of corn flakes tested in bulk. *Journal of Texture Studies*, **29**, 59-69.
- Norziah M.H., Foo, S.L. and Abd.Karim, A. (2006) Rheological studies on mixtures of agar (*Gracilaria changii*) and k-carrageenan. *Food Hydrocolloids*, **20**, 204-217

- Özcan M., and Akgül, A. (1994). Physical and chemical properties and fatty acid composition of tahin (sesame paste). *Gıda*, **19**, 411-416. (in Turkish).
- Özcan, M. (1993). Susam, susam yağı ve tahinde fiziksel-kimyasal analizler ve yağ asitleri bileşimlerinin belirlenmesi. *MS.c Thesis, Selçuk University*.
- Ozdemir, M., and Devres, O. (2000a). Kinetics of color changes of hazelnuts during roasting. *Journal of Food Engineering*, **44**, 31–38.
- Ozdemir, M., and Devres, O. (2000b). Analysis of colour development during roasting of hazelnuts using response surface methodology. *Journal of Food Engineering*, **45**, 17–24
- Ozdemir, M., and Devres, O. (1999). Thin layer drying characteristics of hazelnuts during roasting. *Journal of Food Engineering*, **42**, 225-233.
- Pittia P., Rosa, M.D., and Lericci, C.R. (2001). Textural changes of coffee beans as affected by roasting conditions. *Lebensmittel-Wissenschaft und Technologie*, **34**,168-171.
- Ram, R., Catlin, D., Romero, J., and Cowley, C., (1990). Advances in new crops In: J. Janick and J.E. Simon (Eds.), *Sesame: New approaches for crop improvement*. Timber Press, Portland, OR.
- Rao, M.A., (1999). *Rheology of Fluid and Semisolid Foods-Principles and Applications*, Maryland, Aspen Publications.
- Rapasus, R.S., and Discroll, R.H. (1995). Kinetics of non-enzymatic browning in onion slices during isothermal heating. *Journal of Food Engineering*, **24**, 417-429.
- Rizvi, S.S.H. (1986). Engineering Properties of Foods. In M.A. Rao, and S.S.H. Rizvi (Eds.), *Thermodynamic properties of food in dehydration*. New York: Marcel Dekker Inc.
- Rizvi, S.S.H., and Benado, A.L. (1984). Thermodynamic properties of dehydrated foods. *Food Technology*, **38**, 83-92.
- Ross-Murphy, S.B. (1995). Rheology of biopolymer solutions and gels. In Dickinson, E. (Ed); *New Physico-chemical Techniques for the Characterization of Complex food systems*. pp. 135-156. London: Blackie Academic & Professional
- Rotstein, E. (1983). Exergy balance: a diagnostic tool for energy optimization. *Journal of Food Science*, **48**, 945-950.
- Saguy, I., and Karel, M. (1980). Modeling of quality deterioration during food processing and storage. *Food Technology*, **37**, 78-85.
- Saklar, S., Katnas, S., and Urgan, S. (2001). Determination of optimum hazelnut roasting conditions. *International Journal of Food Science and Technology*, **36**, 271–281.
- Saklar, S., Urgan, S., and Katnas, S. (1999). Instrumental crispness and crunchiness of roasted hazelnuts and correlations with sensory assessment. *Journal of Food Science*, **64**, 1015–1019.
- Sawaya, W.N, Ayaz M., Khalil K.J., and Shalhat A.F. (1985). Chemical composition and nutritional of Tehineh (Sesame Butter). *Food Chemistry*, **18**, 35-45.

- Senadeera, W., Bhandari, B.R., Young, G. and Wijesinghe, B. (2003). Influence of shapes of selected vegetable materials on drying kinetics during fluidized bed drying. *Journal of Food Engineering*, **58**, 277–283.
- Shyu, Y. S., and Hwang, L.S. (2002). Antioxidative activity of crude extract of lignan glycosides from unroasted Burma black sesame meal. *Food Research International*, **35**, 357-365.
- Simal, S., Femenia, A., Garau, M.C, and Rosselló, C. (2005). Use of exponential, Page's and diffusional models to simulate the drying kinetics of kiwi fruit. *Journal of Food Engineering*, **66**, 323–32.
- Skaar, C., and Babiak, M. (1982). A model for bound water transport in wood. *Wood Science and Technology*, **16**, 123-138.
- Smith, J.M., Van Ness, H.C., and Abbott, M.M. (2001). *Introduction to chemical engineering thermodynamics*. Boston: McGraw-Hill.
- Speers, R., and Tung, M. (1986). Concentration and temperature dependence of flow behavior of xanthan gum dispersions. *Journal of Food Science*, **51**, 96–98, 103.
- Steffe, J.F. (1996). *Rheological Methods in Food Process Engineering*. (2<sup>nd</sup> ed.). Freeman Press, USA.
- Tadros, T. (2004). Application of rheology or assessment and prediction of the long-term physical stability of emulsions. *Advances in Colloid and Interface Science*, **108-109**, 227-258.
- Tarrega, A., Duran, L., and Costell, E. (2004). Flow behavior of semi-solid dairy deserts. Effect of temperature. *International Dairy Journal*, **14**, 345-353.
- Telis, V.R.N., Gabas, A.L., Menegalli, F.C., and Telis-Romero, J. (2000). Water sorption thermodynamic properties applied to persimmon skin and pulp. *Thermochimica Acta*, **343**, 49-56.
- The Nut Factory. 1999. The sesame seed family. [thenutfactory.com/ kitchen /edible /facts-sesame.html](http://thenutfactory.com/kitchen/edible/facts-sesame.html).
- Tiu, C., and Boger, D.V. (1974). Complete rheological characterization of time-dependent food products. *Journal of Texture Studies*, **5**, 329–338.
- Tolaba, M.P., Suárez, C., and Viollaz, P. (1995). Heats and entropies of sorption of cereal grains: a comparison between integral and differential quantities. *Drying Technology* **13**, 2097-2111.
- Tsami, E., Marinous-Kouris, D., and Maroulis, Z.B. (1990). Water sorption isotherms of raisins, currants, figs, prunes, and apricots. *Journal of Food Science*, **55**, 1594-1597.
- Tyler, V.E., L.R. Brady, and J.E. Robbers. (1976). Lipids. (pp. 121–122). In: Lea and Febiger, (Eds.) *Pharmacognosy*. Philadelphia, PA.
- Urlacher, B., and Noble, O. (1997). Xanthan. In A. Imeson (Ed.), *Thickening and gelling agents for food* (pp. 284–311). London:Chapman & Hall.
- USDA (2004). National Nutrient Database for Standard Reference, Release 17.
- Van den Berg, C. (1985). Properties of water in foods. In D. Simatos and J.L. Multon (Eds.), *Development of B.E.T. like models for sorption of water on foods, theory and relevance*. Dordrecht: Martinus Nijhoff.

- Van Vliet, T. (1999). Rheological classification of food and instrumental techniques for their study. In A.J. Rosenthal (Ed.), *Food Texture Measurement and Perception*, Gaithersburg, Maryland, Aspen Publishers, 65-98.
- Vincent, J.F.V. (2004). Application of fracture mechanics to the texture of food. *Engineering Failure Analysis*, **11**, 695-704.
- Weltman, R.N. (1943). Breakdown of thixotropic structure as a function of time. *Journal of Applied Physics*, **14**, 343-350.
- William P.A., and Smith G.O. (2003). Use of Hydrocolloids in food systems. In B.M. McKenna, *Texture in Food Vol.1- Semi solid Foods*, Cambridge, Woodhead.
- Yaseen, E.I., Herald, H.J., Aramouni, F.M., and Alavi, S. (2005). Rheological properties of selected gum solutions. *Food Research International*, **38**, 111-119.
- Yoshida, H., and Takagi, S. (1997). Effects of Seed Roasting Temperature and Time on the Quality Characteristics of Sesame Oil (*Sesamum indicum*). *Journal of Science and Food Agriculture*, **75**, 19-26.

## **APPENDICES**



Figure A.1 Hot air roasting system

Table A.1 Experimental data for response parameters of sesame seeds roasted in the hot air roaster

Roasting conditions		Responses						
Temperature (°C)	Time (min)	L-value	a-value	b-value	BI	Hardness (N)	Fracturability (N)	MC (g kg <sup>-1</sup> , db)
150	24	63.67	2.46	15.85	30.90	10.40	12.15	48.8
193	45	62.09	4.61	18.98	41.28	7.27	5.13	11.6
120	30	62.51	2.63	15.57	31.18	10.64	9.40	61.7
150	45	62.61	2.95	16.53	33.52	10.95	8.97	37.2
180	30	63.49	3.74	18.34	37.77	8.07	5.18	35.5
120	60	61.90	2.65	16.79	34.16	9.32	11.88	33.3
150	67	64.44	3.42	16.30	32.52	8.30	6.81	21.0
108	45	61.45	2.68	15.81	32.37	15.63	13.25	69.5
150	45	63.25	2.59	16.24	32.10	10.03	8.75	33.4
180	60	63.41	3.70	18.03	37.11	7.52	6.52	18.8
150	45	63.01	2.43	15.91	31.36	10.89	10.11	39.4
150	45	62.99	2.70	16.08	32.05	9.27	8.13	38.7
150	45	63.15	2.74	16.29	32.44	10.05	9.56	38.3

BI: Browning index, MC: moisture content.

Table A.2 ANOVA and model fitting for response parameters of roasted sesame seeds in the hot air roaster

		df	P-values						
			L-value	a-value	b-value	BI	Hardness (N)	Fracturability (N)	MC (g kg <sup>-1</sup> , db)
Sequential model sum of squares	Linear	2	0.3529	0.0070	0.0043	0.0178	0.0053*	0.0016*	0.0001*
	2FI	1	0.7575	0.9493	0.2875	0.4519	0.8001	0.7243	0.3142
	Quadratic	2	0.0014*	0.0066*	0.0016*	0.0003*	0.3044	0.9392	0.6445
Lack of fit tests	Linear	6	0.0081	0.0327	0.0119	0.0133	0.0538 (NS)	0.0572 (NS)	0.0296 (S)
	2FI	5	0.0061	0.0245	0.0115	0.0112	0.0412	0.0445	0.0278
	Quadratic	3	0.1044 (NS)	0.1774 (NS)	0.1811 (NS)	0.3946 (NS)	0.0368	0.0212	0.0161
r <sup>2</sup>			0.88	0.91	0.95	0.96	0.75	0.73	0.92

\* Shows suggested model;

S: Significant at P<0.05; NS: not significant; df: degree of freedoms; 2FI: two factor interaction term



Table A.3 Experimental data for response parameters of sesame seeds that roasted in the electrical oven

Roasting conditions		Responses						
Temperature (°C)	Time (min)	L-value	a-value	b-value	BI	Hardness (N)	Fracturability (N)	MC (g kg <sup>-1</sup> , db)
150	30	59.05	5.88	19.52	46.75	7.28	5.53	43.5
120	30	61.40	4.51	18.60	40.83	8.39	6.35	59.2
135	45	61.85	4.44	18.85	40.96	6.70	6.03	59.5
150	60	54.14	7.69	19.15	53.36	6.48	5.75	43.1
135	45	61.93	4.46	18.74	40.67	6.00	5.88	58.4
135	45	61.67	4.78	19.17	42.25	6.36	4.83	58.1
120	60	62.57	3.80	18.14	38.06	7.00	6.32	54.0
135	45	62.31	4.49	18.95	40.89	6.91	6.52	56.5
135	45	61.66	4.36	18.79	40.87	6.53	5.24	55.6
114	45	63.45	3.06	17.14	34.42	7.89	6.85	58.2
135	45	61.96	4.41	19.00	41.18	6.51	4.71	56.9
135	67	59.05	5.57	19.16	45.47	6.51	4.71	58.4
157	45	49.25	8.23	17.75	56.24	6.30	4.33	38.2
135	24	62.14	4.26	18.72	40.22	6.94	5.71	58.1

BI: Browning index, MC: moisture content

Table A.4 ANOVA and model fitting for response parameters of roasted sesame seeds in the electrical oven

		P-values							
		df	L-value	a-value	b-value	BI	Hardness (N)	Fracturability (N)	MC (g kg <sup>-1</sup> , db)
Sequential model sum of squares	Linear	2	0.0048	0.0003	0.3287	0.0002	0.0235*	0.0508*	0.0099
	2FI	1	0.2649	0.0813	0.9457	0.0899	0.5883	0.8554	0.6589
	Quadratic	2	0.0019*	0.0014*	0.0056*	0.0060*	0.0598*	0.8131	0.0012*
Lack of fit tests	Linear	6	< 0.0001	0.0014	0.0064	0.0021	0.0902	0.8764	0.0004
	2FI	5	< 0.0001	0.0021	0.0047	0.0031	0.0734	0.8163	0.0003
	Quadratic	3	0.0012 (S)	0.0369 (S)	0.0382 (S)	0.0241 (S)	0.1619 (NS)	0.6567 (NS)	0.0055 (S)
r <sup>2</sup>			0.98	0.98	0.82	0.97	0.80	0.48	0.94

\* Shows suggested model;

S: Significant at P<0.05; NS: not significant; df: degree of freedoms; 2FI: two factor interaction term

Table A.5 Experimental data for response parameters of sesame seeds that roasted in the vacuum oven

Roasting conditions		Responses						
Temperature (°C)	Time (min)	L-value	a-value	b-value	BI	Hardness (N)	Fracturability (N)	MC( g kg <sup>-1</sup> , db )
150	30	62.35	2.76	16.42	33.22	13.18	7.88	28.8
120	30	64.87	2.12	15.88	29.91	20.47	12.65	31.1
135	45	64.45	2.35	16.12	30.88	15.62	10.12	30.8
150	60	61.78	3.12	17.25	35.82	7.54	6.45	24.6
135	45	65.12	2.25	16.52	31.21	10.19	8.92	31.4
135	45	64.87	2.19	16.35	30.93	12.57	9.55	30.1
120	60	63.04	2.01	15.63	30.25	16.66	9.90	27.6
135	45	65.52	2.28	16.67	31.32	12.15	10.18	28.5
135	45	64.71	2.45	16.29	31.20	12.21	9.07	29.1
114	45	62.93	1.83	15.87	30.59	20.07	13.11	32.7
135	45	64.96	2.10	16.44	30.96	11.34	9.89	28.8
135	67	61.13	2.39	16.65	34.03	12.76	8.86	28.4
157	45	60.44	2.96	17.15	36.32	15.14	6.03	25.9
135	24	62.47	1.95	15.10	29.40	13.63	11.22	32.4

BI: Browning index, MC: moisture content

Table A.6 ANOVA and model fitting for response parameters of roasted sesame seeds in the vacuum oven

		df	P-values						
			L-value	a-value	b-value	BI	Hardness (N)	Fracturability (N)	MC (g kg <sup>-1</sup> , db)
Sequential model sum of squares	Linear	2	0.2216	0.0001*	0.0029*	0.0004*	0.0297	< 0.0001*	0.0019*
	2FI	1	0.7148	0.1867	0.1446	0.3388	0.7660	0.2217	0.8190
	Quadratic	2	0.0004*	0.1490	0.1071	0.0018	0.0718*	0.6518	0.4900
Lack of fit tests				0.2601	0.0694	0.0006			0.0148
	Linear	6	0.0029	(NS)	(NS)	(S)	0.1640	0.7032 (NS)	(S)
	2FI	5	0.0022	0.2911	0.0837	0.0006	0.1301	0.7581	0.0111
	Quadratic	3	0.0850 (NS)	0.4167	0.1355	0.0090	0.2623 (NS)	0.6452	0.0074
r <sup>2</sup>			0.92	0.83	0.68	0.96	0.76	0.94	0.71

\* Shows suggested model;

S: Significant at P<0.05; NS: not significant; df: degree of freedoms; 2FI: two factor interaction term

## CURRICULUM VITAE

### PERSONAL INFORMATION

Surname, Name: KAHYAOĞLU Talip  
Nationality: Turkish (TC)  
Date and Place of Birth: 11 August 1975 , Gaziantep  
Marital Status: Married  
Phone: +90 342 360 12 00  
Fax: +90 342 360 11 05  
email: kahyaoglu@gantep.edu.tr

### EDUCATION

Degree	Institution	Year of Graduation
Ph.D	University of Gaziantep	2005
MS	University of Gaziantep	2002
BS	University of Gaziantep	1999
High School	Şahinbey 19 Mayıs	1993

### WORK EXPERIENCE

Year	Place	Enrollment
1999- Present	University of Gaziantep-Food Engineering Department	Research Assistant
2005- Present	Gaziantep TEKMER (Technology Development Center of Gaziantep)	Expert (Half-time)

### FOREIGN LANGUAGES

English (Good)

### PUBLICATIONS

1. **Kahyaoglu, T.** and Kaya, S. (2003). Effects of heat treatment and fat reduction on the rheological and functional properties of Gaziantep cheese. **International Dairy Journal 13: 867-875.**
2. **Kahyaoglu, T.** ,Kaya, S. and Kaya A. (2005). Effects of curd dipping temperatures and fat content on the appearance, texture and viscoelasticity of Gaziantep cheese. **Food Science and Technology International, 11, 191-198.**

3. Kaya, S. & Kahyaoglu T.(2005). Thermodynamic properties and sorption equilibrium of pestil (grape leather). **Journal of Food Engineering**, **71**, 200-207.
4. Kaya S. & Kahyaoglu T. Influence of dehulling and roasting process on the thermodynamics of moisture adsorption in sesame seed. **Journal of Food Engineering (In press, available online)**.
5. Kahyaoglu T. & Kaya S. Modeling of moisture, color and texture changes in sesame seeds during conventional roasting. **Journal of Food Engineering (In press, available online)**.
6. Kahyaoglu, T & Kaya, S. Determination of optimum processing conditions for hot air roasting of dehulled sesame seeds. **Journal of the Science of Food and Agriculture, (In press)**.
7. Kaya, S. and Kahyaoglu, T. Moisture sorption and thermodynamic properties of safflower petals and tarragon. **Journal of Food Engineering, (in press, available online)**.

#### **Symposiums**

1. **KAHYAOĞLU T, S. KAYA.** Use of Dynamic Rheological Data for Prediction of Meltability of Gaziantep Cheese with Various Fat Contents. **2002 Joint Annual ADSA-ASAS-CSAS Meeting, Quebec, Canada, July 21-25, 2002.**
2. **KAHYAOĞLU T, S. KAYA.** Effects of curd dipping temperatures and fat content on the appearance and texture of Gaziantep cheese **International Dairy Symposium, May 24-28, 2004.**
3. **KAHYAOĞLU T, S. KAYA.** Effects of storage conditions and fat reduction on the appearance and texture of Gaziantep cheese. **International Dairy Symposium, May 24-28, 2004.**
4. **KAHYAOĞLU T, S. KAYA.** “Susam kavurma sürecinde meydana gelen renk ve dokusal değişimin analizi” **Geleneksel Gıdalar Sempozyumu, Eylül, 2004.**
5. **KAHYAOĞLU T, S. KAYA.** “Susam kavurma işleminin tepkisel yüzey yöntemiyle optimize edilmesi”, **Ege Gıda Kongresi, Nisan, 2005.**
6. **KAHYAOĞLU T, S. KAYA.** Use of Artificial Neural Networks for Food Process Control and Modeling. **International Congress On Information Technology In Agriculture, Food And Environment, 12-14 October 2005, Adana , TURKEY.**